Centre for Policy Futures
31 July 2020

THE UNIVERSITY OF QUEENSLAND
AUSTRALIA
CREATE CHANGE

National electricity market nodal modelling final report 2020

Dr Phillip Wild,
Centre for Policy Futures
University of Queensland

Contents

Tables

Figures

Executive Overview

The modelling conducted here was commissioned as part of an Advance Queensland research project on the potential for the Queensland electricity system to transition to high levels of variable renewable energy and achieve the Queensland Renewable Energy Target of 50% by 2030.

Modelling outcomes indicate that QRET will not be achieved despite the roll-out of 8,736MW of solar and 4,820MW of wind capacity. This is primarily as a result of high levels of curtailment of solar and wind dispatch due to the high levels of coal plant still in operation by 2030. Multiple iterations were conducted to analyse the effect of coal plant closure on curtailments resulting from surplus renewable energy capacity. Scenarios included modelling the outcome associated with the following closures:

Pipeline scenario A

- Unit 1 Stanwell; Units 1,2,5,6 Gladstone; Unit 1 Tarong; Unit 2 Eraring

Pipeline scenario B

- Units 1,2 Stanwell; Units 1,2,5,6 Gladstone; Units 1,2 Tarong; Units 2-4 Eraring

Pipeline scenario C

- Units 1,2,5,6 Gladstone; Units 1-4 Tarong; Units 2-4 Eraring

To reduce surplus variable renewable energy curtailment during periods of excess supply, 1 GW of pump hydro energy storage (PHES) was assumed at Mt Byron in Moreton North node and Urannah in North Queensland node. In addition to scenarios A to C, scenarios associated with the investment profile of the pipeline scenario considered the consequences of no investment in PHES at Mt Byron and Urannah.

The modelling outcomes of the scenarios without additional pump hydro are detailed in section 4 but in summary PHES enables the increase in the proportion of VRE in the mix of generation by approximately 10% through pump action during the day when there is surplus energy and discharge at evening and morning peak.

The pipeline scenarios are contingent on investment in wind and solar generation as indicated by planning permission already awarded to project proponents. It is recognised that this reflects a bias towards solar generation of 8,736 MW by 2030, against 4,820 MW of wind. For this reason, alternate solar/wind generation mixes as proposed by the Australian Energy Market Operator's (AEMO) Integrated System Plan 2020 (ISP) scenarios were also modelled. These scenarios were associated with the following differences to the pipeline scenarios:

ISP 2030 central scenario

- Coal and gas plant capacity same as for pipeline scenario;
- 2030 solar capacity of 4768 MW (Pipeline: 8736 MW);
- 2030 wind capacity of 3083 MW (Pipeline: 4820 MW)

ISP 2030 step change scenario

- 3080 MW coal plant closures (pipeline scenario B & C: 2520MW);
- 2030 solar capacity of 3278 MW (pipeline: 8736 MW)
- 2030 wind capacity of 7118 MW (pipeline: 4820 MW)

ISP 2040 central scenario

- 3650 MW coal plant closures (pipeline scenario B & C: 2520MW);
- Solar capacity of 7243 MW (pipeline: 8736 MW)
- Wind capacity of 5651 MW (pipeline: 4820 MW)

Outcomes from modelling these scenarios indicate that 2030 pipeline scenario B and 2040 ISP Central Scenario achieve the highest renewable percentage of electricity generated at 42% under unrestricted network conditions.

AEMO's ISP does not indicate priority grid projects for Queensland, and yet modelling outcomes show that transmission has a very large impact on the achievement of QRET. In particular, modelling included 2 transmission scenarios for each of the pipeline and ISP generation scenarios. The first transmission scenario (N) sought to apply the MW thermal limits in the group of transmission lines connecting 2 nodes. This approach effectively assumes no line outages occur, that the transmission lines are always operational and provides an ideal setting for maximising VRE potential within the network. The second transmission scenario (N-1) involved subtracting the largest individual line from the group of transmission lines connecting nodes. This approach more closely matches how AEMO manages the grid in practice, being linked to reliability and security considerations if the largest single line is lost. Modelling outcomes indicate that the 2030 pipeline baseline scenario's VRE contribution to electricity generation reduces to 34.0% from 37.5%, scenario B's VRE contribution reduces to 38.6% from 41.5%, and ISP 2040 central scenario VRE contribution reduces to 38.1% from 41.4% under the restrictive N-1 transmission scenario.

Solar and wind curtailment (or spillage as referred to here) increases from 19% for the 2030 pipeline baseline scenario and 13% for the 2030 pipeline scenario B under unrestricted transmission conditions to 30% for the baseline and 22% for scenario B under restrictive N-1 transmission conditions. Additional spillage will impact on project viability and influence investment levels. If transmission hinders the dispatch of VRE, investment will be restricted and QRET may not be achievable. It is thus particularly important that further attention is paid to the transmission infrastructure in Queensland to ensure that it will facilitate the transition to higher levels of VRE and the achievement of QRET.

Transitioning to high levels of renewable energy results in the emergence of an energy deficit increasing from 2% of energy production in the 2030 pipeline baseline scenario excluding pump hydro storage, to 4% in the 2030 pipeline baseline scenario including pump hydro storage, to 8% in pipeline scenario B, and 11% in the ISP 2040 central scenario. This deficit is energy dispatched not from existing and identified new generation, but from unidentified capacity required to balance supply and demand intermittently at each node. Further detail on the 'Energy Gap' can be found in the discussion of each of the scenarios in the following sections, but in summary, the greater reduction in coal plant in the 2040 ISP central scenario is the primary reason for the increased size of the Energy Gap in the ISP 2040 central scenario.

In all modelled cases however, balancing energy (rather than capacity) is much lower under N than N-1. Resolving both capacity and energy deficits will impact the costs of meeting QRET. Modelling outcomes confirm that transmission losses are higher under the more expansive N scenario, as energy is directed further around the network to meet demand, leading to lower marginal loss factors (MLF). Of interest is the significant change that occurs in the direction of power flows between 2022 and 2030, as the generation mix changes. In 2022, power flows northward to the northern nodes of Far North Queensland, Ross and North Queensland which results in very low marginal losses and MLFs close to unity according to the methodology that was used to calculate MLFs. However, by 2030 with significant investment in VRE in and around the northern nodes and reduced coal plant output from Gladstone and Stanwell, power flows are more predominantly southwards, resulting in an increase in marginal losses and reductions in MLFs for the northern nodes. In tandem with these changes to the northern node MLFs, corresponding MLFs for Central West Queensland, Gladstone, Wide Bay and Tarong all increase as the coal plants reduce output to supply other parts of the network and power flows realign with greater output from generation outside of those nodes.

Modelling outcomes from the N-1 scenario indicate potential for significant branch congestion on the transmission lines connecting:

- Central West Queensland to Gladstone; where power flow from VRE generated in the northern nodes is restricted from reaching Gladstone. This became more noticeable in the ISP 2040 Central Scenario with the complete closure of Gladstone Power Station.
- Wide Bay to Moreton North; where wind and solar at Wide Bay is restricted from reaching the major load centres of South East Queensland, leading to persistent energy deficits at Moreton North.
- South West Queensland to Moreton South; where wind and solar at the AEMO identified Renewable Energy Zone (REZ) in South West Queensland is restricted from reaching the major load centres of South East Queensland.

This potential congestion, the resulting energy and capacity deficits, and VRE spillage could be reduced through transmission augmentation to reflect the changing power flows resulting from coal plant closures and new decentralised VRE generation. Further detail on these changes is provided in Section 6.

The finding of significant capacity and energy deficits at many of the nodes under N-1 perhaps represent a worst possible outcome, but it cannot be ignored if secure supply is to be maintained in a system dominated by variable resource. Analysis should target optimal resolution of the nodal deficits, including consideration of micro-grids in regional locations.

There is also scope for analysing the consequences of possible investment in photovoltaic solar panels and Lithium ion batteries behind the meter for large consumers in Central Queensland, specifically the mines (similar to Sun Metals but without the challenges associated with grid connection currently being experienced by Sun Metals) and the consequences of a change of circumstances at Boyne Smelter.

In summary, analysis of modelling outcomes indicates that transmission really matters. It is therefore recommended that further analysis is required to assess in greater detail the transmission infrastructure that is best suited to meet the transition to high levels of VRE. Consideration could be given to piecemeal transmission augmentation of the lines exhibiting congestion, to consider the effect of each augmentation.

1 Introduction

The author was engaged by The University of Queensland (UQ) Centre for Policy Futures, to undertake research addressing the resiliency of the State of Queensland to achieve the 50% renewable energy target announced by the Queensland State Government by 2030.1

The outline of the report is as follows. In Chapter 2, the key research question governing the research project and associated rationales are provided for the information of interested stakeholders.

In Chapter 3, the wholesale market model that was used in this project is documented, including discussion of the model agents, solution algorithm, modelling assumptions and input requirements.

In Chapter 4, analysis of the "2030 pipeline" scenario is presented, addressing how accelerated retirement of coal generation plant in the NEM together with the existing pipeline of VRE projects might contribute towards attaining 50% renewable energy penetration by 2030.

In Chapter 4, analysis is presented on the results of modelling conducted into a number of selected AEMO ISP scenarios. These are:

- 2030 ISP central scenario;
- 2030 ISP step change scenario applied to 2040 central demand profile; and
- 2040 ISP central scenario.

In all the above modelled scenarios, modelling will investigate the sensitivity of results to specific transmission network augmentation in addition to the different levels and composition of VRE penetration.

In Chapter 5, an assessment of transmission loss outcomes will be presented. This will relate to transmission losses associated with power flow on transmission branches as well as marginal loss factors. The key focus of this research will be on examining key differences in results to generation composition in 2022 and 2030 under the pipeline scenario as well as between two different transmission network scenarios.

In Chapter 6, a discussion of some of the key finding and policy implications of the results reported in Chapters 4 to 5 will be undertaken.

[1] Consult https://www.tiq.qld.gov.au/download/business-interest/invest/19007-MRE-TIQ-Renewables-brochure_v5.pdf for further details.

2 Scope and Objectives of the Electricity Market Modelling Project

2.1 Research Question

Is there an optimal investment strategy for electricity infrastructure, and closure of existing coal generators, to meet Queensland's Renewable Energy Target (QRET) and Queensland's Zero Net Emissions Target (QZNET) whilst advancing regional development?

2.2 Rationale for Research Question

A number of different rationales exist that justify research into the research question identified above.

2.2.1 Complexity of implementation of Queensland's Renewable Energy Target.

Queensland's transition to electricity supplied predominantly from Variable Renewable Energy (VRE) sources is technologically complex. The existing transmission structure has been designed to principally transmit electricity from large coal generators located close to load centres. However, there is a potential conflict in relation to VRE because good VRE resources are likely to be located further away from load centres and even from the existing transmission network. Thus, the ability to take advantage of good wind or solar resources can conflict with the core system design principles of traditional electricity supply.

2.2.2 Existing modelling shortcomings

Modelling Queensland's energy supply to analyse the effect of predicted investment in VRE on the grid is currently undertaken within the Queensland planning and regulatory bureaucracy and preferred consultants at a whole-of-state level. This is because the National Electricity Market (NEM) is designed to resolve optimal power flow and dispatch primarily at a zonal (e.g. state) level. Factors associated with proximity to network, load and generation, especially at an intra-state level, are often estimated annually from historical data and added as static variables in the dispatch optimisation process, if considered at all.

However, intra-regional transmission, generation and load structure of Queensland is considerably more complex and geographically dispersed. A lack of focus on the different nature of a system dominated by VRE could result in the misunderstanding of the technical consequences of high levels of VRE, which, in turn, could serve to derail investment, economic growth and employment in regional Queensland as well as in meeting QRET.

To address these issues, there was a need to utilise a market modelling approach that can overlay the consideration of system cost associated with the wholesale market modelling of generation dispatch and investment on the existing transmission structure at an intra-regional (e.g. nodal) level. This type of modelling can provide more detailed and nuanced understanding of many factors affecting VRE project economics including:

- Re-purposing and estimating transmission losses and Marginal Loss Factors (MLF) linked to real-time inter- and intra-state power flows on transmission branches to determine the real costs of MLF's;
- Assessing transmission network adequacy by identifying and calculating transmission branch congestion in real time and therefore the prospect for volume risk associated with VRE energy spillage if projects become constrained off because of congestion; and
- Assessing VRE spillage and balancing costs associated with the inflexible dispatchability of coal and gas thermal (GT) generation plant in response to variations in VRE output because of these plants':
    - Inability to quickly shut down or start up;

- Limited ramping capability; and
- Operating non-zero minimum stable operating level.

2.3 Research proposal

NEM wholesale market models currently used by consultants, researchers and analysts do not explicitly forecast the cost of intra-regional congestion, MLFs, ramping requirements, storage requirements and coal plant closures to adapt to the installation of large volumes of VRE in more remote locations.

To ensure a managed transition to high levels of VRE, the research undertaken in the project will seek to facilitate knowledge and debate around the transition to reach QRET by focusing on optimal system dispatch cost. This research will seek to model the impact of the role-out of regional based VRE resources based on the existing investment pipeline as well as ISP modelling by AEMO.

The focus of the report will be on assessing:

- Renewable energy production shares as a measure of progress towards achieving the 2030 renewable energy target;
- VRE spillage rates (which affect project volume risk);
- Direction of power flows and congestion on transmission branches; and
- Capacity and energy requirements for system balancing in an environment of high VRE penetration and accelerated coal plant retirements.

3 Wholesale market modelling approach

This chapter discusses the Australian National Electricity Market (ANEM) Model. The ANEM model uses the node and transmission line topology defined in Figures 1 to 6. ANEM is an agent-based model and the agents include demand and supply side participants as well as an Independent System Operator (ISO). The nodes and transmission lines shown in Figures 1 to 6 collectively constrain the behaviour of these agents. The following sections provide an outline of the ANEM model including the principal features of the agents in the model. The formal solution algorithm used to calculate generation production levels, wholesale prices and power flows on transmission lines is also discussed. Practical implementation, data requirements and modelling assumptions are also addressed.

3.1 ANEM model

The methodology underpinning the ANEM model involves the operation of wholesale power markets by an ISO using Locational Marginal Pricing (LMP) to price energy by the location of its injection into, or withdrawal from, the transmission grid. ANEM is a modified and extended version of the American Agent-Based Modelling of Electricity Systems (AMES) model developed by Sun and Tesfatsion (2007a, 2007b). Underpinning the philosophy of this modelling paradigm is to use a realistic representation of the network structure. Important differences between the institutional structures of the Australian and USA wholesale electricity markets are also fully reflected in the modelling undertaken as outlined more fully in Wild, Bell and Foster (2012, Sec. 1).

Key features include realistic transmission network pathways, competitive dispatch of all generation technologies with price determination based upon variable cost and branch congestion characteristics and intra-regional and inter-state trade. Calculation of transmission branch power flows also permits transmission losses to be calculated and allocated to nodes.

A Direct Current Optimal Power Flow (DC OPF) algorithm is used to jointly determine optimal dispatch of generation plant, power flows on transmission branches and wholesale prices. The following unit commitment features are accommodated:

- variable generation costs;
- thermal Megawatt (MW) limits (applied to both generators and transmission lines);
- generator ramping constraints;
- generator start-up costs; and
- generator minimum stable operating levels.

3.2 Principal features of the ANEM model

The ANEM model is programmed in Java using Repast (2014), a Java-based toolkit designed specifically for agent base modelling in the social sciences. The core elements of the model are:

- The wholesale power market includes an ISO and energy traders that include demand side agents called Load-Serving Entities (LSE's) and generators distributed across the nodes of the transmission grid;
- The transmission grid is an alternating current (AC) grid modelled as a balanced three-phase network;
- The ANEM wholesale power market operates using increments of one half-hour;
- The ANEM model ISO undertakes daily operation of the transmission grid within a single settlement system, which consists of a real time market settled using LMP;
- For each half-hour of the day, the ANEM model's ISO determines power commitments and LMP's for the spot market based on generators' supply offers and LSE's demand bids; and

- The inclusion of congestion components in the LMP helps price and manage transmission grid congestion.

3.2.1 Transmission grid characteristics in the ANEM model

The transmission grid utilised in the ANEM model is an AC grid modelled as a balanced three-phase network defined according to the design features outlined in Sun and Tesfatsion (2007a). Figures 1 to 6 outline the transmission grid in the ANEM model, which contains 76 branches and 59 nodes. It combines the Queensland (QLD), New South Wales (NSW), Victorian (VIC), South Australia (SA) and Tasmanian (TAS) state modules. The following interconnectors link the states:

- QNI (line 11) and Directlink (line 14) links QLD and NSW;
- Tumut-Murray (line 36), Wagga-Dederang (line 38) and Buronga-Regional Victoria (line 40) link NSW and VIC;
- Heywood (line 50) and Murraylink (line 56) link VIC and SA; and
- Basslink (line 49) links VIC and TAS.

More generally, the major power flow pathways in the model reflect the major transmission pathways associated with 275, 500/330, 500/330/220, 275 and 220 KV transmission branches in QLD, NSW, VIC, SA and TAS, respectively. Key transmission data required for the transmission grid in the model relate to an assumed base voltage, base apparent power, branch connection and direction of flow information, maximum thermal rating of each transmission branch (in MW's) and estimates of line reactance and resistance parameters (in ohms). Base apparent power is set to 100 MVA, an internationally recognized value.

The direction of flow on a transmission branch (e.g. line) connecting two nodes is defined as 'positive' if the power flows from the lower numbered node to the higher numbered node in Figures 1 to 6. For example, in the case of line 1 connecting Far North Queensland (node 1) and the Ross node (node 2), power flowing from Far North Queensland to Ross on line 1 would have a positive sign (e.g. normal direction flow), whilst power flowing on line 1 from Ross to Far North Queensland would have a negative sign. The latter type of power flow is termed 'reverse' direction flow.

3.2.2 Demand-side agents in the ANEM model: LSE's

A LSE is an electric utility that has an obligation to provide electrical power to end-use consumers (residential, commercial or industrial). The LSE agents purchase bulk power in the wholesale power market each day to service customer demand in the downstream retail market, thereby linking the wholesale power market and retail market. We assume that downstream retail demands serviced by the LSE's exhibit negligible price sensitivity, reducing to daily supplied load profiles which represents the real power demand (in MW's) that the LSE has to service in its downstream retail market for each half-hour of the day. As such, LSE's are modelled as passive entities who submit daily load profiles to the ISO without strategic considerations (Sun & Tesfatsion 2007b).

ANEM requires half-hourly regional load data. Details of the nodal demand data compilation process are presented in Section 3.5 of this report.

Figure 1: Stylised topology of QLD transmission lines and Load Serving Entities

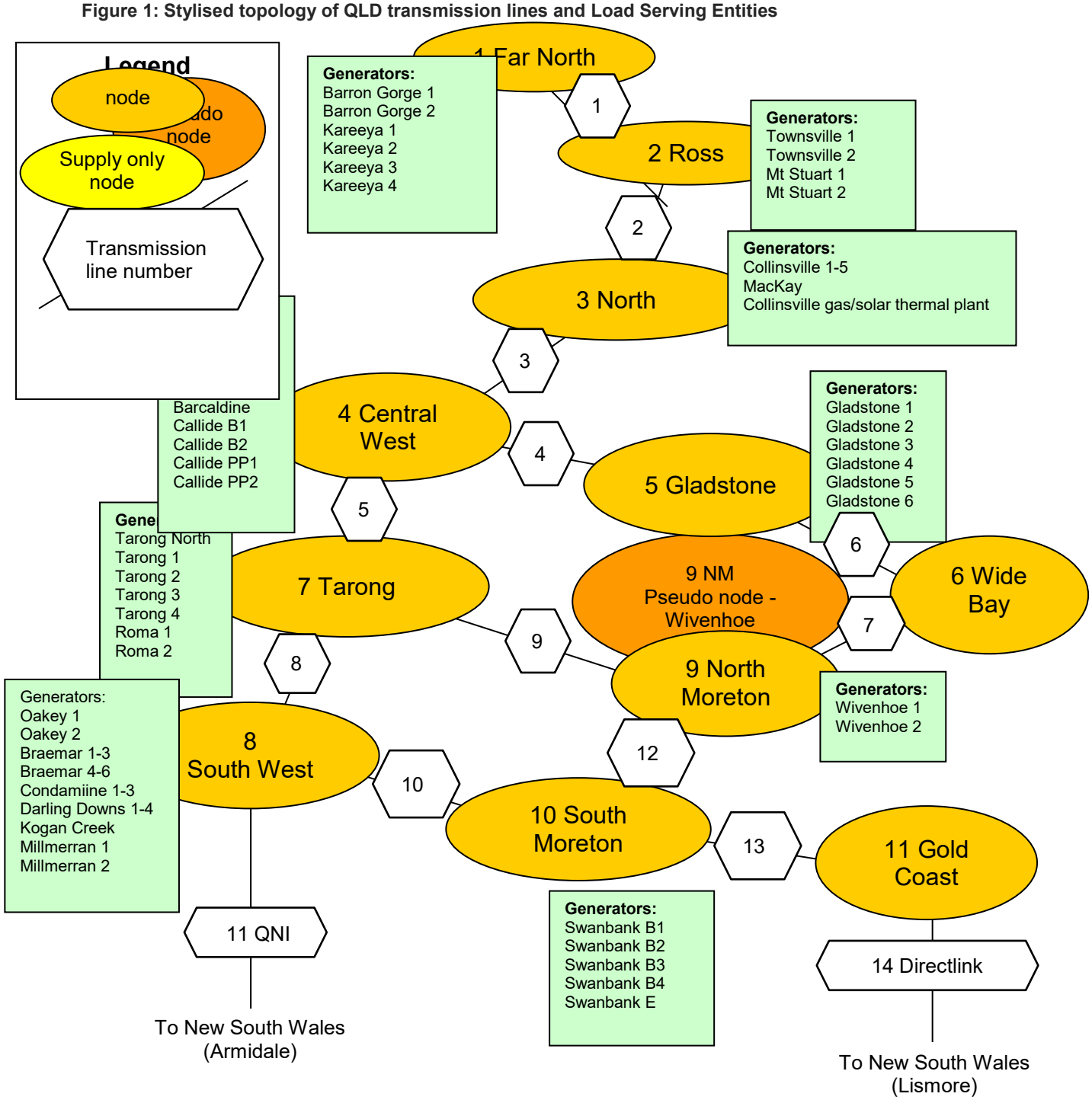

Figure 2: Stylised topology of NSW transmission lines and LSE

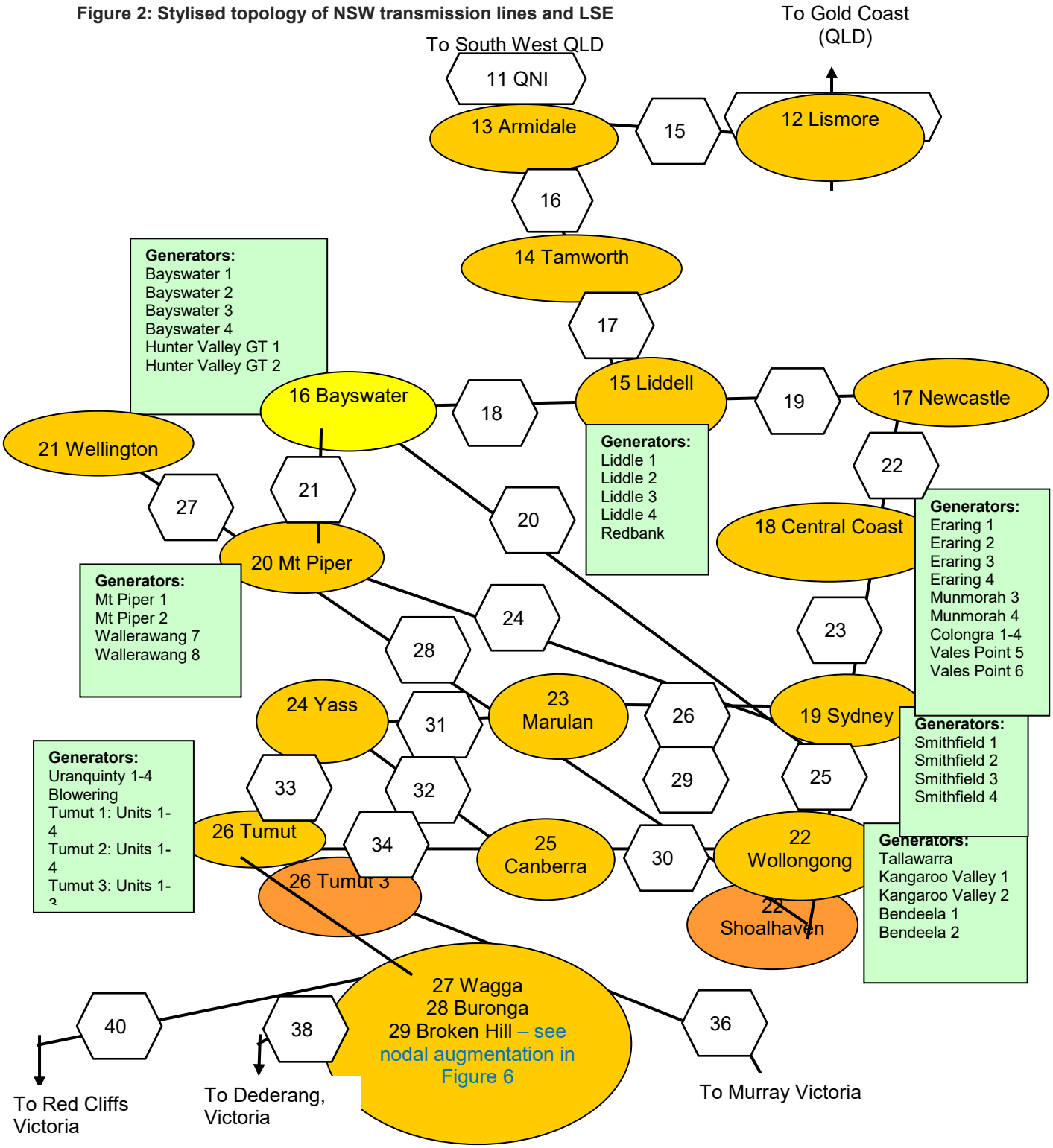

Figure 3: Stylised topology of VIC transmission lines and Load Serving Entities

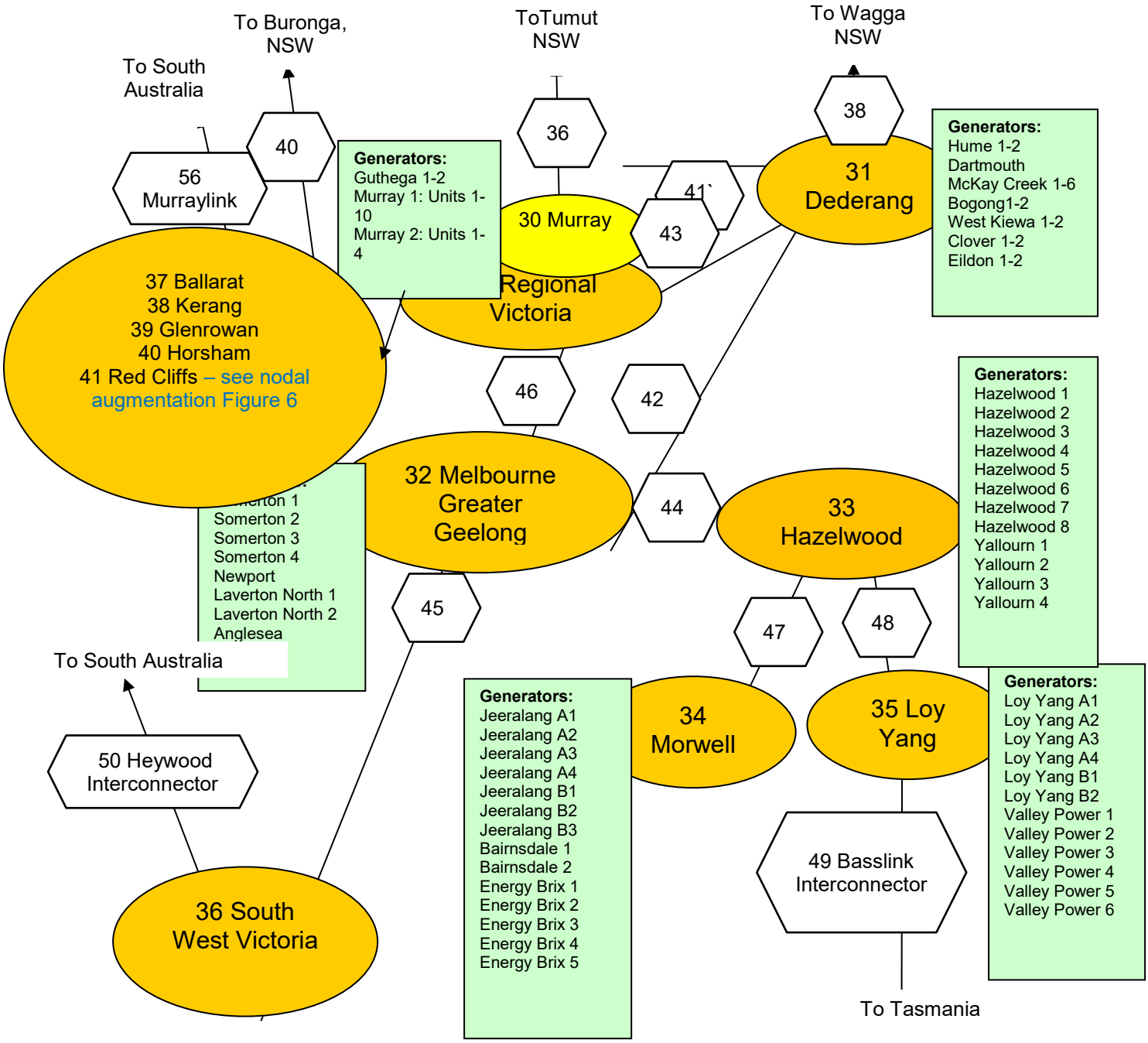

Figure 4: Stylised topology of SA transmission lines and Load Serving Entities

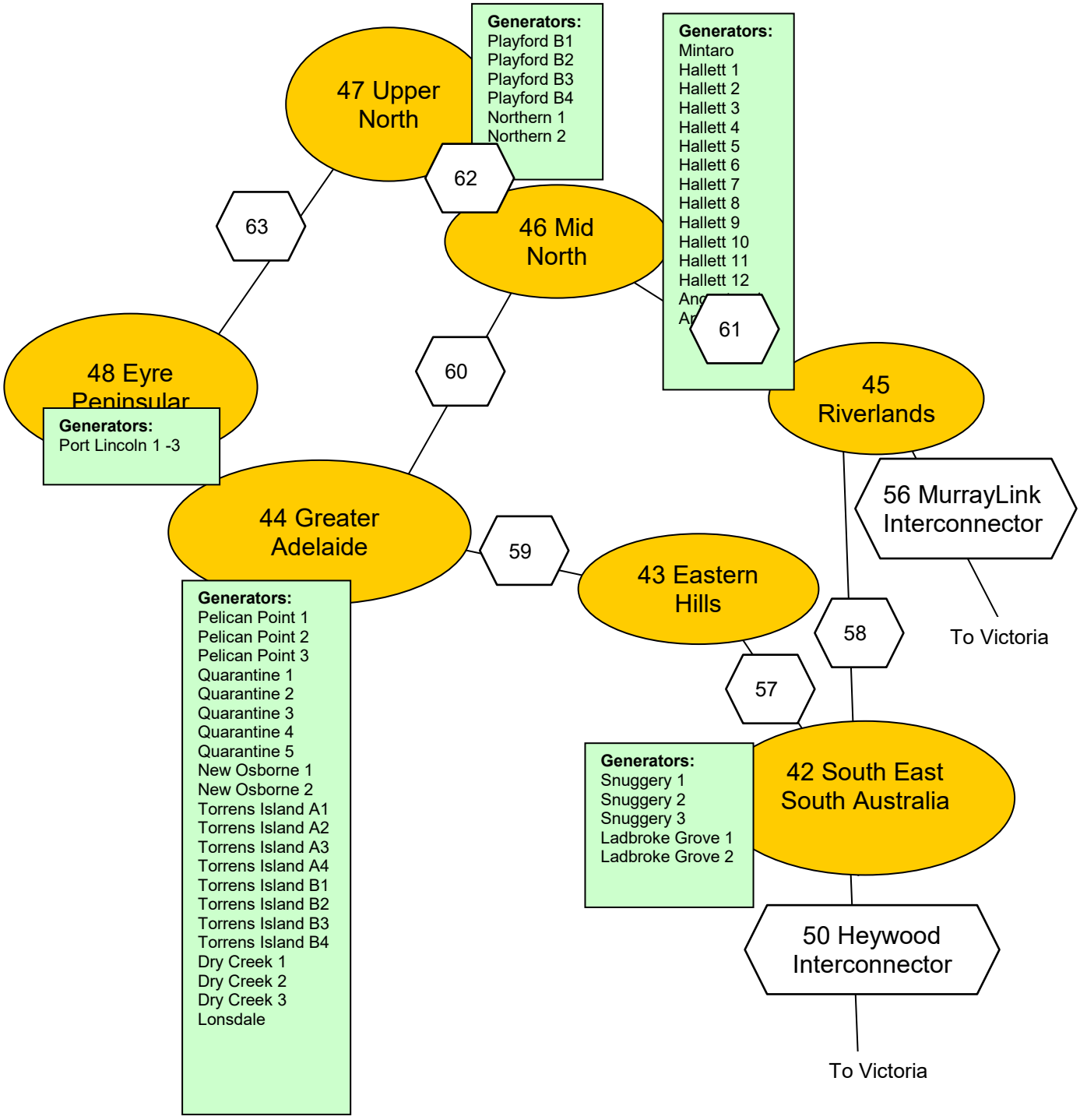

Figure 5: Stylised topology of TAS transmission lines and Load Serving Entities

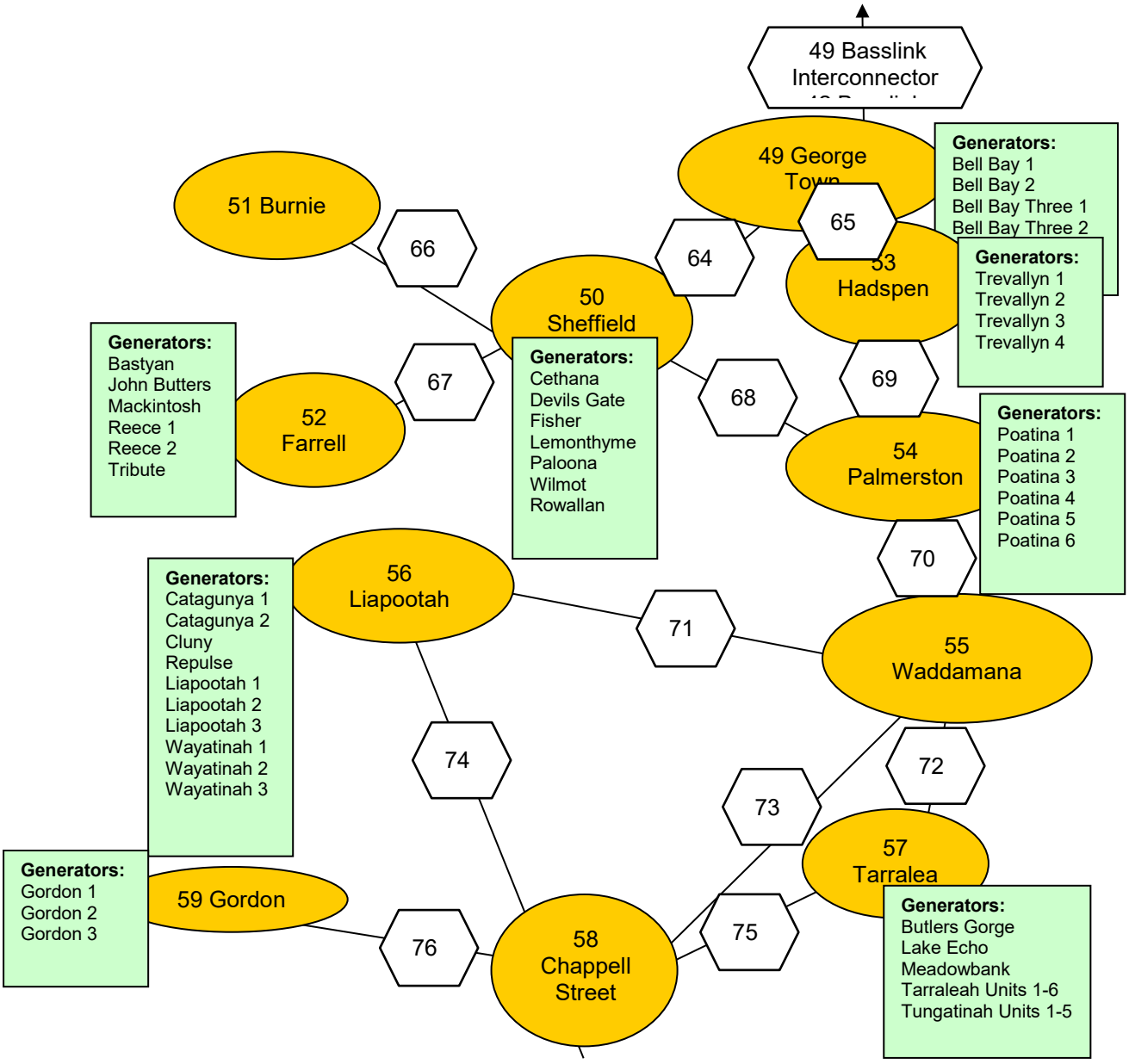

Figure 6: Stylised topology of amended nodal Tumut/Riverina region of NSW and Regional Victoria

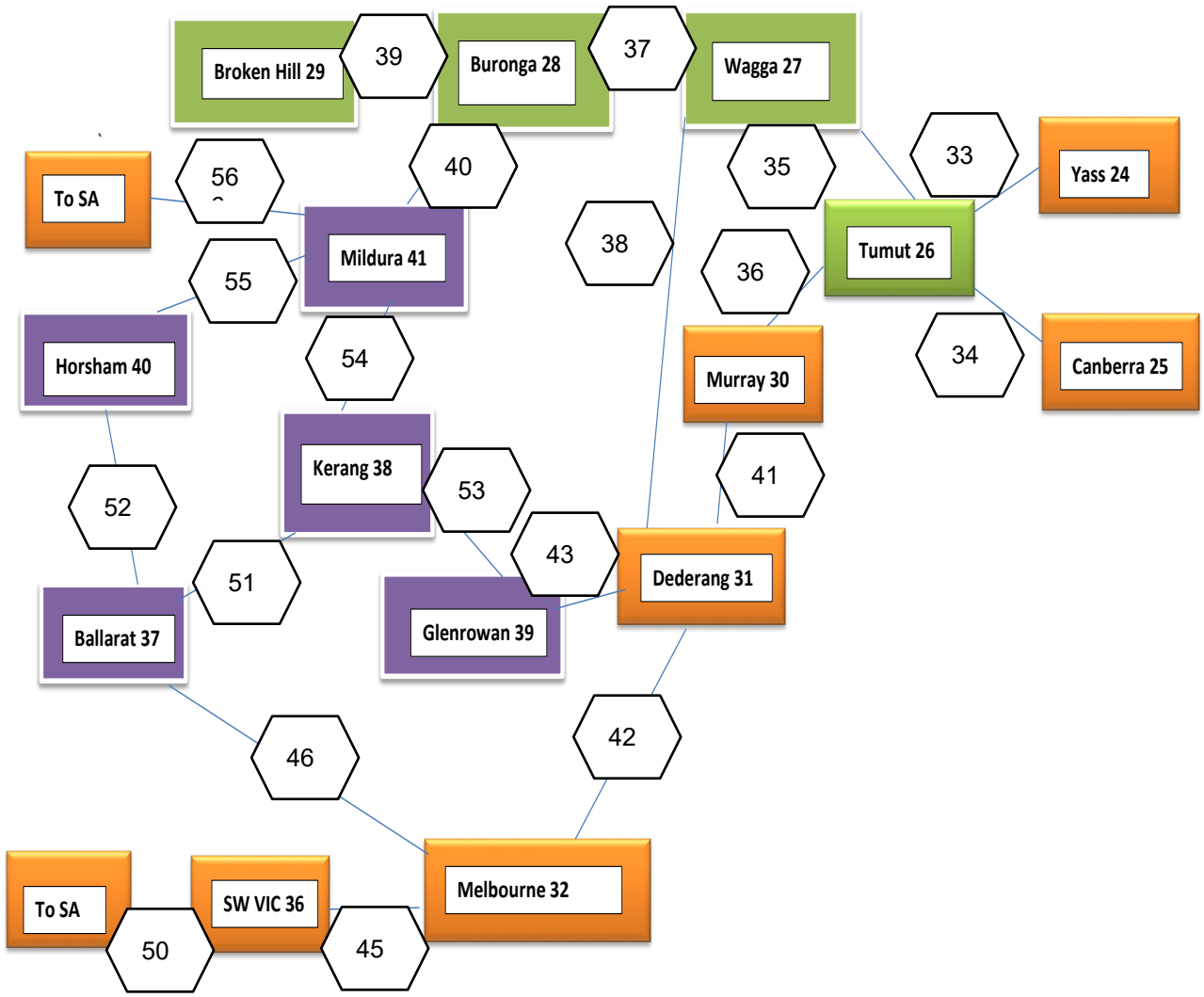

3.2.3 Supply-side agents in the ANEM model: generators

Generators are assumed to produce and sell electrical power in bulk at the wholesale level. Each generator agent is configured with a production technology with assumed attributes relating to feasible production interval, total cost function, total variable cost function, fixed costs and a marginal cost function. Depending upon plant type, a generator may also have start-up costs. Each generator also faces MW ramping constraints that determine the extent to which real power production levels can be increased or decreased over the next half-hour within the half hourly dispatch horizon. Production levels determined from the ramp-up and ramp-down constraints must also fall within the minimum and maximum thermal MW capacity limits confronting each generator.

3.3 DC OPF solution algorithm used

Optimal dispatch, wholesale prices and power flows on transmission lines are determined in the ANEM model by a DC OPF algorithm developed in Sun and Tesfatsion (2007a). This algorithm involves representing the standard DC OPF problem as an augmented strictly convex quadratic programming (SCQP) problem, involving the minimization of a positive definite quadratic form subject to linear equality and inequality constraints. The augmentation entailed utilising an objective function that contains quadratic and linear variable cost coefficients and branch connection coefficients. The solution values are the real power injections and transmission branch flows associated with the energy production levels for each generator and voltage angles for each node. This structure differs significantly from linear programming algorithms in that transmission parameters are included directly in the objective function as well as in equality and inequality constraints of the optimisation problem. Thus, power flows are also optimised within the model solution.

The Mosek (2014) optimisation software that exploits direct sparse matrix methods and utilises a convex quadratic programming algorithm based on the interior point algorithm is used to solve the DC OPF problem. Equation 1 below shows ANEM's implementation of the Mosek DC OPF algorithm inequality constraints.

The ANEM model solves the following optimisation for every half-hour. Equation 1(a) shows the objective function that minimises real-power production levels P_{Gi} for all generators i = 1,…,I and voltage angles δ_k for all transmission lines k = 2,..,K subject to the constraints in Equation 1(b), 1(c) and 1(d).

Equation 1:ANEM's objective function and constraints

(a) Objective function: Minimise generator-reported total variable cost and nodal angle differences

$$\sum_{i=1}^{I}\left[A_i P_{G_i} + B_i P_{G_i}^2\right] + \pi\left[\sum_{I_m \in BR} \delta_m^2 + \sum_{km \in BR,\, k \geq 2} \left[\delta_k - \delta_m\right]^2\right],$$

where:
i = generator number
P_{Gi} = real power (MW) production level of generator i
k = transmission line number
δ_k = phase angle for transmission line k

(b) Constraint 1: Nodal real power balance equality constraint

$$0 = PLoad_k - PGen_k + PNetInject_k$$

where:

$$PLoad_k = \sum_{j \in J_k} P_{L_j}$$ (i.e. aggregate power take-off at node k, e.g. demand)

$$PGen_k = \sum_{i \in I_k} P_{G_i}$$ (i.e. aggregate power injection at node k, e.g. generation)

$$PNetInject_k = \sum_{km \text{ or } mk \in BR} F_{km}$$

$$F_{km} = B_{km}[\delta_k - \delta_m]$$

(i.e. real power flows on branches connecting nodes 'k' and 'm')

$k = 1, \ldots, K$

$\delta_1 \equiv 0$

(c) Constraint 2: Transmission line real power thermal inequality constraints

$F_{km} \geq -F_{km}^{UR}$, (lower bound constraint: reverse direction MW branch flow limit)

$F_{km} \leq F_{km}^{UN}$, (upper bound constraint: normal direction MW branch flow limit),

where:

$km \in BR$

(d) Constraint 3: Generator real-power production inequality constraints

$P_{G_i} \geq P_{G_i}^{LR}$, (lower bound constraint: lower half-hourly MW thermal ramping limit)

$P_{G_i} \leq P_{G_i}^{UR}$ (upper bound constraint: upper half-hourly MW thermal ramping limit),

where:

$P_{G_i}^{LR} \geq P_{G_i}^{L}$,

(lower half-hourly thermal ramping limit $\geq$ lower thermal MW capacity limit)

$P_{G_i}^{UR} \leq P_{G_i}^{U}$

(upper half-hourly thermal ramping limit $\leq$ upper thermal MW capacity limit)

$i = 1, \ldots, I.$

U and L denote upper and lower limits, A_i and B_i are linear and quadratic cost coefficients from the generator's variable cost function. δ_k and δ_m are the voltage angles at nodes 'k' and 'm' (measured in radians). Parameter π is a positive soft penalty weight on the sum of squared voltage angle differences. Variables F_{km}^{UN} and F_{km}^{UR} are the (positive) MW thermal limits associated with real power flows in the 'normal' and 'reverse' direction on each connected transmission branch km ∈ BR.

The linear equality constraint refers to a nodal balance condition, which requires that, *at each node*, power take-off (by LSE's located at that node) equals power injection (by generators located at that node) and net power transfers from other nodes on 'connected' transmission branches. On a *node-by-node* basis, the shadow price associated with this constraint gives the LMP (e.g. regional wholesale spot price) associated with that node. Accounting for power flows in the equality constraints of the DC OPF algorithm allows the incorporation of congestion components in regional wholesale spot prices, which can produce divergence in regional spot prices associated with congestion on intra-state transmission branches, thus providing local price signals for investment in network and non-network augmentation options. Importantly, given the network structure outlined in Figures 1 to 6, these regional spot prices will be intra-state regional spot prices, thus deviating significantly from zonal based regional reference prices estimated by other wholesale market models.

The linear inequality constraints ensure that real power transfers on connected transmission branches remain within permitted 'normal' and 'reverse' direction thermal limits and the real power produced by each generator remains within permitted lower and upper thermal MW capacity limits while also meeting MW ramp up and ramp down generator production limits.

3.4 Modelling transmission losses

Two transmission loss concepts were calculated in this project. The first concept refers to transmission losses on transmission branches associated with power flows on those branches determined by the DC OPF solution. Within this context, these transmission losses are calculated for each transmission branch using the methodology outlined in (AEMO, 2012, Section 5). That is, transmission losses are calculated by multiplying the square of the power flow on each transmission branch determined by the DC OPF solution by that branch's line resistance. Losses are allocated to nodes connecting each respective transmission branch by two alternative methods. The first involves allocating transmission losses to the receiving end node as an additional fictitious nodal demand. This method necessarily takes account of the direction of power flow to determine the receiving end node – that is, the node that power flows towards on the transmission branch. The second method involves allocating transmission loss as additional fictitious nodal demands to each of the connected nodes at each end of the transmission branch on a 50:50 basis. The key impact of this operation is to ensure that enough power is generated by generators to both transmit (e.g. cover transmission losses) and meet demand offtake at each node.

Transmission losses will depend on two different factors:

- Line resistance which declines as the voltage level of the transmission branches increases; and
- Directly with the square of the magnitude of power flow on transmission branches. Formally, this relation can be expressed (AEMO, 2012) as:

$$TL = I^2 \times R \quad \text{... (1)}$$

where TL represents transmission losses, I represents current and R denotes line resistance. Equation (1) is implemented in the modelling to calculate transmission losses as:

$$TL = P^2 \times R \quad \text{... (2),}$$

assuming a proportionality factor of unity in terms of equation (iv) of (AEMO, 2012, Section 5) and where P represents three phase active power. For reporting purposes, however, we apply equation (ii) in (AEMO, 2012, Section 5), employing their assumptions that $V = 1, Q = 0$ to derive:

$$I = \frac{\sqrt{P^2}}{\sqrt{3}} \quad \text{... (3).}$$

After squaring and substituting this equation into equation (1):

$$Tl = \left(\frac{1}{\sqrt{3}}\right)^2 \times \left(\sqrt{P^2}\right)^2 \times R \quad \text{... (4),}$$

which simplifies further to:

$$Tl = 0.3333 \times R \times P^2 \quad \text{... (5).}$$

Compared to (2), equation (5) applies a proportionality factor of 0.3333 and produces results consistent with reported losses by Transmission Network Service providers (TNSP) like Powerlink.

The second loss concept is marginal losses. Marginal losses are partial derivatives relating to the incremental change in transmission losses to an incremental net injection of power at a specific node. This is calculated given an existing solution from the DC OPF solution and typically involves adding one extra MW of load at a node and then numerically calculating the change in transmission losses that result from this incremental nodal injection. The change in transmission losses are defined relative to the transmission losses associated with the existing solution. For further details consult (AEMO, 2012, Section 5).

Numeric partial derivatives are typically calculated by applying an extremely small constant positive and negative increment and calculating the change in the variable of interest (e.g. transmission losses) under both increment and de-incrementing operations. Let the increment/de-increment quantity be represented by Δx. Define the resulting change in the variable of interest to be Δy. Then the partial derivative can be calculated numerically as:

$$PD = \frac{(\Delta y^{+} - \Delta y^{-})}{(2 \times \Delta x)}, \ldots (6)$$

where Δy^{+} is the change in y associated with a positive increment to x, Δx and Δy^{-} is the change in y associated with a negative increment to x, $(-\Delta x)$. In the current context, Δy is the change in transmission losses and Δx and $(-\Delta x)$ are positive and negative increments to nodal demand.

Assume that beq_i is the nodal demand at node i and $genInject_i$ is nodal generation at node i. The incrementing/de-incrementing operations are applied as:

$$beq_i^{*} = beq_i \pm 0.01\, pu, \ldots (7)$$

for each node i, holding nodal demand and generation fixed at all other nodes. The change in demand of $\pm 0.01\, pu$ is calculated by applying ± 1 MW of additional demand which is converted to a per unit basis by dividing by base apparent power which has a value of 100, producing the $0.01\, pu$ demand increment listed in equation (7).

For each incrementing and de-incrementing operation, a new net nodal injection vector is calculated for all nodes as the difference between $genInject_i$ and the new perturbed demand vector for all i:

$$netInject_i = genInject_i - beq_i^{*}, \ldots (8)$$

recalling that apart from node i at which the demand incrementing is being applied, all other nodal generation and demand values will be unchanged from their original values for the purpose of calculating marginal losses.

The solution method involves calculating new real power flow results using the shift matrix (Sun and Tesfatsion, 2007, footnote, 15, p. 20), given by:

$$S = D \times Adj \times BInv, \ldots (9)$$

where D is the diagonal admittance matrix and Adj is the adjacency matrix. $BInv$ is the bus admittance matrix with the row and columns associated with the slack bus removed. This matrix is then inverted and then a row and column of zeros are added back into the inverted matrix at the row and column corresponding to the slack bus. In this project, the slack bus corresponds to the Loy Yang node (see Figure 3).

Once S is calculated, the new power flow vector can be calculated from:

$$PF = S \times netInject, \ldots (10)$$

(Sun and Tesfatsion, 2007, footnote, 15, p. 20). Note that PF denotes a vector of power flows and $netInject$ is the new net injection vector associated with the perturbed demand vector defined in equation (7). Once PF is calculated, transmission losses can be calculated using equation (2) and then the change in branch transmission losses can be calculated according to equation (6) for the incrementing/de-incrementing operations outlined in (7). Recall that (6) corresponds to partial derivatives and as such, in the current context, will calculate marginal losses. Then the calculated branch marginal losses can be allocated to nodes according to a commonly applied allocation methodology.

Once the marginal loss has been determined, Marginal Loss Factors (MLF) can be calculated simply as one plus the marginal loss. The allocation methodology applied in relation to the marginal loss calculations is to allocate the marginal losses to the sending node. This approach was adopted because power flow on a transmission branches commences at the sending node end of the

transmission branch with power flowing over the transmission branch to the receiving end node and, in doing so, incurring the transmission loss.

It is notable that the allocation of marginal losses differs markedly from how transmission losses are allocated in the DC OPF model as additional fictitious nodal demands. In the latter case, these additional nodal demands are allocated either to the receiving node or on a 50:50 basis to both the receiving and sending nodes. This difference reflects different objectives associated with allocation of transmission losses and marginal losses. The former is to ensure that nodal demand is completely satisfied while the latter is to more fully reflect the nodal location from which power flow commences and from where the transmission losses are incurred.

3.5 Methodology and data sources underpinning state and nodal demand traces to be used in the modelling

Application of a nodal model requires demand traces for each node within the network structure. This section will document how these nodal demand traces were derived.

3.5.1 Background

The source state-based demand traces were compiled from demand traces produced by AEMO for the 2018-19 Integrated System Planning (ISP) process. The projection horizon is half-hourly data defined over the period beginning 12.30 am on 1 July 2019 to 12.00 am on 30 June 2050. Further details about the AEMO forecast methodology used to generate this source data is documented in AEMO (2019a).

The demand traces are compiled for each NEM region (e.g. state) and according to different target demand concepts relating to maximum summer and winter demands, minimum demand (all calculated relative to a defined 'Probability-Of-Exceedance (POE) statistical threshold) and annual energy (consumption). The POE thresholds used relate to average (e.g. POE50) and high (e.g. POE10) thresholds. In this context, 'POE50' signifies a fifty percent chance that the POE50 demand value would be exceeded. In contrast, POE10 signifies that there is only a ten per cent chance that the POE10 demand value would be exceeded.

In compiling half-hourly demand projections, a number of different representative historical years are used encompassing the period 2011-2019. Included in each of these reference years are residential and commercial demand impacts associated with underlying weather patterns, economic conditions, observed uptake rates of newer technologies (e.g. distributed solar PV, energy storage, energy efficiency savings and electrical vehicles) as well as network losses prevailing in each respective historical reference year. Forecasts of technology up-take and adoption traces and climate change effects (e.g. via heating and cooling degree days) for each financial year in the projection period (2019-20 to 2049-50) was determined by AEMO.[2]

In calculating the demand traces, the key demand concept utilised is operational demand sent-out (OPSO). Sent-out output refers to the total energy generated by each generator less auxiliary power used internally within the power production process. More generally, this demand definition refers to electricity used by residential, commercial and larger industrial users as supplied to the grid on a 'sent-out' basis by scheduled, semi-scheduled and non-scheduled generation over 30 MW. This demand concept, however, excludes generation supplied by non-scheduled generation less than 30 MW and exempt generation. However, output of some exempt generation is included in the calculation of operational demand including Yarwun Power Station, Mortons Lane and Yalock South

[2] Account for energy efficiency savings are incorporated into econometric estimates of residential and commercial demand as a consumption driver but is treated differently to distributed solar PV, energy storage and electric vehicles in that separate data traces were not produced for it by AEMO when compared with the other demand drivers mentioned above.

wind farms, Hughenden and Longreach solar farms and all non-scheduled diesel generation plant in South Australia.

The principal methodology used by AEMO to generate half-hourly forecast demand traces was to use a constrained optimisation algorithm to scale up historical reference year demand to match pre-determined energy and demand targets in forecast years. A two-pass methodology was used to calculate the half-hourly demand traces (AEMO, 2019a, Chapter 6). The first pass involved 'growing' each respective historical reference year's OPSO demand to a pre-determined target corresponding to a target year in the projection period 2019-20 to 2049-50. A growth (scaling) algorithm sought to preserve seasonal, weekly and intra-day demand patterns. In calculating this first run pass, AEMO's forecast of technology up-take during the projection interval was excluded from both the underlying energy and demand target. This forecast was termed 'OPSO-Lite' and can be interpreted as sent-out operational demand that has been 'cleaned' to remove atypical demand events as well as the impact of the following technologies (AEMO, 2019a, Section 6.2):

Rooftop solar PV;

- Non-scheduled PV;
- Energy storage systems;
- Electric vehicles; and
- Coal Seam Gas (CSG) in Queensland.

The second pass runs re-imposes AEMO's forecasts of technology up-take during the projection period (including CSG demand in Queensland) and reconciled these new sets of forecasts to some pre-determined target value. These forecasts are termed 'OPSO' forecasts (AEMO, 2019a, Section 6.3)[3].

3.5.2 Derivation of state demand traces used in modelling

In considering the demand traces to include in the modelling, the demand traces chosen were related to AEMO's neutral scenario. Key facets of this scenario include:

- Neutral growth in consumption and demand;
- Moderate economic growth and DER uptake;
- Generation expansion planning determined by central estimates of technology cost reductions; and
- Existing market and policy settings.

See (AEMO, 2018a, Section 2.7.1) for further details.

For each NEM region (e.g. state) and all historical reference years (encompassing years 2011-2019), two representative half-hourly demand profiles were extracted based on the following high and average demand scenarios:

High demand:

- POE10 OPSO.

Average demand:

- POE50 OPSO.

For all NEM states (e.g. 5 states), 9 reference years and 2 demand scenarios identified above, this gives a total of 90 individual half-hourly demand traces, each defined over the interval commencing at 12.30 am on 1/7/2019 12.30 am and ending at 12.00 am on 30/6/2050. In compiling this data, the additional day corresponding to February 29 associated with leap years was removed. Hence, each year corresponds to a 365-day interval. In this case, a half-hourly demand trace over the forecast interval 2019-2020 to 2049-50 would encompass 543,504 data points.

For each state and each of the two demand scenarios listed above, a representative demand trace was calculated as the maximum of the average or median of each half hour of all 9 reference year

[3] The demand trace data is available at: https://www.aemo.com.au/Electricity/National-Electricity-Market-NEM/Planning-and-forecasting/Integrated-System-Plan/2019-Integrated-System-Plan/ISP-database.

demand traces. This implies taking the average and median values for a specific demand scenario and state over the nine available reference year's demand traces, conducted over each successive data point in the associated 543,504 sets of data points in the reference year's demand traces. In performing these operations, the calculated representative demand trace would encapsulate averaging performed over different weather patterns, climate change trends, economic activity and technology up-take relating to: (1) the historical reference year demand traces; and (2) technology up-take and climate change assumptions of AEMO applicable to the 2019-20 to 2049-50 forecast interval.

3.5.3 Derivation of nodal demand traces used in modelling

The ANEM wholesale electricity market model used in this project is a nodal based model. The model's current nodal structure contains 60 separate nodal demand entities, three of which are pseudo nodal demands to accommodate pumping actions by pumped hydro plant located in Moreton North node (Wivenhoe Power Station), Wollongong node (Shoalhaven Scheme) and Tumut node (Tumut 3 Power Station). Nodal demands are calculated by allocating the state based aggregate demand data to various regions (nodes) within each respective state.

Historically, two different methods were utilised to determine nodal demand allocation shares in different states in the NEM in ANEM. For Queensland, New South Wales and Tasmania, supplied demand data from Powerlink, Transgrid and Transend transmission companies was used to determine nodal demand allocations in those states. In the cases of Victoria and South Australia, summer and winter terminal station demand forecasts published by Vencorp (latter AEMO) and Electranet were used in conjunction with spline-based interpolation methods to determine nodal demand allocation shares for Victoria and South Australia. The state-based nodal shares determined by both methods summed to unity, by construction, and the nodal based demands were calculated by multiplying each respective nodal share by the relevant state aggregate demand time series data. For this project the aggregate state demand time series data will be the representative AEMO ISP demand traces discussed in the previous section.

The nodal demand shares to be utilised in the modelling typically reflect the composition of electricity demand in different regional areas within each in the NEM. Some nodes have a heavy baseload consumption component such as Gladstone and South West Queensland (SWQ) Queensland nodes, Newcastle (New South Wales), South West Victoria, Upper North South Australia and George Town (Tasmania) reflecting baseload electricity consumption associated with aluminium smelting, mining, CSG processing and steel making. Large residential centres including nodes based around state capital cities have a significant mixture of residential, commercial and industrial demand whilst rural communities tend to have lower demand, reflecting smaller residential and commercial populations and economic activity.

In general, the shares have tended to remain reasonably constant notwithstanding some emergent volatility in both average and peak demand over the last decade associated with swings in economic activity, improved energy efficiency and emergent technologies like distributed solar PV. That is, these trends whilst affecting both average and peak demand, have tended to be spread in line with existing demand shares across different regions in the NEM. Two exceptions however have arisen. First, there has been a noticeable increase in demand in South West Queensland associated with development of the CSG industry in Queensland. Second, emergent vulnerability of aluminium smelting to increases in wholesale electricity prices and potential closures of legacy coal-fired generation plant or PPA arrangements with such plant in the NEM. Both factors can adversely affect the profitability of aluminium smelting and can potentially change nodal demand shares in significant ways if the smelters were to subsequently close. A case in point, in the latter context, relates to the viability of the Boyne smelter in Gladstone Queensland[4]. Additional methods were needed to

[4] Another case was the closure of the Port Henry smelter in Victoria in 2014. Hourly baseload electricity consumption of this smelter was estimated to be 360 MWh for annual output of 185,000 tonnes per year.

accommodate the impacts on nodal demand of CSG and aluminium smelting in Queensland. These are discussed in the next section.

3.5.4 Methodology used to calculate nodal demand for Gladstone and South West Queensland Nodes

Particular care was exercised in updating nodal demand estimates for Gladstone and South West Queensland (SWQ) nodes to reflect recent changes occurring in the operation of Boyne Smelter in Gladstone during 2017 and also the ramp up and plateau of CSG gas production in Surat and Bulli zones of SWQ to levels consistent with supply rates required to supply natural gas to LNG processing facilities at Gladstone.

In the latter context, energy for LNG production in Gladstone itself is accomplished by using natural gas and not from electricity drawn from the main electricity grid. Rather, mains electricity is primarily used for field and plant gas compression and groundwater pumping activities located in SWQ locations where the operational CSG fields and plant suppling natural gas to LNG processing in Gladstone are located.

CSG demand data was sourced from AEMO 2019 ISP data for the period 2020 to 2050. This data was forecast annual consumption (GWh) associated with the neutral ISP scenario. Average hourly MWh values were calculated assuming a 365-day year with the additional 29th of February day being excluded for leap years. This compilation assumes that CSG demand serving gas processing for LNG export activity is essentially a baseload demand that is met 24 hours a day, 365 days in each year in the time interval being investigated. Values for 2018 and 2019 were calculated using earlier data published by AEMO[5] for annual CSG electricity consumption, but back-cast from the 2020 annual consumption values provided in the 2019 ISP dataset.

The GWh annual consumption data and calculated average hourly MWh values used for SWQ CSG demand are listed in Table 1.

Table 1. CSG electricity forecasts for SWQ nodal region

Time	Annual CSG Electricity Consumption	Average Hourly Demand	Upper Hourly Demand Bound
	GWh	MWh	MWh
2018	5762.27	657.79	1229.75
2019	6311.06	720.44	1191.67
2020	6402.52	730.88	1206.75
2021	6461.44	737.61	1235.55
2022	6512.17	743.40	1219.20
2023	6562.02	749.09	1202.49
2024	6611.95	754.79	1202.49
2025	6662.00	760.50	1181.40
2026	6670.23	761.44	1181.40
2027	6678.55	762.39	1144.32
2028	6686.89	763.34	1144.32
2029	6677.77	762.30	1144.32
2030	6677.38	762.26	1144.32

SWQ nodal demand data was calculated using the original ANEM SWQ nodal demand data and then adding each respective year's average MWh CSG baseload demand values reported in column 3 of Table 1 to the source half-hourly ANEM nodal SWQ demand data. The original SWQ nodal data primarily reflected demand associated with the Middle Ridge terminal station servicing Toowoomba

[5] These earlier estimates were determined from eye-balling GWh neutral scenario values contained in the Figure in the AEMO report listed at: https://www.aemo.com.au/Electricity/National-Electricity-Market-NEM/Planning-and-forecasting/NEM-Electricity-Demand-Forecasts/Electricity-Forecasting-Insights/2017-Electricity-Forecasting-Insights/Key-component-consumption-forecasts/Business-consumption/CSG.

and Darling Downs communities with some allowance for ramp up allocation for CSG developments prior to 2015. After 2015, significant expansion in demand was observed reflecting accelerated ramp up and plateauing of CSG supply.

In compiling the SWQ nodal demand data, allowance was also made for upper bounds on demand associated with Powerlink maximum transmission delivered zonal demand forecasts outlined in (Powerlink, 2019). Those for the SWQ node are listed in column 4 of Table 1. For each year, half-hourly demand estimates for SWQ cannot exceed the upper bound values for each respective year listed in column 4 of Table 1. These upper bound values were calculated by multiplying the maximum summer and winter transmission delivered demand values reported in Tables 2.16 and 2.18 by the average ratio of zonal maximum delivered demand values reported in Table 2.13 of (Powerlink, 2019). The aggregated SWQ bounds were calculated as the sum of maximum transmission delivered demand for the Surat and Bulli zones and 85% of the SW Queensland zone.[6] The higher of the calculated summer or winter maximum transmission delivered demand values was chosen as the upper bound as reported in column 4 of Table 1.

The original ANEM Gladstone nodal demand data was based upon demand estimates for this region over the period 2007-2015. Given the heavy contributions of aluminium and alumina smelting in this node, the underlying nodal demand for Gladstone has a high baseload content. During 2017, the operators of the Boyne Smelter in Gladstone reduced hourly electricity consumption by 150 MWh following a sharp rise in wholesale electricity prices. This 150 MWh value represented the amount of electricity used at the smelter that was not under a long term PPA. Therefore, the Gladstone nodal demand was updated by subtracting 150 MW from the source ANEM half-hourly nodal demand data for the Gladstone node.

In compiling the nodal demand data for Gladstone, a lower half-hourly bound of 980 MW was imposed, equalling the baseload hourly electricity demand of Boyne Smelter (810 MWh), Queensland Alumina (90 MWh) and Yarwun Alumina (80 MWh). Furthermore, as with the case of the SWQ nodal demand, an upper bound MW value was also imposed using the same methodology that was used in relation to SWQ, except now utilising the Gladstone zonal data instead of Surat, Bulli and SW Queensland zonal data in (Powerlink, 2019). This upper bound data is presented in column 2 of Table 2. As such, for each year, half-hourly demand estimates for Gladstone cannot exceed the upper bound values for each respective year listed in column 2 of Table 2.

Table 2. Upper Bound Demand Limits for Gladstone

Time	Upper Hourly Demand Bound
	MWh
2018	1146.08
2019	1148.16
2020	1107.25
2021	1104.48
2022	1105.52
2023	1108.64
2024	1110.72
2025	1111.76
2026	1112.80
2027	1112.80
2028	1113.84
2029	1113.84
2030	1113.84

[6] Note that the remaining 15% of the Powerlink SW Queensland zonal demand is allocated to the Tarong node.

3.5.5 Methodology used to account for electricity demand associated with aluminium smelting in other ANEM nodes

Aluminium smelting is also an important driver of electricity demand in the following nodes: Newcastle (Tomago Smelter); South West Victoria (Portland Smelter) and George Town (Bell Bay Smelter). The approach taken was to ensure that the nodal demands could not fall below the underlying baseload MWh electricity demand estimates associated with the various smelters listed in Table 3.

Table 3. Nodal location and baseload consumption of Aluminium Smelters

Smelter	State	Node	Baseload demand (MWh)
Boyne	QLD	Gladstone	810
Tomago	NSW	Newcastle	850
Portland	VIC	South West VIC	594
Bell Bay	Tasmania	George Town	355

3.6 Practical implementation

The solution algorithm employed involves applying a 'competitive equilibrium' solution. This means that all generators submit their true marginal cost coefficients without strategic bidding. As such, the analytic framework is a conventional DC OPF analysis with generator supply offers based upon Short Run Marginal Cost (SRMC) coefficient. In this context, nodal LMP's would reflect their conventional definition of defining the incremental cost of satisfying an additional MW of demand at each node.

3.6.1 Scheduled O&M

An extensive and aggressive set of assumptions was made about scheduled outages of baseload generation plant, namely Coal and Natural Gas Combined Cycle (NGCC) or Gas Thermal (GT) plant. The assumed profile posits scheduled O&M on each turbine of these plant on a *yearly* basis to ensure their highest degree of reliability over the peak summer period (December to February). On an annual basis, the targeted periods for O&M are Spring, Winter and Autumn, thereby targeting periods when demand will be lower compared to summer. This schedule can also be viewed as a mechanism for capacity withdrawal during periods of lower demand. The scheduled O&M profiles are listed in Table 1.

Table 1: Generator scheduled outage profile

Generator	Scheduled O&M
Queensland	
Yabulu	August
Stanwell 1	June-July[7]
Stanwell 2	August
Stanwell 3	October
Stanwell 4	September
Callide B 1	July
Callide B 2	September
Callide C 1	May
Callide C 2	June
Gladstone 1	August-September
Gladstone 2	October
Gladstone 3	July
Gladstone 4	April
Gladstone 5	May
Gladstone 6	June
Yarwun	July

[7] Multi-month outages listed for some Queensland generators including Stanwell 1, Gladstone 1, Tarong 1 and Kogan Creek (shaded in orange) could be associated with more extensive O&M requirements or a desire on the part of the operators to withdraw some capacity during seasonal periods experiencing lower levels of demand.

Tarong North	June
Tarong 1	July-August
Tarong 2	May
Tarong 3	April
Tarong 4	September
Kogan Creek	October-November
Millmerran 1	April
Millmerran 2	September
Darling Downs	July
Condamine	October
Swanbank E	November
New South Wales	
Liddell 2	April
Liddell 3	September
Liddell 4	November
Bayswater 1	May
Bayswater 2	August
Bayswater 3	October
Bayswater 4	March
Eraring 1	May
Eraring 2	June
Eraring 3	August
Eraring 4	September
Vales Point 5	March
Vales Point 6	October
Smithfield	September
Mt Piper 1	October
Mt Piper 2	November
Tallawarra	August
Victoria	
Newport	August
Yallourn 1	May
Yallourn 2	October
Yallourn 3	April
Yallourn 4	September
Loy Yang A 1	June
Loy Yang A 2	July
Loy Yang A 3	November
Loy Yang A 4	March
Loy yang B 1	September
Loy Yang B 2	April
South Australia	
Torrens Island B 1	April
Torrens Island B 2	August
Torrens Island B 3	September
Torrens island B 4	July
Pelican point	June
Osbourne	July
Quarantine 5	October
TGN (CCGT)	April
Tasmania	
Tamar Valley CCGT	September

Modelling using the scheduled outage profiles listed in Table 1 reflect an 'ideal' set-up to the extent that outages are preferable during lower demand periods than, for example, during peak load events arising during summer. Capacity withdrawal for baseload plant during low demand periods is also an

option if the penetration of distributed and utility-scale solar PV begins to produce very low or negative prices associated with an emergent duck-curve effect. Some evidence of this type of effect began to emerge in the cases of South Australia and Queensland during Spring of 2019.

The O&M profile in Table 1 differs from industry practice where routine short-term O&M is often performed over two- or four-year cycles often depending upon underlying ash content of coal in the case of coal-fired generators. Major O&M on turbines typically occurred on a decade timescale and on a twenty-year time frame for control systems. Potential arguments in favour for the more frequent O&M regime listed in Table 1 when compared to industry practice alluded to above might be linked to both aging of plant and reduced reliability associated with extreme weather conditions linked to climate change. However, to the extent that Table 1 overstates scheduled O&M, then the results cited in this report, in terms of Variable Renewable Energy (VRE) targets and production shares, will be more conservative as production from baseload thermal plant would be higher in relative terms under the 'industry practice' O&M regime outlined above, thus driving the renewable energy share production downwards. Further modelling will be undertaken to examine how sensitive the findings are to deviations in O&M arrangements.

3.6.2 General use of 2019-20 ISP assumptions

In order to make the model response to the various scenarios more realistic, we have taken account of the fact that baseload and intermediate coal and gas plant typically have 'non-zero' must run MW capacity levels termed minimum stable operating levels. These plants cannot run below these specified MW capacity levels without endangering the long-term productive and operational viability of the plant itself or violating statutory limitations relating to the production of pollutants and other toxic substances. In including these constraints, the assumptions included in the '2019 ISP Input and Assumptions workbook v1 3 Dec 19' workbook were adopted with the following exception[8]:

- Darling Downs NGCC plant minimum stable operating level was set to 23% of the plant's nameplate capacity (645 MW), reflecting lower values of other NGCC plant in the NEM. In the ISP workbook, in contrast, this value was set to 58 MW which seemed very low in comparison to other similar plant, being below 10% of nameplate capacity.

More generally, other assumptions relating to ($/GJ) fuel cost, ($/MWh) VOM costs, ($/MW/year) FOM costs, minimum and maximum MW capacities, emission intensity rates, auxiliary load rates and plant closures were also sourced from the '2019 ISP Input and Assumptions workbook v1 3 Dec 19' ISP workbook. Plant closure information incorporated in the modelling is listed in Table 2 below. As such, for the 2030 timeframe, major baseload plant closures include Callide B (QLD), Liddell, one unit of Eraring and Vales Point (NSW), Yallourn (VIC), and Torrens Island A in SA.

Table 2: Generator scheduled closures

Generator	Scheduled Closure
Queensland	
Kareeya	2037
Mt Stuart	2033
Mackay GT	2021
Stanwell	2042-2043
Barcaldine	2034
Callide B	2028-2029
Gladstone	2034-2036
Tarong	2035-2037
Roma	2034
Swanbank E	2028

[8] This input data file can be accessed at the following web-address:https://aemo.com.au/en/energy-systems/major-publications/integrated-system-plan-isp/2020-integrated-system-plan-isp#2019 Scenarios, Inputs, Assumptions and Methodologies.

New South Wales	
Liddell	2022-2023
Bayswater	2034-2036
Eraring	2030-2032
Vales Point	2029-2030
Smithfield	2044
Mt Piper	2042-2043
Victoria	
Newport	2039
Hazelwood	2018
Yallourn	2028-2030
Loy Yang A	2038-2040
Loy Yang B	2039-2040
South Australia	
Torrens Island A	2021-2022
Torrens Island B	2034-2036
Pelican Point	2037
Osbourne	2033

3.6.3 New entrant generation

For new entrant fossil-fuel generation, we follow the Australian Energy Market Operator's (AEMO), assumptions for the Integrated Systems Plan 2019 (ISP), and more specifically the Neutral Scenario. For VRE new entrant generation, two broad approaches were adopted. The first was to assume that projects with planning permission, hereinafter called the project pipeline, would be deployed and commissioned. We understand that the project pipeline differs from the ISP Neutral Scenario but the ISP Neutral Scenario does not forecast the achievement of 50% renewable energy by 2030. Therefore, we needed to assume greater deployment of VRE by 2030 to achieve the state-based renewable energy targets (RET). The second approach was to replicate the new entrant VRE profiles calculated within the ISP process, namely, those associated with the 2030 central, 2030 step change and 2040 central scenarios.

In relation to the pipeline scenario, a consequence of high levels of solar in the generation mix, in conjunction with coal and gas plant with must-run characteristics, is high levels of VRE spillage to accommodate the coal and gas plant minimum stable operating levels. High levels of VRE spillage, indicate a requirement for energy storage so that energy generated during periods of excess supply can be stored until periods of higher demand. As well as not forecasting the achievement of state RETs, the ISP makes few assumptions about energy storage for Queensland. For this reason, prior modelling indicates that approximately 2 GW of storage in Queensland is required to facilitate a daily energy shift from periods of excess supply to periods of excess demand. For this energy storage, we assume that pump hydro will be able to facilitate the daily energy shift, as it is currently the cheapest source of utility scale energy storage.

In Table 3, we detail the new entrant pump hydro plant included in the modelling. By 2025, some additional pump hydro plant are assumed to be operational including Kidston in QLD and Baroota and Goats Head pump hydro plant in SA. By 2030, it is assumed that some larger pump hydro plant become operational including Urannah and Mt Byron in QLD and Snowy 2.0 in NSW as well as the smaller Middleback Range plant in SA. For pump hydro potential in QLD, apart from Kidston, there is little in the way of detailed public studies. The only other projects the authors know about is the Urannah and Mt Bryon proposals. In both cases, however, there is a paucity of public information. Both projects were modelled on published information on Snowy 2.0 particularly in terms of individual 340 MW hydro turbine design characteristics. Both projects are sizable at 1020 MW capacity and have the capability of supplying power at full capacity for several hours. In the case of both projects, there are advantages with their geographical location with Urannah located in the North Queensland node and Mt Bryon in the Moreton North node, close to the existing Wivenhoe power station. Thus,

both can provide crucial network balancing and support services to the VRE pipeline for North and Central QLD and South East and South West QLD.

Table 3: New generation

Generator	Assumed Commencement of Operations
Queensland	
Kidston pumped hydro (250 MW)	2025
Urannah pumped hydro (1020 MW)	2030
Mt Bryon pumped hydro (1020 MW)	2030
New South Wales	
Newcastle GT (250 MW)	2022
Snowy 2.0 (2040 MW)	2030
South Australia	
Barkers Inlet GT	2020
Baroota pumped hydro (250 MW)	2025
Goat Hill pumped hydro (250 MW)	2025
Middleback Ranges pumped hydro (110 MW)	2030

3.6.4 Conventional hydro

In this project, hydro supply offers were constructed to target peak demand periods and a broader system balancing function, including any ramping requirements needed in late afternoon as solar PV output tailors off. In this case, the bids are based around each plant's Long Run Marginal Cost (LRMC) with escalation around these estimates across separate turbines within individual hydro gensets. In this case, hydro offers often shadow supply offers of peak load OCGT generation plant.

3.6.5 Modelling Pump hydro

The treatment of pump hydro plant will differ in important respects from the approach defined immediately above for standard hydro plant. A key advantage of pump hydro is its ability to use pump actions to enable greater output from both solar PV and wind generation[9]. Given the typical nightly diurnal cycle of wind and daily cycle of solar PV, both night-time and day-time pump actions could help facilitate increased power from wind and solar generation, if otherwise, this output would be spilled. Supply offers for pump hydro plant were developed to target morning and evening peak periods – that is, from 6 am to 9 am and 5 pm to 9 pm, respectively. Pump actions were defined to support these operations and are outlined in Tables 4-5. Recall that many of the larger pump hydro plant listed in Table 4 are assumed to be operational by 2030. In overall terms, the pump actions are expected to facilitate greater power production from particularly solar PV generation, thereby contributing to the attainment of state clean energy targets. An additional advantage of combined pump and dispatch operations or if operating in 'Syncon' mode would be to additionally provide synchronous inertia and system strength.

Assuming a round trip efficiency of 0.8, the ability to supply full output for a period of seven hours would notionally require equivalent pumping action for a period of 9 hours (e.g. 7/0.8). Therefore, the need to conduct pumping actions for a longer period than the full power that can be supplied has to be factored into the design of pumping actions. It should also be recognised that apart from Snowy 2.0, all other pump hydro plant have relatively small upper or lower reservoirs thereby restricting their supply and pumping activities to a daily operational cycle. That is, they do not constitute seasonal storages, but instead, are more suitable for daily balancing requirements.

[9] This will particularly arise once the minimum stable must-run requirement of baseload thermal plant has been met. In this case, additional output would be sourced from cheaper sources of generation including wind and solar PV generation.

Table 4: Pump loads (MW) assumed for pump hydro generators in QLD and NSW

Half-hour	Time	Kidston	Urannah	Wivenhoe	Mr Bryon	Shaolhavn	Tumut 3	Snowy 2.0
1		240	680	480	680		600	680
2	1am							
3								
4	2 am							
5								
6	3 am							
7								
8	4 am							
9								
10	5 am						600	
11			680		680		400	
12	6 am	240	340	480	340		200	680
13								
14	7 am							
15								
16	8 am							
17								
18	9 am							
19		120	680	240	340	160	200	340
20	10 am	240	1020	240	680	240	400	680
21		240	1020	480	1020	240	600	1020
22	11 am	240	1020	480	1020	240	600	1020
23		240	1020	480	1020	240	600	1020
24	12 pm	240	1020	480	1020	240	600	1020
25		240	1020	480	1020	240	600	1020
26	1 pm	240	1020	480	1020	240	600	1020
27		240	1020	480	1020	240	600	1020
28	2 pm	240	1020	480	1020	240	600	1020
29		240	1020	480	1020	240	600	1020
30	3 pm	240	1020	480	1020	240	600	1020
31		240	1020	480	1020	240	600	1020
32	4 pm	240	1020	480	1020	240	600	1020
33		240	1020	480	1020	240	600	1020
34	5 pm	340	680	240	680	160	400	680
35		120	340	240	340	80	200	340
36	6 pm							
37								
38	7 pm							
39								
40	8 pm							
41								
42	9 pm							
43								
44	10 pm							
45								
46	11 pm		340	240	340		200	340
47		240	680	240	680		400	680
48	12 am	240	1020	480	680		600	680

Table 5: Pump loads (MW) assumed for pump hydro generators in SA

Half-hour	Time	Baroota	Goat Hill	Middleback Ranges
1		240	240	110
2	1am			

3				
4	2 am			
5				
6	3 am			
7				
8	4 am			
9				
10	5 am			
11		240	240	
12	6 am	120	120	110
13				
14	7 am			
15				
16	8 am			
17				
18	9 am			
19		120	120	110
20	10 am	240	240	110
21		240	240	110
22	11 am	240	240	110
23		240	240	110
24	12 pm	240	240	110
25		240	240	110
26	1 pm	240	240	110
27		240	240	110
28	2 pm	240	240	110
29		240	240	110
30	3 pm	240	240	110
31		240	240	110
32	4 pm	240	240	110
33		240	240	110
34	5 pm	240	240	110
35		120	120	110
36	6 pm			
37				
38	7 pm			
39				
40	8 pm			
41				
42	9 pm			
43				
44	10 pm			
45				110
46	11 pm	120	120	110
47		240	240	110
48	12 am	240	240	110

3.6.6 Transmission network scenarios and augmentations

In the modelling performed for this project, we have investigated two particular transmission scenarios:

- N transmission scenario; and
- N-1 transmission scenario.

The first scenario involves applying the MW thermal limits determined from the sum of all individual transmission line thermal ratings in the group of transmission lines connecting two nodes. This

approach effectively assumes no line outages occur and that the transmission lines are all in good working condition. As such, this approach represents, from the perspective of operational constraints of the transmission network, an ideal setting consistent with maximising VRE potential within the network.

The second N-1 transmission scenario involves subtracting the largest individual line from the group of transmission lines connecting nodes (when appropriate). This approach more closely matches how AEMO manages the grid in practice, being linked to reliability and security considerations if the largest single line is lost. This approach might also more closely match outcomes in which the capacity of the transmission branches is determined by voltage, transient or oscillatory stability limits which tend to produce capacity limits that are more restrictive (e.g. lower) than those determined from consideration of thermal ratings alone.

Some uncertainty exists over the exact technical specification of some of the ISP based transmission network augmentations currently undergoing assessment through the RIT-T process that have been included in the modelling. However, where possible, the preferred options identified by the project proponents as part of the RIT-T process have been subsequently adopted.

In the 2030 timeframe underpinning the modelling outcomes reported in this report, the following transmission network augmentations have been incorporated:

- EnergyConnect - double circuit 330 kV branch;
- HumeLink - two double circuit 500 kV branches;
- KerangLink - 500 kV double circuit branch with 330 kV branches also to the Red Cliffs and Glenrowan nodes;
- QNI Stage 2 - double circuit 500 kV branch linking QNI to Newcastle and Bayswater nodes through the Armidale, Tamworth and Liddell nodes;
- Stage 1 'Battery-Of-The-Nation' (BON): 750 MW HVDC branch from Burnie (Tasmania) to Hazelwood (Victoria); and
- Stage 2 'Battery-Of-The-Nation' (BON): 750 MW HVDC branch from Burnie (Tasmania) to Hazelwood (Victoria) applied specifically to the ISP 2040 central scenario.

In the case of EnergyConnect, technical parameters were sourced from ElectraNet (2019). In the case of KerangLink and HumeLink, technical parameters used in the modelling were based upon those of existing 500 kV branches in both NSW and VIC.

Unfortunately, much less public information is available on the ISP Stage 2 QNI upgrade. No formal RIT-T process has commenced at the time of writing. Given the recent identification of northern NSW as a potential renewable energy zone centred on Armidale and Tamworth regions by the NSW government[10], the Stage 2 QNI upgrade included in the modelling encompassed a double circuit 500 kV branch setup linking QNI to Newcastle and Bayswater nodes through the Armidale, Tamworth and Liddell nodes listed in Figure 2. This would complete the northern arm of the 500kV network serving the greater Sydney area whilst HumeLink would, in turn, complete the southern arm, connecting Snowy Mountains, Riverina and Southern Highland regions to the greater Sydney region.

An intra-state QLD project CopperString 2.0 was also assumed in the modelling in 2030. In the latter context, the CopperString project is assumed to fall fully within the Ross node, however, allowing significant additional VRE output to be sourced from the previously electrically remote Hughenden region (see Figure 1).

Finally, in all cases, an N-1 specification is applied to these augmentations for both N and N-1 transmission scenarios with one 330 or 500 kV line being dropped in determining the MW capacity

[10] As incorporated in the 2040 ISP central scenario, for example.

limits on these new branches. In all cases, it is assumed that the existing 330 and 220 kV backbones also remain in operation.

For the information of stakeholders, the derivation of capacity limits under the N and N-1 scenarios will be presented in the following subsection. The transmission branches listed were chosen because they experienced some congestion impacts under one or more scenarios.

3.6.6.1 Assessment of MW capacity limits on key transmission lines subject to congestion under both pipeline and ISP scenarios

This sub-section will outline the derivation of the capacity limits used in the ANEM modelling that are crucial to congestion outcomes produced by the modelling. Focus will be concentrated on transmission pathways linking NQ, CWQ, Gladstone, WB, and MN, as well as the SWQ and MS nodes. See Figure 1 for further details.

NQ to CWQ (Line 3) transfer capacity

Definitionally, the NQ node includes the terminal stations at Nebo and Strathmore with four 275 kV transmission branches connecting the NQ and CWQ nodes. These branches together with their summer and winter capacity limits are: [11]

- Nebo to Broadsound 1 (1x275 kV): 788 MW 912 MW;
- Nebo to Broadsound 2 (1x275 kV): 1096 MW 1231 MW;
- Nebo to Broadsound 3 (1x275 kV): 1096 MW 1231 MW; and
- Nebo to Bouldercombe (1x275 kV): 363 MW 363 MW.[12]

The normal direction summer and winter N-1 capacity limit associated with the above set of transmission lines correspond to 2247 MW and 2506 MW, respectively.

CWQ (Node 4) intra-node transfer capacity

The CWQ node includes the following terminal stations: Lilyvale, Broadsound, Bouldercombe and Calvale. It therefore includes the Rockhampton-Mackay load centre and Stanwell and Callide B and C power stations. Key internal transmission branches within the CWQ node include:

- Lilyvale to Broadsound (2x275 kV): (1) 440 MW 570 MW; (2) 548 MW 760 MW – potentially establishing an important internal upper transfer limit for output of solar farms located in the Emerald-Lilyvale region;[13]
- Calvale to Stanwell (1x275 kV): 861.9 MW 861.9 MW;
- Stanwell to Bouldercombe (2x275 kV): (1) 934 MW 1296 MW; (2) 934 MW 1296 MW; and
- Stanwell to Broadsound (2x275 kV): (1) 1225 MW 1225 MW; (2) 992 MW 992 MW.

Note the restrictive summer and winter N-1 transfer limit on the internal Lilyvale to Broadsound line of 440 MW and 570 MW, respectively. Significant new investment in CWQ would need to take this into account and possibly locate elsewhere within the CWQ node without further augmentation of the transfer capacity limit on the Lilyvale to Broadsound line.

CWQ-GLAD (Line 4) transfer capacity

The Gladstone node includes the Raglan, Mt Larcom, Boyne and Wurdong terminal stations. The key 275 kV circuits determining the capacity transfer limits on Line 4 (CWQ to Gladstone) are:

[11] The original limits were defined in terms of Megavoltamperes (MVA) which is a measure of apparent power. In the ANEM modelling, a power factor of unity is assumed for all major transmission branches meaning that MVA values will equate to MW values which are subsequently used in the rest of this document.

[12] Capacity limits for powerflow in the reverse direction (e.g. Bouldercombe to Nebo) is slightly higher in magnitude, between 471 MW and 568 MW, depending upon season.

[13] This possibility was not modelled in ANEM.

- Bouldercombe to Gladstone (1x275 kV): 483 MW 557 MW;
- Bouldercombe to Raglan (1x275 kV): 497 MW 569 MW; and
- Calvale to Wurdong (1x275 kV): 548 MW 615 MW.

The normal direction summer and winter N-1 capacity limit associated with the above set of transmission lines are 980 MW and 1126 MW, respectively. Therefore, in comparison with the transfer capacity between NQ and CWQ outlined above, the N-1 transfer capacity between CWQ and Gladstone is significantly lower in magnitude. This reflects the loss of one 275 kV circuit as well as the lower capacity limits generally applicable to the latter set of 275 kV circuits.

It should also be noted that another key 275 kV transmission pathway southward is an inland route connecting CWQ (Calvale) and the Tarong nodes. This particular transmission line (Line 5 in the ANEM structure) comprises two 275 kV circuits: (1) 1096 MW 1230 MW; (2) 1096 MW 1230 MW, with a summer and winter N-1 transfer capacity equal to one of the circuits – namely, 1096 MW and 1230 MW, respectively.

GLAD-WB (Line 6) transfer capacity

The Wide Bay node includes the Gin Gin, Teebar and Woolooga terminal stations. The key 275 kV circuits connecting the Gladstone and Wide Bay nodes are:

- Gladstone to Gin Gin (1) (1 x 275 kV): 797 MW 883 MW;
- Gladstone to Gin Gin (2) (1 x 275 kV): 797 MW 883 MW; and
- Wurdong to Gin Gin (1 x 275 kV): 797 MW 883 MW.

In this case, the normal direction summer and winter N-1 capacity limit associated with the above set of transmission lines are 1594 MW and 1766 MW, respectively.

WB (Node 6) intra-node transfer capacity

The internal transfer capacity within the Wide Bay node is determined by:

- Gin Gin to Woolooga (1) (1 x 275 kV): 761 MW 886 MW;
- Gin to Woolooga (2) (1 x 275 kV): 737 MW 737 MW; and
- Gin Gin-Teebar-Woolooga (1 x 275 kV): 737 MW 737 MW,

thereby producing internal summer and winter N-1 transfer capacity limits of 1474 MW and 1474 MW. This result is slightly lower than the Gladstone to Wide Bay transfer capacity mentioned above but greater than the CWQ to Gladstone transfer capacities.

WB-MN (Line 7) transfer capacity

The transfer capacity between the Wide Bay and Moreton North nodes on Line 7 is determined by two 275 kV circuits:

- Woolooga to South Pine (1x275 kV): 798 MW 884 MW; and
- Woolooga-Palmwoods-South Pine (1 x 275 kV): 797 MW 883 MW.

The implied summer and winter N-1 transfer limits for summer and winter are 797 MW and 883 MW, respectively. Thus, compared to the transfer capacity on the branch connecting Gladstone and Wide Bay as well as the internal transfer capacity within the Wide Bay node, the transfer capacity on Line 7 between Wide Bay and Moreton North has declined significantly in comparison, with the loss of a 275 kV circuit (e.g. down from two to one circuits 275 kV circuits under N-1).

SWQ-MS (Line 10) transfer capacity

The transfer capacity on Line 10 (connecting the SWQ and Moreton South nodes) are:

- Middle Ridge to Greenbank 1 (1x275 kV): 1096 MW 1231 MW; and
- Middle Ridge to Greenbank 2 (1x275 kV): 1096 MW 1231 MW.

The implied summer and winter N-1 transfer limits in this case are 1096 MW and 1231 MW, respectively.

GC-LIS (Line 14) transfer capacity

Finally, Line 14 Directlink connects the Gold Coast node with the NSW Lismore node. The thermal capacity of this line is very small in magnitude at 180 MW.

3.7 VRE data compilation

Various scenarios were modelled involving the increased penetration of wind and solar PV over the 2022 to 2030 time period with targeted simulation year of 2030. Recall that two broad modelling approaches were undertaken. The first, termed the '2030 Pipeline Scenario', involved using historical based resource VRE assessment carried out for operational, under construction, and planned projects (i.e. investment pipeline projects). These projects are listed for each state in Tables 1 to 9 of Appendix B.

The second approach that was investigated involved modelling VRE penetration scenarios determined by AEMO as part of its ISP process. Specifically, three ISP scenarios were investigated:

- 2030 ISP central scenario;
- 2030 ISP step change scenario; and
- 2040 ISP central scenario.

This section will outline the compilation of VRE resources used in both the pipeline and ISP modelled scenarios.

3.7.1 VRE compilation: 2030 pipeline scenario

Three broad construction pipelines were envisaged. The first, termed '2022' mainly encapsulated operational, under construction or projects with financial close that are likely to be completed by 2022.

The second scenario envisaged a target completion year of 2025. In the case of Queensland, many projects included were shortlisted Q400 projects as well as the Aldoga solar farm which had an existing PPA with the QLD Government and was expected to be completed by 2025. Additional projects chosen in QLD were largely in nodal areas favoured by AEMO in its ISP modelling and included both wind and solar projects in SWQ and CWQ regions. These projects also had proponents with a history of successful project completion and strong connection prospects through close location to major 275 kV Powerlink terminal stations.

The last completion year was 2030. These additional projects were also chosen on the basis of location, grid connectivity and strong proponents.

Two general sources of VRE output data was utilised in the modelling conducted for the project. The first source of VRE data was output traces produced by AEMO as part of the ISP process. Two ISP datasets are available. The first is half-hourly Solar PV and wind output traces for operational solar and wind projects from 1 July 2017 to end of June 2050 based upon a 2014 reference year. The second is a shorter but more extensive set of output projections for operational and under construction solar and wind farms projects released with the 2019 ISP dataset encompassing a projection period of 1 July 2019 to the end of June 2030. In this latter case, the projections are based upon solar and wind resource yields over nine reference years encompassing years 2011 to 2019. This latter set of data was used extensively in relation to the three ISP scenarios mentioned above.

A potential shortfall of the ISP data mentioned immediately above is that detailed yield assessments have only been produced for operational or under construction solar and wind farms occurring during 2019 at the time the ISP database was produced. No similar yield assessments have been done for planned projects that are likely to proceed under any serious state based clean energy target. However, regional based solar PV and wind generation output traces have been produced for numerous renewable energy zones, including South West QLD, Isaac, Fitzroy, North QLD and the North QLD energy hub (centred around Hughenden). Interestingly, no data appeared to have been released for the Wide Bay renewable energy zone which has attracted interest within policy circles in QLD. However, in all cases, only one solar PV and wind trace is supplied per renewable energy zone and encompasses half hourly output projections for the period 1 July 2017 to end of June 2058. While useful for modelling purposes, such single traces are not likely to account for specific variability and complexities associated with the effects of terrain on wind farms locating on exposed hills or ranges or emergent efficiencies associated with use of larger wind turbine generators. Finally, the only solar PV technology considered in the renewable energy zone traces was single-axis tracking technology. This is a potential limitation because larger projects such as Bulli Creek and Wandowan South are likely to favour the use of fixed tilt arrays rather than single-axis tracking arrays because the former require less ground area coverage for a given MW capacity.

In the second instant, wind and solar output calculated from climate and solar irradiance data from Australia Bureau of Meteorology (BOM) in the case of solar PV and from a meso-scale weather model in the case of wind generation will be utilised. This data has been developed previously by one of the authors as part of other projects and is project pipeline centric. In contrast to the ISP data mentioned above, considerable effort was also applied to producing project specific wind and solar yield traces for planned projects as well as operational or under construction projects. In this context, this data is particularly suitable for assessing VRE production trends linked to the staged role out of planned projects that are part of each state's existing investment pipeline. This data was used to expand VRE capacity in accordance with the VRE expansion scenarios outlined in detail in Appendix B. The focus of this data was to use historical based estimates of median project yields to underly the scenario-based capacity expansions listed in Appendix B for target year 2030. This, in turn, encompassed output traces associated with full set of projects listed cumulatively under the '2022', '2025' and '2030' headings in each table in Appendix B.

In the following two sections, an outline is provided about how the wind and solar PV traces used in the modelling were developed.

3.7.2.1 Wind generation

Wind data came from the Weather Research & Forecasting Model (WRF 2015), a "mesoscale numerical weather prediction system", configured to model the geographical region surrounding the windfarms of interest, to produce weather predictions consisting of 5-minute interval wind speed vectors. The latitude and longitude coordinates of representative clusters of Wind Turbine Generators (WTGs) identified from windfarm layouts in planning approval documents formed the basis of geographical locations for WRF data extraction points within each selected windfarm site. WRF data extraction at these latitude and longitude coordinates related to wind climatology results at 80 meters 'Above Ground Level', taking account of the elevation and nature of the terrain surrounding these coordinates when applying the 80 meters above ground level requirement.

The average wind speeds calculated from WRF wind climatology results formed the basis for calculating the MW output of each windfarm. The initial calculation involves determining the MW output for a single representative WTG in a windfarm for each five-minute average wind speed for each consecutive five-minute period in years 2010, 2011 and 2012, respectively. Thus, there were three representative years. The MW output is read off an appropriate WTG power curve for a given average meters per second (m/s) wind speed value. Because the choice of WTG can differ from windfarm to windfarm and even within a single windfarm, different WTG power curves were used to calculate WTG output traces. In order to fill in the detail of the power curves, a cubic spline technique was used to disaggregate the horizontal axes of the standard power curves so that they incremented

in terms of 0.05 m/s instead of the more aggregated 1 m/s typically displayed in the case of standard power curves.

Information on WTG power curves were sourced from different resources. The first was published power curves in excel files available from Idaho National Renewable Laboratory (INL 2015). The second was power curves available with the Windpower Program (Bradbury 2015). The third source was power curves available with the WASP Wind Flow Modelling Program (Jacobsen 2015). Finally, for any WTG not listed at these three sites, internet searches for power curves at the web sites of the manufactures of the WTG usually provided power curves in sales and technical documents outlining technical characteristics of the WTG. Alternatively, interpolation methods were also used to extrapolate new power curves from existing power curves.

The original research into wind farms encompassed calculating wind traces over the three representative years 2010, 2011 and 2012 for the following wind farms listed in Table 6. Many wind farms listed under Scenarios C, D and E in Table 6 denote wind farms that have been constructed more recently or are part of the remaining investment pipeline. In these cases, WTG type was appropriately updated to reflect actual investment technology to derive updated wind farm output traces. In the case of newer emerging wind farms such as Murra Warra or Dulucca and MacIntyre wind farms in south west QLD, wind climatology had to be subsequently proxied by that of other wind farms.

In all cases, median wind farm output traces were calculated as the median results across the three representative years for which data was available. Half-hourly wind output traces were calculated by averaging across the six five-minute periods comprising each half-hourly period.

Table 6: List of windfarm WTG by scenario and wind climate proxy

Windfarm	**WTG Type**	**Wind Climatology Proxy**
Scenario A – no wind generation		
Scenario B – operational non- and semi-scheduled and under construction		
Operational: Non-scheduled		
Blayney	VESTAS V47-660	
Canunda	VESTAS V80-2000	
Capital 1	SUZLON S88-2100	
Cathedral Rocks	VESTAS V80-2000	
Challicum Hills	NEG MICON NM72C	
Codrington	AN Bonus 1300	
Crookwell	VESTAS V44-600	
Cullerin Range	REPower MM82-2000 (8) and MM92-2000 (9)	
Hepburn	REPower MM82-2000	
Lake Bonney 1	VESTAS V66-1.75MW	
Morton's Lane	Goldwind GW82/1500	
Mt Millar	ENERCON E70-2000	
Portland 2 and 3	REPower MM82-2000	
Starfish Hill	NEG MICON NM72C	
Toora	VESTAS V66-1.75MW	
Wattle Point	VESTAS V82_1.65MW	
Waubra	ACCIONA AW77-1500	
Windy Hill 1	ENERCON E40-600	
Wonthagi	REPower MM82-2000	
Woolnorth	VESTAS V66-1.75MW (37) and V90-3000 (25)	
Yambuk	NEG MICON NM72C	
Operational: Semi-scheduled		

Windfarm	WTG Type	Wind Climatology Proxy
Clements Gap	SUZLON S88-2100	
Gunning	ACCIONA AW77-1500	
Hallett 1	SUZLON S88-2100	
Hallett 2	SUZLON S88-2100	
Lake Bonney 2	VESTAS V90-3000	
Lake Bonney 3	VESTAS V90-3000	
Macarthur	VESTAS V112-3000	
Musselroe	VESTAS V90-3000	
North Brown Hill	SUZLON S88-2100	
Oaklands Hills	SUZLON S88-2100	
Snowtown 1	SUZLON S88-2100	
The Bluff	SUZLON S88-2100	
Waterloo	VESTAS V90-3000	
Woodlawn	SUZLON S88-2100	
Under Construction		
Bald Hills	REPower MM92-2050	
Boco Rock 1	GE 1.6-100 (9) and 1.7-100 (58)	Woodlawn
Gullen Range	Goldwind GW82/1500 (17) and GW2.5/103 (56)	
Mt Mercer	REPower MM92-2050	
Portland 4	REPower MM92-2050	
Snowtown 2	Siemens 3 s101 (10) and 3 s108 (80)	
Taralga	VESTAS V90-2000 (21), V100-1800 (21) and V90-3000 (9)	
Scenario C: Advanced planning (+all the windfarms above)		
Ararat	VESTAS V112-3000	
Barn Hill	VESTAS V112-3000	
Boco Rock 2	GE 1.6-100 (7) and 1.7-100 (48)	Woodlawn
Bodangora	VESTAS V112-3000	Crudine Ridge
Capital 2	VESTAS V112-3000	
Cherry Tree	VESTAS V112-3000	Hepburn
Collector	VESTAS V112-3000	
Coonooner Bridge	VESTAS V112-3000	Ararat
Crookwell 2	VESTAS V112-3000	
Forsayth	VESTAS V112-3000	average of Mt Emerald/High Road
Glen Innes	VESTAS V112-3000	
Hornsdale	VESTAS V112-3000	
Lal Lal	VESTAS V112-3000	
Mt Gellibrand	VESTAS V112-3000	
Salt Creek	VESTAS V112-3000	Penhurst
Silverton 1	VESTAS V112-3000	
Stockyard Hill	VESTAS V112-3000	
Stony Gap	VESTAS V112-3000	
Waterloo 2	VESTAS V112-3000	
Woolsthorpe	VESTAS V112-3000	
Yaloak South	VESTAS V112-3000	Lal Lal
Scenario D: Less advanced planning (+all the windfarms above)		
Ben Lomond	VESTAS V112-3000	
Berrybank	VESTAS V112-3000	
Chepstowe	VESTAS V112-3000	Mt Mercer
Conroy's Gap 1	VESTAS V112-3000	

Windfarm	WTG Type	Wind Climatology Proxy
Coopers Gap	VESTAS V112-3000	
Crookwell 3	VESTAS V112-3000	
Crowlands	VESTAS V112-3000	
Crudine Ridge	VESTAS V112-3000	
Flyers Creek	VESTAS V112-3000	
Granville Harbour	VESTAS V112-3000	Woolnorth
Hawkesdale	VESTAS V112-3000	
High Road	VESTAS V112-3000	
Keyneton	VESTAS V112-3000	Waterloo
Lincoln Gap	VESTAS V112-3000	average of Clements Gap, Hallett 1 and 2, Mt Millar, North Brown Hill and The Bluff
Low head	VESTAS V112-3000	average of Woolnorth/Musselroe
Moorabool	VESTAS V112-3000	Lal Lal
Mortlake South	ACCIONA AW77/1500	Macarthur
Mt Bryan	VESTAS V112-3000	
Mt Emerald	VESTAS V112-3000	
Ryans Corner	VESTAS V112-3000	
Sapphire	VESTAS V112-3000	
Silverton 2	VESTAS V112-3000	
White Rock	VESTAS V112-3000	
Winchelsea	VESTAS V112-3000	
Woakwine Range	VESTAS V112-3000	
Scenario E: Least advanced planning (+all the windfarms above)		
Cattle Hill 1 and 2	VESTAS V112-3000	average of Woolnorth/Musselroe
Ceres 1 and 2	REPOWER 3.4MW 104	
Conroy's Gap 2	VESTAS V112-3000	Conroy's Gap
Crows Nest	VESTAS V112-3000	
Liverpool Range	VESTAS V112-3000	
Yass Valley	VESTAS V112-3000	

3.7.2.2 Solar generation

Output traces were developed for the utility scale solar PV investment pipeline using the US National Renewable Energy Laboratory (NREL) System Advisor Model (SAM), see (Gilman, 2015). To run simulations in SAM, various user supplied inputs are required. These relate to: (1) hourly solar and weather data; (2) technical information about modules, inverters and array sizing and design; (3) soiling effects; (4) shading effects; and (5) DC and AC electrical losses.

The solar and weather data needed included Global Horizontal Irradiance (GHI) and Direct Normal Irradiance (DNI) data together with weather data on ambient temperature and wind speed. The GHI and DNI data used in the simulations were obtained from the Australian Bureau of Meteorology's (BOM) hourly solar irradiance gridded data (BOM, 2015) whilst weather data was sourced from BOM automatic weather station data.[14]

Technical information about modules, inverters and array sizing and design were sourced from product data sheets provided by module and inverter suppliers and from planning documents if available. Soiling effects were calculated for some selected sites located in arid, pastoral and coastal

[14] This solar irradiance data can also be conveniently sourced from the AREMI database located at: https://nationalmap.gov.au/renewables/.

settings[15]. In calculating soiling impacts, rainfall was a key determinant of soiling impact and module cleansing effects. Shading effects were restricted to assessment of self-shading impacts. These impacts refer to the impact of shadows thrown on modules by nearby rows of other modules and crucially depend upon row spacing, module tilt angle and orientation (e.g. portrait or landscape orientation).

Solar PV yield traces were developed for all the solar PV projects listed in Appendix B, calculated over the representative years 2007 to 2015. Median traces were then calculated from these nine reference years of hourly traces, excluding the additional day associated with leap years. Half hourly output traces were then calculated from the hourly traces within Matlab using a linear interpolation technique.

Given the large number of solar farms being investigated, some homogenisation was undertaken in terms of module choice. Module types accommodated in solar PV yield calculations were thin film (First Solar) or mono-crystalline (Trina) with different provisions for different orientations of the modules.

3.7.3 VRE compilation: ISP scenarios

In this report, an investigation of selected AEMO ISP scenarios will be presented. Recall that the chosen ISP scenarios were: (1) 2030 central scenario; (2) 2040 central scenario; and (3) 2030 step change scenario, but utilising 2040 central scenario demand profiles.

The source of the VRE output traces employed in the modelling was drawn from information contained in the 2019-20 ISP documentation and accompanying databases [AEMO (2018b,2020)]. Recall that two ISP datasets are available. The first is half-hourly solar PV and wind output traces for operational solar and wind projects from 1 July 2017 to end of June 2050 based on a 2014 reference year. The second is a shorter but more extensive set of output projections for operational and under construction solar and wind farms projects released with the 2019/20 ISP dataset encompassing a projection period of 1 July 2019 to the end of June 2030. In this latter case, the projections are based on solar and wind resource yields over nine reference years encompassing years 2011 to 2019. This latter set of data was used extensively to develop the output traces for various operational/under-construction solar and wind farms for the ISP based modelling.

A similar approach was taken to the approach adopted in deriving demand traces outlined in Section 3.5. Specifically, the median VRE output profiles were obtained from the set of profiles derived by AEMO for each reference year in the interval 2011 to 2019. As with the demand profiles, this entailed averaging over different weather conditions encapsulated in each of the reference year profiles to determine the median profile.

Because the available AEMO data relating to wind and solar PV farms ended at midnight ending 30 June 2030, other data sources had to be used to extrapolate the output trace out to the end of December 2030 for calendar-year based model simulations. Wind and solar PV traces associated with renewable energy zones were used in this case. In the case of wind farms, some splicing had to be done to rebase the renewable energy zones wind trace to the wind farm data. In the case of solar PV, splicing was not necessary as there was no solar output during the period where the data exchange occurred, i.e. at and around mid-night on 1 July 2030.

The sizing of the nodal based VRE resources was sized to accommodate the zonal VRE capacities determined from the original 2019 ISP modelling by AEMO (AEMO, 2019b), after taking account of existing capacity of solar and wind farms located in each node, including any recently announced projects that have achieved financial close and/or decision to proceed to construction. For example, this included the 1026 GW McIntyre wind farm located in the SWQ node.

[15] Soiling refers to the build-up of substances like dust on module surfaces which are capable of reducing output over time. Remedies for this include depending upon rainfall for cleaning or building in provisions for module cleaning in O&M contracts.

For the information of interested stakeholders, the nameplate MW capacities and potential GWh energy available from these VRE resources for use in the modelling employed for each ISP scenario are reported in Tables 11 and 12. From inspection of Table 11, the ISP scenarios incorporated NEM wide wind farm capacity between 10 and 14.7 GW's and between 21.5 and 23.9 GW's for solar PV. In terms of GWh energy reported in Table 12, this falls within a range of 52.5 to 80.9 TWh's for wind and between 26.9 to 64.4 TWh of energy for solar PV. It should also be noted that the energy estimates in Table 12 refers to the potential energy available of the VRE resource available for dispatch.

Table 7: Nameplate MW capacities of nodal based VRE resources employed in ISP modelling by VRE resource type and ISP scenario

Node	Wind	Wind	Wind	Solar	Solar	Solar
	2030 central	2030 step change	2040 central	2030 central	2030 step change	2040 central
FNQ	700.0	1500.0	1675.0	49.0	49.0	49.0
ROSS	43.2	43.2	43.2	477.0	477.0	477.0
NQ	0.0	1000.0	1000.0	356.6	356.6	356.6
CWQ	306.0	900.0	900.0	1494.0	343.0	1494.0
GLAD	0.0	0.0	0.0	515.0	515.0	515.0
WB	0.0	0.0	0.0	173.0	500.0	500.0
TAR	728.5	1549.0	728.5	19.9	19.9	19.9
SWQ	1305.3	2125.8	1305.3	1683.5	1017.5	3830.5
ARM	445.0	1308.7	1945.7	280.0	1395.0	3706.0
TAM	0.0	0.0	1000.0	80.0	948.0	3259.0
MTP	143.1	143.1	143.1	0.0	0.0	0.0
WELLI	113.2	656.9	656.9	749.4	847.4	1322.6
MARU	473.2	473.2	473.2	10.0	10.0	10.0
YASS	255.6	255.6	255.6	0.0	0.0	0.0
CAN	576.5	776.5	776.5	33.0	33.0	33.0
WAGG	0.0	0.0	0.0	764.0	1823.8	1847.2
BURG	0.0	0.0	0.0	450.0	1009.8	1033.2
BRK H	198.9	198.9	198.9	53.0	53.0	53.0
MORW	139.6	139.6	139.6	0.0	0.0	0.0
SWV	3093.7	2843.7	2880.2	0.0	0.0	0.0
BALL	1762.4	1562.4	1609.8	0.0	0.0	0.0
KER	19.8	19.8	19.8	404.4	614.8	614.8
GLEN	457.6	457.6	244.1	462.8	673.2	673.2
HORSH	1012.1	812.1	859.5	0.0	369.0	319.0
RED CL	0.0	0.0	0.0	997.8	1208.2	1208.2
SESA	320.4	397.4	593.8	100.0	100.0	100.0
ADEL	33.7	33.7	142.7	0.0	0.0	0.0
RIV L	0.0	0.0	0.0	200.0	908.0	1126.7
MNSA	1432.1	2237.6	1842.2	0.0	0.0	0.0
UNSA	422.4	422.4	422.4	444.0	350.0	1091.3
EYRE P	136.0	136.0	136.0	220.0	220.0	220.0
BURN	139.8	139.8	139.8	0.0	0.0	0.0
FARRI	111.6	111.6	111.6	0.0	0.0	0.0
HADSP	168.0	168.0	168.0	0.0	0.0	0.0
WADDA	0.0	1069.8	451.8	0.0	0.0	0.0
TARREL	200.4	1219.2	601.2	0.0	0.0	0.0
Total	10016	14738	13841	22702	23859	21464

Table 8: Potential nodal VRE GWh energy available in ISP modelling by VRE resource type and ISP scenario

Node	Wind	Wind	Wind	Solar	Solar	Solar
	2030 central	2030 step change	2040 central	2030 central	2030 step change	2040 central
FNQ	2928.8	5817.2	6507.1	132.0	132.0	132.0
ROSS	145.0	145.0	145.0	1291.6	1291.6	1291.6
NQ	0.0	3148.9	3148.9	932.1	932.1	932.1

CWQ	1051.9	3096.3	3096.3	4076.9	946.3	4076.9
GLAD	0.0	0.0	0.0	1400.7	1400.7	1400.7
WB	0.0	0.0	0.0	451.3	1310.3	1310.3
TAR	2615.0	5278.0	2527.6	54.6	54.6	54.6
SWQ	4782.2	7125.0	4374.6	4723.4	2852.3	10755.1
ARM	1529.1	4542.8	6765.4	782.6	3867.1	10260.3
TAM	0.0	0.0	3413.4	214.4	2545.0	8749.1
MTP	499.5	499.5	499.5	0.0	0.0	0.0
WELLI	399.5	2314.0	2314.0	2058.8	2327.6	3630.9
MARU	1696.1	1696.1	1696.1	19.7	19.7	19.7
YASS	945.7	945.7	945.7	0.0	0.0	0.0
CAN	2169.6	2910.8	2910.8	84.7	84.7	84.7
WAGG	0.0	0.0	0.0	1984.0	4622.6	4680.8
BURG	0.0	0.0	0.0	1224.0	2746.9	2810.5
BRK H	693.7	693.7	693.7	139.3	139.3	139.3
MORW	477.3	477.3	477.3	0.0	0.0	0.0
SWV	11177.4	10281.5	10412.3	0.0	0.0	0.0
BALL	6038.9	5362.6	5522.9	0.0	0.0	0.0
KER	61.4	61.4	61.4	1064.5	1618.6	1618.6
GLEN	1382.3	1382.3	756.7	1068.9	1554.9	1554.9
HORSH	3500.6	2861.5	3012.9	0.0	918.6	794.1
RED CL	0.0	0.0	0.0	2628.4	3183.1	3183.1
SESA	1026.3	1272.5	1900.6	258.7	258.7	258.7
ADEL	103.6	103.6	498.9	0.0	0.0	0.0
RIV L	0.0	0.0	0.0	507.2	2341.2	2907.7
MNSA	5160.1	8027.9	6620.2	0.0	0.0	0.0
UNSA	1519.6	1519.6	1519.6	1274.5	997.4	3182.7
EYRE P	407.8	407.8	407.8	538.5	538.5	538.5
BURN	411.5	411.5	411.5	0.0	0.0	0.0
FARRI	321.1	321.1	321.1	0.0	0.0	0.0
HADSP	679.5	679.5	679.5	0.0	0.0	0.0
WADDA	0.0	4482.8	1891.8	0.0	0.0	0.0
TARREL	795.5	5065.6	2475.6	0.0	0.0	0.0
Total	52519	80932	76008	26911	36684	64367

The location of the nodes referenced in Tables 11 and 12 can be found in the schematic diagrams of the nodal structure of the model documented in Figures 1 to 6.

3.7.4 Analysis of 2030 pipeline and 2030 ISP central scenario VRE penetration capacity results for QLD

In Table 9 below, the comparative state GW capacities of wind and solar PV generation is outlined for the pipeline scenario and for the AEMO ISP (Neutral Scenario) modelling conducted for the 2019-20 ISP process for target years 2022, 2025 and 2030. The pipeline results are linked to the project installation assumptions reported Appendix B for the main completion years identified above. In contrast, the ISP results refer to VRE capacities determined from generation-expansion planning modelling, without reference, to the author's knowledge, to any particular planned projects in any of the existing State investment pipelines.

In Panel (A) of Table 9 for year 2022, some slight differences emerge between the ANEM and ISP results. In the case of QLD, the solar PV difference can be largely attributed to the inclusion of two additional solar farms in the pipeline modelling that were recently announced including Coloomboola (162 MW) and Gangarri (120 MW). Similar arguments extend to the other states as well in accounting for the slight differences between pipeline and ISP results.

Noticeable differences emerge between the GW capacities at 2025 as cited in Panel (B). In the case of QLD, pipeline capacity for wind is 2.96 GW compared with an ISP value of 1.28 GW. For solar PV, pipeline capacity is 5.52 GW compared with ISP value of 2.53 GW. The ISP results implies investment of 600 MW for wind and 700 MW for solar over the period 2022 to 2025. In contrast, the pipeline results point to investment in wind generation of 2280 MW and 3410 MW for solar PV over the same time period.

Noticeable differences continue to emerge between the GW capacities in 2030 reported in Panel (C). Specifically, for QLD, the 2030 pipeline baseline capacities for wind and solar PV are 4.82 GW and 8.73 GW. These compare with ISP values of 3.08 GW and 4.77 GW. The ISP implied investment rates for wind and solar PV over the period 2025 to 2030 are 1800 MW and 2240 MW compared with pipeline investment rates of 1860 MW and 3210 MW, respectively. Thus, ISP modelling results requires slightly lower rates of investment in both wind and solar PV over the 2025 to 2030 period than associated with the pipeline scenario. However, over the total 2022-2030 time period, the 2030 pipeline investment requirements are significantly higher than comparable ISP results. Specifically, the comparative results point to investment of 4140 MW and 6620 MW in wind and solar PV compared with 2400 MW and 2950 MW in the case of the ISP modelling over the period 2022 to 2030.

As a further point of comparison, investigation of the results in Table 9 also show that the pipeline results for completion year 2025 (in Panel B) for QLD are closest in magnitude to the ISP results for 2030 (in Panel C). Examining the results for QLD reported in Panel (B) indicate for pipeline modelling capacity values of 2.96 GW for wind and 5.52 GW for solar PV. This compares with 2030 ISP capacity values for wind and solar PV of 3.08 GW and 4.77 GW as listed in Panel (C). These results signify a deficit in pipeline wind generation capacity relative to the 2030 ISP result of 120 MW and a surplus capacity of 750 MW in the case of solar PV relative to the 2030 ISP result.

Table 9: VRE capacity (GW) by scenario, state and technology types

Panel (A). 2022 VRE Capacity (GW)

Scenario 2022	GW Wind	GW Solar PV	ISP GW Wind	ISP GW Solar PV
QLD	0.68	2.11	0.68	1.82
NSW	2.21	2.22	1.50	1.74
VIC	4.11	1.09	3.98	0.96
SA	2.34	0.87	2.14	0.38
TAS	0.57	0.00	0.57	0.00
Total	9.91	6.29	8.87	4.90
Combined Total		16.20		13.77

Differences between ANEM and ISP assumptions are primarily as a result of including recently announced, Coloomboola (162 MW) and Gangarri (120 MW) projects in Qld, and similar recent announcements in the other states.

Panel(B). 2025 VRE Capacity (GW)

Scenario 2025	GW Wind	GW Solar PV	ISP GW Wind	ISP GW Solar PV
QLD	2.96	5.52	1.28	2.53
NSW	3.60	3.69	1.50	1.74
VIC	4.87	1.88	4.56	1.22
SA	3.16	1.88	2.14	0.38
TAS	1.34	0.00	0.57	0.00
Total	15.94	12.98	10.05	5.87
Combined Total		28.91		15.92

ANEM modelling assumes that Q400 shortlisted projects and other projects proposed by reliable proponents are completed to full capacity whereas ISP modelling makes no assumptions about planned projects whatsoever.

Panel (C) 2030 VRE Capacity (GW)

Scenario 2030	GW Wind	GW Solar PV	ISP GW Wind	ISP GW Solar PV
QLD	4.82	8.73	3.08	4.77
NSW	5.67	8.02	1.50	2.14
VIC	6.48	2.08	6.48	1.86
SA	3.66	4.21	1.90	0.84
TAS	2.30	0.00	0.62	0.00
Total	22.94	23.04	13.58	9.61
Combined Total		45.98		23.19

ANEM modelling recognises project pipeline to ensure achievement of QRET.

4 Outcomes from of Modelled Scenarios

4.1 Modelled scenarios

Various scenarios were modelled involving the increased penetration of wind and solar PV over the 2022 to 2030 time period with targeted simulation year of 2030. Recall that two broad modelling approaches were undertaken. The first, termed the '2030 Pipeline Scenario', involved using historical based VRE resource assessment carried out for operational, under construction, and planned projects (i.e. investment pipeline projects). These projects are listed for each state in Tables 1 to 9 of Appendix B.

The second approach that was investigated involved modelling VRE penetration scenarios determined by AEMO as part of its ISP process. Specifically, three ISP scenarios were investigated:

- 2030 ISP central scenario;
- 2030 ISP step change scenario; and
- 2040 ISP central scenario.

4.1.1 2030 pipeline scenarios

Three broad construction pipelines were envisaged. The first, termed '2022' mainly encapsulated operational, under construction or projects with financial close that were likely to be completed by 2022.

The second scenario envisaged a target completion year of 2025. In the case of Queensland, many projects included were shortlisted Q400 projects as well as the Aldoga solar farm which had an existing PPA with the QLD Government and was expected to be completed by 2025. Additional projects chosen in QLD were largely in nodal areas favoured by AEMO in its ISP modelling and included both wind and solar projects in SWQ and CWQ regions. These projects also had proponents with a history of successful project completion and strong connection prospects through close location to major 275 kV Powerlink terminal stations.

The last completion year was 2030. These additional projects were also chosen on the basis of location, grid connectivity and strong proponents.

The base 2030 pipeline scenario was named the '2030 pipeline baseline scenario'. In accordance with the plant closures assumed in the AEMO ISP 2030 central scenario, the following plant closures were assumed under this particular scenario[16]:

- Callide B;
- Liddell;
- Vales Point;
- Unit 1, Eraring; and
- Yallourn.

The possibility of further leveraging higher renewable energy production share outcomes linked with the implementation of a policy of accelerated coal plant retirements was also investigated in the project. As such, additional scenarios were crafted around the 2030 pipeline baseline scenario outlined immediately above, but with more accelerated coal plant closures, including:

2030 pipeline scenario A additional closures:

[16] The Natural Gas Combined Cycle (NGCC) generator Swanbank E is also assumed to be closed by 2030.

- Unit 1, Stanwell;
- Units 1, 2, 5, 6 of Gladstone;
- Unit 1, Tarong; and
- Unit 2 of Eraring.

2030 pipeline scenario B additional closures:

- Units 1 and 2, Stanwell;
- Units 1, 2, 5, 6 of Gladstone;
- Units 1 and 2, Tarong; and
- All units of Eraring (i.e. units 2 to 4).

2030 pipeline scenario C additional closures:

- Units 1, 2, 5, 6 of Gladstone;
- All units of Tarong (i.e. units 1 to 4); and
- All units of Eraring.

4.1.2 ISP scenarios

The ISP time frames encapsulated either a 2030 or 2040 perspective with two scenarios utilising the 2040 ISP central scenario demand profiles within the modelling. These two scenarios, the 2040 central scenario and 2030 step change scenario can be viewed as separate 2030 step change scenarios with both accelerated demand and generation plant closure assumptions that move beyond the assumptions employed in relation to the ISP 2030 central scenario. Specifically, the broader step change process involved:

- Bringing forward later year demand profiles constructed around greater levels of behind the meter technology adoption rates especially reflected in rooftop solar PV uptake; and
- Applying a more accelerated programme of generation plant closures, especially amongst coal generation plant currently operating in the NEM.

Distinct sets of plant closure assumptions are applied for each ISP scenario. In the case of the 2030 ISP central scenario, the following plant closures were assumed[17]:

- Callide B;
- Liddell;
- Vales Point;
- Unit 1, Eraring; and
- Yallourn.

In the case of the 2040 ISP central scenario, the following additional plant retirements were also assumed:

- Gladstone and Tarong, all units;
- Tarong North;

[17] The Natural Gas Combined Cycle (NGCC) generator Swanbank E is also assumed to be closed by 2030.

- Bayswater and Eraring, all units; and
- Loy Yang A and B, all units.

In the case of the 2030 step change scenario, the following additional plant closure assumptions were applied:

- Gladstone and Tarong, all units;
- Loy Yang A.

In common with the modelling of the 2030 pipeline scenarios, the sensitivities discussed in relation to transmission structure, modelling of conventional and pump hydro generation and transmission losses continued to hold.

4.2 Analysis of 2030 pipeline scenario

The 2030 pipeline scenario targets year 2030. The baseline scenario includes VRE projects consistent with achieving State based 50% renewable energy targets. The composition of VRE projects are listed in Appendix B. Recall also that this scenario included the following transmission augmentations: (1) EnergyConnect; (2) HumeLink; (3) KerangLink; (4) Stage 2 QNI upgrade; and (5) Stage 1 of MarinusLink. Snowy 2.0 is also included in the modelling. Moreover Copperstring 2.0 is also assumed to be operational in order to open up the Far North Renewable Energy Zone around Hughenden. However, this transmission branch is internalised in the Ross node. However, this branch does not have any power flow implications apart from facilitating more VRE power production (both solar PV and wind) in the Ross node.

Four areas of analysis were investigated. First, in order to gauge the degree of VRE and renewable penetration, production shares by technology/fuel type was calculated. Second, the nature and extent of any VRE spillage was examined. Third, the direction of power flows on transmission branches and the incidence of transmission branch congestion was investigated to assess whether the grid structure currently supported the role out of renewable energy in the state. Fourth, the adequacy of existing generation resources was investigated from the perspective of system balancing.

These areas will be addressed in Sections 4.2.1 to 4.2.3, respectively.

4.2.1 Analysis of production shares by technology/fuel type

To assess production trends by technology type, production shares were calculated by summing half hourly production of all generators in Queensland according to technology and/or fuel type, converted to a GWh basis and then represented as a percentage of total production for the year of interest, in this case, 2030.

These calculations were performed for modelled scenarios based on: (1) P50 average demand; and (2) allocation of transmission losses according to receiving node (determined by the direction of power flow). Another defining feature of the modelled scenarios was whether the N or N-1 transmission structure was imposed in the modelling.

Production shares are reported in Table 10. Because of the focus on network adequacy for the broader transition process, transmission scenarios were distinguished with results associated with the N transmission scenario reported in Panel (A) and those associated with the N-1 transmission scenario reported in Panel (B).

In interpreting the results in Table 10, the fossil fuel component share is calculated as the sum of coal, and gas generation with the latter defined to include NGCC/GT, OCGT and diesel generation. The VRE share is calculated as the sum of wind and solar PV production shares. Finally, the renewable energy share is calculated as the sum of VRE and conventional hydro production shares. As such, dispatch from pump hydro is excluded from the calculation of renewable energy share.

It should also be noted that the results reported in Table 10 relate to the 'centralised' power system. Thus, production shares include that of utility-scale solar PV only and excludes the contribution of distributed (e.g. rooftop) solar PV. This reflects the focus of this report on decarbonisation options for the centralised power system. The report also focuses exclusively on production trends arising in Queensland.

The results in Table 10 point to a failure to achieve a 50% renewable energy target across all of the 2030 pipeline baseline scenarios. Renewable energy shares of 37.6% and 34.0% were obtained in Panels (A) and (B) respectively. In Panel (A), for scenario A, the renewable energy share is still well below 50% at 40.7%, increasing marginally to 41.8% and 41.5% under scenarios B and C. In the case of the N-1 transmission scenario, the renewable energy shares remain well below 50% for all scenarios, in the range of 37.7% to 38.8%.

Both wind and solar PV production shares increase across the scenarios reported in Table 10, falling between 17.7% and 18.6% for wind and between 19.8% and 22.9% for solar PV under the N transmission scenario. The equivalent range, under the N-1 scenario, is slightly lower for both VRE resources. In overall terms, VRE production share falls between 34.0% and 38.6% under the N-1 scenario and increases to between 37.5% and 41.5% under the N transmission scenario. Conventional hydro production shares are very low, between 0.03% and 0.24% whilst dispatch from pump hydro falls between 2.7% and 4.7%. In terms of annual GWh production, the pump hydro production shares equivalently fall between 2350 GWh and 3843 GWh as indicated in the last row of Table 10. Further, slightly higher levels of pump hydro dispatch arise under the N-1 transmission scenario.

Of further note is the observed drop in coal production share from between 52.3% and 52.6% under the baseline scenario, to between 37.7% and 38.4% under scenarios B and C. This result is on the back of significant closure of Queensland coal plant, including Gladstone units 1,2,5 and 6, and combinations of units 1 and 2 of Stanwell and Tarong or all units of Tarong, depending on the specifics of scenarios B and C.

Table 10: Production shares for 2030 pipeline scenarios: Large-scale QLD pump hydro included

Panel (A): N transmission scenario

Technology type	Baseline	Scenario A	Scenario B	Scenario C
Coal	52.32%	42.67%	37.82%	37.67%
Gas & Diesel	3.53%	6.06%	8.33%	8.56%
Hydro	0.03%	0.17%	0.24%	0.24%
PHES dispatch	2.71%	3.82%	4.16%	4.22%
Solar	19.81%	21.98%	22.87%	22.72%
Wind	17.71%	18.57%	18.63%	18.50%
Energy-Gap	3.88%	6.73%	7.94%	8.10%
Thermal	55.86%	48.73%	46.15%	46.23%
VRE	37.52%	40.55%	41.50%	41.22%
Renewable	37.55%	40.72%	41.75%	41.46%
Energy-Gap	3.88%	6.73%	7.94%	8.10%
Total Energy (GWh)	86589	84310	84214	84287
Spillage (GWh)	7594	5897	5134	5346
Solar (GWh)	6625	5248	4521	4634
Wind (GWh)	969	649	613	712
Energy-Gap (GWh)	3356	5670	6688	6824
PHES Dispatch (GWh)	2350	3222	3505	3554

Panel B: N-1 transmission scenario

Technology type	Baseline	Scenario A	Scenario B	Scenario C
Coal	52.60%	43.35%	38.42%	38.17%
Gas & Diesel	3.83%	5.69%	7.30%	8.17%
Hydro	0.03%	0.13%	0.22%	0.15%
PHES dispatch	3.26%	4.10%	4.73%	4.58%
Solar	17.74%	19.86%	20.94%	20.44%
Wind	16.23%	17.71%	17.67%	17.55%
Energy-Gap	6.32%	9.17%	10.72%	10.93%
Thermal	56.42%	49.04%	45.72%	46.34%
VRE	33.97%	37.57%	38.60%	37.99%
Renewable	34.00%	37.70%	38.83%	38.14%
Energy-Gap	6.32%	9.17%	10.72%	10.93%
Total Energy (GWh)	83075	81119	81228	80456
Spillage (GWh)	11864	9610	8729	9520
Solar (GWh)	9045	7671	6774	7333
Wind (GWh)	2820	1938	1955	2187
Energy-Gap (GWh)	5250	7438	8707	8796
PHES Dispatch (GWh)	2709	3324	3843	3686

An additional generation source that is identified in Table 10 is an item called 'Energy-Gap'. This component reflects the additional energy that has to be dispatched from new sources of generation over and above that of the existing generation fleet (whether thermal or renewable) to balance the network.

The modelling approach that has been utilised is technologically agnostic towards considerations of technology type in calculating the balancing requirements. The governing principal used in the modelling is to fully exhaust the potential contribution of existing generation resources in balancing the system during each dispatch interval. As such, any new additional balancing supply capacity is priced extremely high relative to the existing generation sources and thus represents a network balancing dispatch resource of last resort.[18] The new capacity will be dispatched if either unit commitment or transmission congestion prevents energy that is needed to balance the network on a node-by-node basis from reaching nodes requiring extra power in order to balance demand.

Inspection of Table 10 indicates that this component falls between 3.9% and 6.3% under the baseline scenario, depending on transmission scenario. This component then ramps up across scenarios A to C as increased plant retirements are incorporated into the modelling. Under the N transmission scenario, values increase from 6.7% under scenario A to 8.1% under scenario C. Under the N-1 scenario, the range of this component is larger in magnitude, increasing from 9.2% in scenario A to 10.9% in scenario C. These production shares translate into annual GWh energy requirements of between 3356 and 6824 GWh's under the N transmission scenario [listed in second last row of Panel (A)], and a higher range between 5250 to 8796 GWh's under the N-1 transmission scenario [listed in the second last row of Panel (B)].

Therefore, energy required for balancing is notably higher for the N-1 transmission scenario and increases as the extent of coal plant retirements increase, e.g. increasing across Scenarios A, B and C respectively. Although the MW capacity of coal plant closures is the same for Scenarios B and C

[18] This new balancing capacity offers supply at $20000/MWh, an offer well above any other competing supply offer of existing generation resources.

(e.g. 3220 MW)[19], the closure of all units of Tarong under Scenario C appears to generate lower VRE and larger system balancing requirement principally because of its closer geographic location to the large Queensland demand centres located in South East Queensland.

The higher values under the N-1 transmission scenario reflects the lower power transfer capacity arising under this scenario relative to the more expansive N transmission scenario. In the case of the former scenario, transmission branch congestion is more likely with an implied requirement of nodes possibly having to source required power from more 'localised' generation resources when branch congestion binds. In this circumstance, if the localised generation resource is not sufficient, then additional localised generation capacity would be required to balance the network regions adversely impacted by transmission branch congestion.

Finally, the annual GWh energy production values are also listed in Table 10. Inspection of these values indicate higher values under the N transmission scenario when compared with the N-1 transmission scenario. This outcome can be attributed to the greater transmission losses incurred under the N transmission scenario reflecting the higher MW capacities underpinning power transfers under this transmission scenario when compared to the more restrictive N-1 transmission scenario. Recall that the higher transmission losses are allocated as fictitious nodal demands to receiving end nodes of interconnected transmission branches, thereby increasing nodal demands and energy required to balance that demand.

4.2.2 VRE spillage

The spillage results for the 2030 Pipeline scenarios are reported in Table 11. For each scenario (e.g. baseline, A, B and C), the N and N-1 transmission scenario spillage results for both wind and solar generation are reported as separate panels.

For all scenarios, the spillage results are generally lower under the N transmission scenario reflecting the greater reach of energy from VRE sources associated with higher power transfer capabilities arising under the N transmission scenario when compared to the N-1 scenario[20]. Moreover, apart from the case of wind at the Wide Bay (WB) node, the spillage of wind power is generally significantly lower than is the case for solar PV at most Queensland nodes.

These two broad results are also discernible from inspection of Table 10. In the case of the N transmission scenario [Panel (A)], annual VRE energy spillage falls in the range 5134 GWh (scenario B) and 7594 GWH (baseline scenario). The annual totals can be further split between solar PV (4521 GWh to 6625 GWh) and wind (613 GWh to 969 GWh). In the case of the N-1 transmission scenario [Panel (B)], the annual VRE energy spillage outcomes were in the range of range 8729 GWh (scenario B) and 11864 GWH (baseline scenario). These outcomes represent notably significant increases over the equivalent results cited in Panel (A) of Table 10. Further, under the N-1 transmission scenario, the above annual totals can be further split between solar PV (6774 GWh to 9045 GWh) and wind (1938 GWh to 2820 GWh). Again, these compositional splits are much higher in magnitude than the equivalent results reported in Panel (A) of Table 10 associated with the N transmission scenario. More generally, spillage results are notably higher across both solar PV and wind power under the N-1 transmission scenario relative to the N transmission scenario across all pipeline scenarios.

From Table 11, for the Baseline scenario [Panels (A) and (B)], under the N-1 transmission scenario, spillage effects are particularly noticeable for both solar and wind power at the WB node, solar PV at Ross and South West Queensland (SWQ) nodes and to a slightly lower extent for solar PV at North Queensland (NQ), Central West Queensland (CWQ) and Gladstone nodes. In general, these nodes also experience spillage under the N transmission scenario [Panel (A)] although at lower rates (apart

[19] Specifically, coal closures underpinning Scenario B include Callide B (700 MW), units 1,2,5 and 6 of Gladstone (1120 MW), two units of Stanwell (700 MW) and two units of Tarong (700 MW), totalling 3220 MW. For Scenario C, coal closures include Callide B (700 MW), Gladstone units 1,2,5 and 6 (1120 MW) and all units of Tarong (1400 MW), also totally 3220 MW.

[20] The exception is solar PV spillage in the SWQ node which is marginally higher under the N transmission scenario.

from SWQ solar). However, a significant reduction in spillage is observed for both wind and solar PV at the WB node under the N scenario relative to the N-1 transmission scenario, e.g. down from 61.2% and 86.5% (under N-1) to 19.3% and 27.7% (under N).

In general, for both the N and N-1 transmission scenarios, the extent of spillage at the nodes identified above in relation to the baseline scenario (and identified VRE fuel types) decline in magnitude in the cases of scenarios A, B and C relative to the baseline outcomes. Notable reductions include wind and solar PV at WB node and solar PV at the Gladstone node especially for the N-1 scenario. Reductions are also recorded for solar PV spillage at NQ and CWQ nodes, especially under scenarios A and B. In the case of scenario C, Stanwell power station is unaffected by assumed coal plant closures thereby mitigating most of the reduction in solar PV spillage observed in the cases of scenarios A and B. Of further note, solar PV spillage at the Ross and SWQ nodes appear to be less affected by the additional coal plant retirements underpinning scenarios A, B and C.

From inspection of Table 11, a few key results are worth noting. First, the spillage rates for both solar and wind at the WB node most crucially depend upon the transmission scenario being assumed – much smaller spillage rates are recorded under the N scenario than under the N-1 scenario across all the Pipeline scenarios considered. Prospective coal plant closures play a much less important role but do drive some reductions under the N-1 scenario, e.g. down from 61% and 86% under the Baseline scenario to around 40% and 65% under scenarios A and B.

Table 11: Average VRE spillage rates for 2030 pipeline scenarios: Large-scale QLD pump hydro included

Node	FNQ	Ross	NQ	CWQ	GLAD	WB	TAR	SWQ	ARM	TAM
Panel (A): 2030 Pipeline Baseline Scenario: N Transmission Scenario										
Wind	1.02%	0.67%	1.79%	0.15%	NA	19.33%	0.21%	1.87%	2.77%	11.51%
Solar	0.19%	40.08%	20.24%	17.75%	15.98%	27.70%	2.42%	40.62%	33.72%	25.07%
Panel (B): 2030 Pipeline Baseline Scenario: N-1 Transmission Scenario										
Wind	**3.39%**	**2.41%**	**4.81%**	**0.33%**	**NA**	**61.17%**	**0.12%**	**1.62%**	**2.50%**	**10.11%**
Solar	0.69%	51.96%	28.61%	25.55%	23.44%	86.50%	0.65%	39.74%	29.60%	21.97%
Panel (C): 2030 Pipeline Scenario A: N Transmission Scenario										
Wind	**0.56%**	**0.42%**	**1.08%**	**0.32%**	**NA**	**13.00%**	**0.15%**	**1.29%**	**2.45%**	**10.79%**
Solar	0.28%	33.11%	14.05%	11.85%	8.55%	16.46%	1.19%	36.50%	31.71%	23.16%
Panel (D): 2030 Pipeline Scenario A: N-1 Transmission Scenario										
Wind	**3.41%**	**2.55%**	**4.46%**	**0.98%**	**NA**	**40.15%**	**0.12%**	**1.13%**	**2.21%**	**9.36%**
Solar	1.06%	48.87%	25.01%	21.96%	8.13%	64.84%	0.42%	35.83%	27.41%	20.08%
Panel (E): 2030 Pipeline Scenario B: N Transmission Scenario										
Wind	**0.64%**	**0.57%**	**1.01%**	**0.78%**	**NA**	**11.95%**	**0.30%**	**1.11%**	**2.16%**	**9.62%**
Solar	0.72%	28.29%	11.24%	9.40%	6.92%	15.01%	1.12%	32.33%	28.10%	19.95%
Panel (F): 2030 Pipeline Scenario B: N-1 Transmission Scenario										
Wind	**3.39%**	**2.68%**	**3.77%**	**2.27%**	**NA**	**40.84%**	**0.16%**	**0.96%**	**1.85%**	**7.87%**
Solar	2.48%	42.23%	19.45%	16.80%	6.86%	65.58%	0.36%	31.92%	22.95%	16.32%
Panel (G): 2030 Pipeline Scenario C: N Transmission Scenario										
Wind	**0.75%**	**0.66%**	**1.15%**	**0.87%**	**NA**	**13.98%**	**0.30%**	**1.08%**	**2.15%**	**9.55%**
Solar	0.80%	29.74%	11.95%	10.06%	6.97%	17.92%	1.16%	31.05%	27.95%	19.83%
Panel (H): 2030 Pipeline Scenario C: N-1 Transmission Scenario										
Wind	**4.84%**	**3.87%**	**5.50%**	**2.68%**	**NA**	**44.10%**	**0.14%**	**0.63%**	**1.84%**	**7.82%**
Solar	3.41%	48.92%	26.00%	23.32%	5.53%	69.27%	0.27%	28.33%	22.85%	16.25%

Second, solar PV spillage rates in the SWQ node do not appear to be very sensitive to either the underlying transmission scenarios or coal plant closure assumptions implemented. Across all scenarios and both transmission scenarios, SWQ spillage rates fall between 28.3% and 40.6%. This outcome most likely reflects limitations placed on VRE dispatch by the thermal plant located in this node which, because of its relatively young age, are not scheduled for closure until after 2040. This could have potential implications for AEMO ISP scenarios which target SWQ as a prominent Queensland renewable energy zone.

Third, solar PV spillage rates in the Ross node also appear to be quite invariant to coal plant retirement assumptions especially under the N-1 transmission scenario. More generally, solar PV spillage rates at northern and central nodes remain higher under scenario C when compared to scenario B. This reflects some further 'crowding-out' of VRE production associated with non-closure of the two Stanwell units occurring under scenario C.

Fourth, spillage of solar PV in SWQ and Ross nodes appear to remain the most persistent, being the least affected by transmission or coal closure assumptions.

Fifth, solar PV spillage rates at the Gladstone node fall significantly from 23.4% under baseline N-1 scenarios to around 6% to 7% under scenarios B and C.

4.2.3 Power flow direction and congestion

The ANEM model co-optimises transmission branch power flows along with generator dispatch. As part of this process, it applies nodal balance constraints which ensure that demand and supply balance at each node. A part of this balancing process is to optimise power flow between nodes to ensure that power flows from nodes with surplus generation to nodes with excess demand arise to balance supply and demand though out the network. This power flow is defined according to the nodal structure of the electricity network underpinning the modelling which defines power flow direction according to whether power flows towards or away from higher numbered nodes. The nodal structure of ANEM is documented in Figures 1 to 6. Normal direction power flow is defined as power flowing from a lower to higher numbered node interconnected by a transmission branch. In contrast, reverse direction power flow on the same transmission branch occurs when power flows from the higher to lower numbered node. Normal direction power flows will have a positive sign whilst reverse direction power flow will have a negative sign.

The power flow results are reported in Tables 12 and 13 for the N and N-1 transmission scenario for the four 2030 Pipeline Scenarios. Inspection of Table 12 indicates the predominance of normal direction power flows on all Queensland transmission branches. This generally signifies power flows from a north to south direction. Under the N transmission scenario, congestion is restricted primarily to Lines 7 and 14 which connect the WB and MN nodes, and Gold Coast and Lismore nodes.

As the level of coal plant retirements increase, moving from Pipeline scenarios A to C, the extent of normal direction power flows increase as more power from northern based generators is required to fill the supply gaps left by the coal plant retirements. There is some evidence of reduced congestion on Line 7 connecting WB and MN nodes and slightly higher congestion on Line 4 connecting NQ and Gladstone nodes particularly under scenario C. Recall that scenarios A to C involve the retirement of four units of Gladstone power station.

In overall terms, under the N transmission scenario and the four Pipeline scenarios, branch congestion appears to be quite mild except on Line 14 (Gold Coast to Lismore) which experiences congestion rates between 35% and 41%. The line next most impacted by congestion is Line 7 connecting WB and MN nodes which experiences congestion rates between 12% and 23.4%.

In Table 13, for the N-1 scenario, the extent of normal direction flows on Lines in north and central Queensland has moderated slightly although they still dominate power flow direction in absolute terms. This implies slightly higher dependence on localised sources of generation under the N-1 scenario. Congestion has become more prominent, especially on Lines 4 (connecting NQ and

Gladstone nodes), Line 7 (connecting WB and MN nodes), Line 10 (connecting SWQ and MS nodes) and Line 14 (connecting Gold Coast and Lismore nodes).

Congestion remains problematic on Line 4 connecting NQ and Gladstone under scenarios A to C, increasing under all of these scenarios relative to the baseline congestion result. For example, the congestion rate increases from 32.5% under the baseline scenario to 50.1% under scenario C (its highest value). The latter outcome is most likely linked to increased power flows from North Queensland towards Southern Queensland nodes to compensate for the loss of energy associated with the retirements of the Gladstone and Tarong units under scenario C. Recall under scenario C that no units of Stanwell were retired meaning that a greater composition of power generation remains operational in North and Central Queensland that can serve demand in more southern located nodes.

Congestion also remains problematic on Line 7 which connects the WB and MN nodes. In this case, there is a trend reduction in congestion over scenarios A to C relative to the baseline result, declining from 52.6% under the baseline scenario to 35.8% under scenario B (its lowest value). The slightly lower result under scenario B is likely linked to the partial retirement of Tarong units (i.e. only two units) which provides more local resources to help balance the large South East Queensland demand than arises under scenario C with the retirement of all Tarong units. In the latter case, more power from both northern and centrally located generators would be needed to help balance the supply-demand gap following the loss of all units of Tarong, prompting larger north to south power flows and an increased likelihood of congestion arising under the more restrictive transfer capacity of the N-1 transmission scenario.

Another transmission line experiencing congestion under the N-1 transmission scenario is Line 10 connecting the SWQ and MS nodes. Congestion on this line increases in magnitude from 28.9% under the baseline scenario to 37.9% under scenario C. This increased congestion would reflect increased power flows from the significant generation capacity located in the SWQ node to meet the large demand in MS node in response to retirements of coal plant especially at Tarong. This would be the principal reason accounting for the slightly higher congestion rates observed under scenario C (i.e. 37.9%) relative to scenario B (i.e. 34.5%). This is also borne out by the slightly lower extent of normal power flows on Line 8 connecting the Tarong and SWQ nodes under scenario C compared to scenario B. This points to relatively more power flowing from generators in the SWQ node to the Tarong node which can then be directed into South East Queensland via the MN node.

The other line experiencing considerable congestion is Line 14 that connects Gold Coast and Lismore nodes. Power flows predominately in a reverse direction on this Line, from Lismore to the Gold Coast. This trend increases as more coal retirements are modelled as power is sourced from NSW to help balance demand at the Gold Coast node. Congestion on this line also increases as more energy is sourced to offset the supply gap associated with coal plant retirement. The highest results under scenario C reflect the consequences on supply-demand balance in South East Queensland of the closure of all units of Tarong power station which is located much closer to the critical demand centres in South East Queensland than are Stanwell or Gladstone power stations

Table 12: Average transmission branch congestion and direction of flow results for 2030 pipeline scenarios: N transmission scenario

Panel (A): Baseline Scenario

	Line 1 FNQ-ROSS	Line 2 ROSS-NQ	Line 3 NQ-CWQ	Line 4 CWQ-GLAD	Line 5 CWQ-TAR	Line 6 GLAD-WB	Line 7 WB-NM	Line 8 TAR-SWQ	Line 9 TAR-SWQ
Node Paths	1-2	2-3	3-4	4-5	4-7	5-6	6-9	7-8	7-9
Flow direction: Normal (%)	71.74%	67.03%	68.24%	98.70%	98.70%	99.86%	99.99%	99.92%	100.00%
Flow direction: Reverse (%)	28.26%	32.97%	31.76%	1.30%	1.30%	0.14%	0.01%	0.08%	0.00%
Congestion (%)	0.00%	0.00%	0.00%	1.80%	0.00%	0.00%	23.40%	0.00%	0.00%

	Line 10 SWQ-SWQ-SM	Line 11 QNI-ARM	Line 12 NM-SM	Line13 SM-GC	Line 14 GC-DL-LIS
Node Paths	8-10	8-13	9-10	10-11	11-12
Flow direction: Normal (%)	100.00%	100.00%	100.00%	100.00%	50.08%
Flow direction: Reverse (%)	0.00%	0.00%	0.00%	0.00%	49.92%
Congestion (%)	0.00%	0.00%	0.00%	0.00%	36.38%

Panel (B): Scenario A

	Line 1 FNQ-ROSS	Line 2 ROSS-NQ	Line 3 NQ-CWQ	Line 4 CWQ-GLAD	Line 5 CWQ-TAR	Line 6 GLAD-WB	Line 7 WB-NM	Line 8 TAR-SWQ	Line 9 TAR-SWQ
Node Paths	1-2	2-3	3-4	4-5	4-7	5-6	6-9	7-8	7-9
Flow direction: Normal (%)	81.36%	74.47%	78.38%	99.95%	91.87%	95.81%	97.35%	98.78%	100.00%
Flow direction: Reverse (%)	18.64%	25.53%	21.62%	0.05%	8.13%	4.19%	2.65%	1.22%	0.00%
Congestion (%)	0.00%	0.00%	0.00%	3.96%	0.00%	0.00%	15.89%	0.00%	0.00%

	Line 10 SWQ-SWQ-SM	Line 11 QNI-ARM	Line 12 NM-SM	Line13 SM-GC	Line 14 GC-DL-LIS
Node Paths	8-10	8-13	9-10	10-11	11-12
Flow direction: Normal (%)	100.00%	100.00%	100.00%	100.00%	33.81%
Flow direction: Reverse (%)	0.00%	0.00%	0.00%	0.00%	66.19%
Congestion (%)	0.01%	0.00%	0.00%	0.00%	40.83%

Panel (C): Scenario B

	Line 1 FNQ-ROSS	Line 2 ROSS-NQ	Line 3 NQ-CWQ	Line 4 CWQ-GLAD	Line 5 CWQ-TAR	Line 6 GLAD-WB	Line 7 WB-NM	Line 8 TAR-SWQ	Line 9 TAR-SWQ
Node Paths	1-2	2-3	3-4	4-5	4-7	5-6	6-9	7-8	7-9
Flow direction: Normal (%)	85.52%	78.94%	82.57%	99.91%	90.14%	93.56%	95.70%	95.19%	100.00%
Flow direction: Reverse (%)	14.48%	21.06%	17.43%	0.09%	9.86%	6.44%	4.30%	4.81%	0.00%
Congestion (%)	0.00%	0.01%	0.00%	2.12%	0.00%	0.00%	12.38%	0.00%	0.00%

	Line 10 SWQ-SWQ-SM	Line 11 QNI-ARM	Line 12 NM-SM	Line13 SM-GC	Line 14 GC-DL-LIS
Node Paths	8-10	8-13	9-10	10-11	11-12
Flow direction: Normal (%)	100.00%	100.00%	99.97%	100.00%	31.70%
Flow direction: Reverse (%)	0.00%	0.00%	0.03%	0.00%	68.30%
Congestion (%)	0.03%	0.00%	0.00%	0.00%	36.00%

Panel (D): Scenario C

	Line 1 FNQ-ROSS	Line 2 ROSS-NQ	Line 3 NQ-CWQ	Line 4 CWQ-GLAD	Line 5 CWQ-TAR	Line 6 GLAD-WB	Line 7 WB-NM	Line 8 TAR-SWQ	Line 9 TAR-SWQ
Node Paths	1-2	2-3	3-4	4-5	4-7	5-6	6-9	7-8	7-9
Flow direction: Normal (%)	85.45%	78.85%	82.61%	99.98%	99.20%	98.61%	99.63%	90.56%	100.00%
Flow direction: Reverse (%)	14.55%	21.15%	17.39%	0.02%	0.80%	1.39%	0.37%	9.44%	0.00%
Congestion (%)	0.00%	0.00%	0.00%	7.38%	0.00%	0.00%	16.20%	0.00%	0.00%

	Line 10 SWQ-SM	Line 11 SWQ-QNI-ARM	Line 12 NM-SM	Line13 SM-GC	Line 14 GC-DL-LIS
Node Paths	8-10	8-13	9-10	10-11	11-12
Flow direction: Normal (%)	100.00%	100.00%	99.97%	100.00%	29.17%
Flow direction: Reverse (%)	0.00%	0.00%	0.03%	0.00%	70.83%
Congestion (%)	0.01%	0.00%	0.00%	0.00%	35.35%

Table 13: Average transmission branch congestion and direction of flow results for 2030 pipeline scenarios: N-1 transmission scenario

Panel (A): Baseline Scenario

	Line 1 FNQ-ROSS	Line 2 ROSS-NQ	Line 3 NQ-CWQ	Line 4 CWQ-GLAD	Line 5 CWQ-TAR	Line 6 GLAD-WB	Line 7 WB-NM	Line 8 TAR-SWQ	Line 9 TAR-SWQ
Node Paths	1-2	2-3	3-4	4-5	4-7	5-6	6-9	7-8	7-9
Flow direction: Normal (%)	67.92%	63.83%	64.87%	98.53%	98.03%	99.31%	100.00%	100.00%	100.00%
Flow direction: Reverse (%)	32.08%	36.17%	35.13%	1.47%	1.97%	0.69%	0.00%	0.00%	0.00%
Congestion (%)	0.07%	0.03%	0.00%	32.49%	0.00%	0.00%	52.60%	0.00%	0.00%

	Line 10 SWQ-SM	Line 11 SWQ-QNI-ARM	Line 12 NM-SM	Line13 SM-GC	Line 14 GC-DL-LIS
Node Paths	8-10	8-13	9-10	10-11	11-12
Flow direction: Normal (%)	100.00%	100.00%	98.46%	100.00%	30.17%
Flow direction: Reverse (%)	0.00%	0.00%	1.54%	0.00%	69.83%
Congestion (%)	28.86%	0.00%	0.00%	0.00%	38.79%

Panel (B): Scenario A

	Line 1 FNQ-ROSS	Line 2 ROSS-NQ	Line 3 NQ-CWQ	Line 4 CWQ-GLAD	Line 5 CWQ-TAR	Line 6 GLAD-WB	Line 7 WB-NM	Line 8 TAR-SWQ	Line 9 TAR-SWQ
Node Paths	1-2	2-3	3-4	4-5	4-7	5-6	6-9	7-8	7-9
Flow direction: Normal (%)	77.86%	69.09%	76.36%	99.97%	94.02%	95.90%	98.63%	99.93%	100.00%
Flow direction: Reverse (%)	22.14%	30.91%	23.64%	0.03%	5.98%	4.10%	1.37%	0.07%	0.00%
Congestion (%)	0.13%	0.03%	0.00%	45.06%	0.00%	0.00%	42.41%	0.00%	0.00%

	Line 10 SWQ-SM	Line 11 SWQ-QNI-ARM	Line 12 NM-SM	Line13 SM-GC	Line 14 GC-DL-LIS
Node Paths	8-10	8-13	9-10	10-11	11-12
Flow direction: Normal (%)	100.00%	100.00%	97.48%	100.00%	18.87%
Flow direction: Reverse (%)	0.00%	0.00%	2.52%	0.00%	81.13%
Congestion (%)	33.88%	0.00%	0.00%	0.00%	45.05%

Panel (C): Scenario B

	Line 1 FNQ-ROSS	Line 2 ROSS-NQ	Line 3 NQ-CWQ	Line 4 CWQ-GLAD	Line 5 CWQ-TAR	Line 6 GLAD-WB	Line 7 WB-NM	Line 8 TAR-SWQ	Line 9 TAR-SWQ
Node Paths	1-2	2-3	3-4	4-5	4-7	5-6	6-9	7-8	7-9
Flow direction: Normal (%)	83.31%	76.66%	86.28%	99.99%	93.73%	94.96%	97.82%	99.00%	100.00%
Flow direction: Reverse (%)	16.69%	23.34%	13.72%	0.01%	6.27%	5.04%	2.18%	1.00%	0.00%
Congestion (%)	0.34%	0.15%	0.00%	37.12%	0.00%	0.00%	35.78%	0.00%	0.00%

	Line 10 SWQ-SM	Line 11 SWQ-QNI-ARM	Line 12 NM-SM	Line13 SM-GC	Line 14 GC-DL-LIS
Node Paths	8-10	8-13	9-10	10-11	11-12
Flow direction: Normal (%)	100.00%	100.00%	96.81%	100.00%	19.95%
Flow direction: Reverse (%)	0.00%	0.00%	3.19%	0.00%	80.05%
Congestion (%)	34.75%	0.00%	0.00%	0.00%	40.88%

Panel (D): Scenario C

	Line 1 FNQ-ROSS	Line 2 ROSS-NQ	Line 3 NQ-CWQ	Line 4 CWQ-GLAD	Line 5 CWQ-TAR	Line 6 GLAD-WB	Line 7 WB-NM	Line 8 TAR-SWQ	Line 9 TAR-SWQ
Node Paths	1-2	2-3	3-4	4-5	4-7	5-6	6-9	7-8	7-9
Flow direction: Normal (%)	79.22%	69.81%	74.96%	100.00%	99.67%	98.67%	99.80%	95.05%	100.00%
Flow direction: Reverse (%)	20.78%	30.19%	25.04%	0.00%	0.33%	1.33%	0.20%	4.95%	0.00%
Congestion (%)	0.11%	0.02%	0.00%	50.14%	0.00%	0.00%	39.11%	0.00%	0.00%

	Line 10 SWQ-SM	Line 11 SWQ-QNI-ARM	Line 12 NM-SM	Line13 SM-GC	Line 14 GC-DL-LIS
Node Paths	8-10	8-13	9-10	10-11	11-12
Flow direction: Normal (%)	100.00%	100.00%	96.26%	100.00%	14.15%
Flow direction: Reverse (%)	0.00%	0.00%	3.74%	0.00%	85.85%
Congestion (%)	37.92%	0.00%	0.00%	0.00%	47.34%

Another key consequence of branch congestion is its potential impact on volume risk of VRE projects located in nodes adversely affected by branch congestion. VRE spillage is one form of volume risk. Another is congestion induced reductions in the maximum dispatched capacity relative to nameplate capacity. In the current context, nameplate capacities can be viewed as the maximum potential dispatch capacity while the maximum dispatched capacity is the actual dispatch MW level which could be lower than the nameplate capacity if spillage occurs. This outcome can be linked to spillage effects but not all spillage effects will necessarily involve a reduction in the maximum dispatched capacity relative to nameplate. These effects are demonstrated in Table 14 for both wind and solar PV under the N-1 transmission scenario for all four 2030 Pipeline scenarios.

The results for wind generation are reported in Panel (A). Results includes nameplate MW capacity and all maximum MW dispatched capacities for the four 2030 Pipeline Scenarios. The results for the WB node are shaded in green. In Section 4.2.2 of this chapter, significant levels of spillage of wind power were reported at the WB node, with spillage rates between 61.2% under the baseline scenario and increasing to 69.3% under scenario C. However, as seen from Panel (A) of Table 14, no reduction in maximum dispatched capacity was recorded for all Pipeline scenarios relative to this wind resource's nameplate MW capacity.

In contrast, reductions in maximum installed capacity relative to nameplate capacity was observed for solar PV as indicated in Panel (B) of Table 14. These cases are shaded in yellow in this panel. The most notable result can be seen in the case of maximum dispatch results for solar PV in the WB node which are all well below its nameplate capacity of 808 MW for each of the Pipeline Scenarios – falling between 396 MW and 614 MW. Similar situations also arise in relation to solar PV located at the Ross and SWQ nodes as also indicated through yellow shading.

This outcome not only affects project economics of individual projects locating in affected nodes, but also planning assessments because the maximum dispatched capacities indicate the maximum sizing of nodal VRE capacity that is consistent with dispatch and system balancing.

Table 14: Comparison of nameplate and maximum dispatched MW capacities for 2030 Pipeline scenarios: N-1 transmission scenario

Panel (A): Wind generation outcomes

Node	Nameplate Capacity	Baseline	Scenario A	Scenario B	Scenario C
FNQ	705	705	705	705	705
Ross	644	644	644	644	644
NQ	799	799	799	799	799
CWQ	180	180	180	180	180
GLAD	0	0	0	0	0
WB	1200	1200	1200	1200	1200
TAR	513	513	513	513	513
SWQ	779	779	779	779	779

Panel (B): Solar PV generation outcomes

Node	Nameplate Capacity	Baseline	Scenario A	Scenario B	Scenario C
FNQ	320	320	320	320	320
Ross	1785	1635	1700	1769	1644
NQ	1027	1027	1027	1027	1027
CWQ	943	943	943	943	943
GLAD	795	775	795	795	795
WB	808	396	566	614	500
TAR	620	620	620	620	620
SWQ	2439	2336	2353	2355	2356

4.3 Sensitivity of 2030 pipeline results to the inclusion of Mt Bryon and Urannah pump hydro plant in the modelling

One notable feature of the 2030 Pipeline scenarios discussed in Section 4.2 relates to the inclusion of the Mt Bryon and Urannah pump hydro plant in the modelling. Both of these pump hydro plants are sizeable with capacities of 1020 MW. Urannah is located in the NQ node whilst Mt Bryon is located in the MN node (adjacent to the existing Wivenhoe pump hydro power station). The intention underpinning the inclusion of these two pump hydro plants was to investigate how hydro generation might contribute towards attaining the 2030 renewable energy target and system balancing via two particular pathways:

- Indirect contribution using aggressive charging profiles utilising predominantly day-time charging profiles to enable greater production from solar PV resources which exhibited more spillage; and
- Direct contribution through active dispatch targeting morning and evening peak demand periods.

In this section, the consequences of dropping these two pump hydro plants will be investigated. Two particular metrics will be employed. The first will be to compare production shares arising when these two pump hydro plants are excluded from the modelling. The second metric will be to investigate any high-level impact on the underlying requirements for network balancing.

4.3.1 Analysis of production shares by technology/fuel type and VRE spillage

The production share results for the 2030 scenario with Mt Bryon and Urannah excluded from the modelling are presented in Table 15 with the results for the N transmission scenario reported in Panel (A) and the N-1 transmission scenario results in Panel (B).

The results in Table 15 point again to a general failure to achieve a 2030 50% renewable energy target across all of the 2030 Pipeline scenarios considered. *This outcome is not different from that experienced under the pipeline scenarios with the two-pump hydro plant included as discussed in Section 4.2.1.*

In Table 15, the maximum renewable production share achieved was under scenario B at 41.4% (N transmission scenario) and the lowest was under the baseline Scenario at 33.0% (N-1 transmission scenario). Equivalent VRE production rates fell between 32.9% and 41%. Conventional hydro production shares remained very small between 0.04% and 0.44% whilst pump-hydro dispatch contribution fell between 1.8% and 2.4%, marginally lower than the results reported in Table 10 in Section 4.2.1. In the latter case, this translates into an annual GWh energy range for pump-hydro dispatch of 1402 GWh to 1774 GWh in Table 15. This compares with the equivalent range of 2350 GWh to 3843 GWh in Table 10.

Comparison of the results for renewable energy production shares cited in Table 15 indicates a reduction in production share of 10.5% and 9.8% under the N and N-1 transmission scenarios, respectively, relative to the equivalent results cited in Table 10. Note that these results were obtained by calculating the percentage change in the renewable energy production shares in both Tables 10 and 15 and then averaging across all four scenarios, that is, the baseline as well as scenarios A, B and C.

These results indicate that the inclusion of these two pump hydro plants materially contributed towards attaining higher renewable production shares.

Table 15: Production shares for 2030 Pipeline scenarios: Large-scale QLD pump hydro excluded

Panel (A): N transmission scenario

Technology type	Baseline	Scenario A	Scenario B	Scenario C
Coal	56.07%	45.68%	40.30%	40.22%
Gas & Diesel	4.36%	8.82%	11.83%	12.06%
Hydro	0.04%	0.27%	0.41%	0.42%
PHES dispatch	1.77%	2.21%	2.31%	2.31%
Solar	17.49%	20.05%	21.16%	20.95%
Wind	18.65%	19.72%	19.81%	19.70%
Energy-Gap	1.63%	3.24%	4.18%	4.34%
Thermal	60.43%	54.50%	52.13%	52.28%
VRE	36.13%	39.77%	40.97%	40.65%
Renewable	36.17%	40.05%	41.38%	41.07%
Energy-Gap	1.63%	3.24%	4.18%	4.34%
Total Energy (GWh)	79089	76674	76616	76764
Spillage (GWh)	11510	9593	8698	8882
Solar (GWh)	9952	8408	7571	7699
Wind (GWh)	1558	1184	1126	1183
Energy-Gap (GWh)	1288	2487	3204	3330
PHES Dispatch (GWh)	1402	1698	1770	1774

Panel B: N-1 transmission scenario

Technology type	Baseline	Scenario A	Scenario B	Scenario C
Coal	57.33%	47.20%	41.89%	41.60%
Gas & Diesel	4.63%	7.49%	9.54%	10.68%
Hydro	0.10%	0.28%	0.44%	0.32%
PHES dispatch	1.96%	2.23%	2.38%	2.29%
Solar	15.99%	18.50%	19.68%	19.02%
Wind	16.89%	18.91%	18.90%	18.57%
Energy-Gap	3.11%	5.38%	7.17%	7.52%
Thermal	61.96%	54.69%	51.43%	52.28%
VRE	32.88%	37.42%	38.58%	37.59%
Renewable	32.98%	37.70%	39.03%	37.91%
Energy-Gap	3.11%	5.38%	7.17%	7.52%
Total Energy (GWh)	75713	73697	73613	73183
Spillage (GWh)	15191	15191	11685	12578
Solar (GWh)	11672	11672	9291	9864
Wind (GWh)	3518	3518	2393	2715
Energy-Gap (GWh)	2351	3964	5278	5503
PHES Dispatch (GWh)	1483	1645	1750	1676

Comparing the results for VRE energy production shares in Table 15 also indicate a reduction in production share of 10.8% under the N transmission scenario and 10.2% under the N-1 transmission scenario relative to the equivalent results cited in Table 10. Once again, these results were obtained

by calculating the percentage change in the VRE energy production shares in both Tables 10 and 15 and then averaging these results across all four Pipeline scenarios. *These results indicate that the uplift in VRE production associated with the charging profiles of the pump hydro plant was slightly greater under the N transmission scenario with an average uplift of 10.8%.*

The higher results associated with the N transmission scenario reflects the greater transfer capability arising under this scenario which produces a greater nodal reach for power transfer from VRE generation across the network thereby contributing to production share. This ability can be reduced under the more restrictive N-1 transmission scenario with the increased likelihood of congestion potentially islanding regions of the network thereby constraining output from all generation sources including VRE. In this circumstance, potential uplift in VRE production from pump actions of pump hydro plant would be mitigated.

In common with the results listed previously in Table 10 for VRE spillage, higher spillage rates were obtained for solar PV compared to wind power in Table 15. Moreover, more spillage occurred under the N-1 transmission scenario than arising under the N transmission scenario. Across the four pipeline scenarios and two transmission scenarios, spillage was greater in magnitude in Table 15 when compared to results reported in Table 10. *Thus, VRE spillage rates were higher in magnitude when Urannah and Mt Bryon were excluded in the modelling.*

Inspection of Table 15 also indicates that the production shares of both coal and thermal generation more generally are higher than comparable rates cited in Table 10 for both transmission scenarios and across all of the pipeline scenarios.

Examination of Table 15 also indicates that the energy-gap component has declined relative to the comparable results listed in Table 10. For example, the range in Table 15 encompasses production share of between 1.6% and 7.5% compared with an equivalent range of between 3.9% and 10.9% in Table 10 (e.g. with Urannah and Mt Bryon pump hydro included in the modelling). This translates into a GWh range of 1288 GWh to 5503 GWh in Table 15 compared with the equivalent range of 3356 GWh to 8796 GWhs in Table 10.

The lower energy-gap results associated with the case of excluding Urannah and Mt Bryon reflect two particular aspects. First, when the two pump-hydro plant are excluded, production shares of coal and thermal generation more generally were observed to increase notably compared to the case where the two-pump hydro plant are included in the modelling. This is likely to reduce variability in energy supply thereby reducing the need for balancing services whilst working against the renewable target and de-carbonising of the electricity supply. Second, and in contrast, when the two pump-hydro plant are included, VRE production shares increases notably whilst the production share of coal and other thermal generation declines. In this case, variability in electricity supply is likely to be increased with the underlying intermittency of VRE resources, thereby increasing the need for balancing services encapsulated in the energy-gap component.

4.4 Analysis of ISP 2030 central scenario

The 2030 ISP central scenario was a default scenario developed by AEMO. In this scenario, the following plant retirements were assumed: (1) Callide B (2) Swanbank E; (3) Liddell; (4) Vales Point; (5) one unit of Eraring; and (6) Yallourn. The Queensland production share results for the 2030 ISP central scenario are presented in Table 16 with the results for the N transmission scenario reported in Column 2 while the N-1 transmission scenario results are listed in Column 3.

A number of conclusions can be made. First, the renewable energy share for QLD under both transmission scenarios are well below 50%, instead, approximately 27.1%. Second, the VRE shares are quite close in magnitude under both transmission scenarios, between 27.0% and 27.1%. Conventional hydro production shares are very small, between 0.06% and 0.09% whilst pump hydro share is in the range of 3.5% to 4.0%. This translates into annual GWh production values between 3157 GWh and 3533 GWh. Third, the production shares of both wind and solar PV remain quite close across both transmission scenarios, in the range of 12.8% to 13.0% for wind and 14.0% to 14.3% for

solar PV. Fourth, the fossil fuel share remains well above 50%, in the range 61.5% to 63.8%. Finally, the energy used for balancing (e.g. the energy-gap component) falls between 5.5% and 7.3%. These production shares imply an annual GWh production range of 4905 GWh to 6389 GWh with the higher value arising under the more restrictive N-1 transmission scenario.

Table 16: Production shares for 2030 ISP Central Scenario

Technology Type	N Transmission Scenario	N-1 Transmission Scenario
Coal	59.38%	57.57%
Gas & Diesel	4.46%	3.97%
Hydro	0.06%	0.09%
PHES Dispatch	3.53%	4.05%
Solar	14.26%	14.04%
Wind	12.84%	12.96%
Energy-Gap	5.48%	7.32%
Thermal	63.84%	61.54%
VRE	27.09%	27.00%
Renewable	27.15%	27.09%
Energy-Gap	5.48%	7.32%
Total Energy (GWh)	89464	87291
Spillage	354	1029
Solar (GWh)	312	809
Wind (GWh)	42	220
Energy-Gap (GWh)	4905	6389
PHES Dispatch (GWh)	3157	3533

VRE spillage results for the 2030 ISP central scenario are reported in Panels (A) and (B) of Table 17 for the N and N-1 transmission scenarios respectively. Inspection of Panel (A) indicates very little spillage with the highest rate being 7.3% for solar PV at the WB node. The magnitude of spillage rates increased marginally in the case of the N-1 transmission scenario reported in Panel (B) with again WB solar having the highest rate of 18.6% followed by SWQ solar PV at 9.7%. Further, spillage of wind power across the nodes tends to be lower than comparable spillage rates of solar PV.

Inspection of Table 16 also indicates much higher spillage rates in the case of the N-1 transmission scenario. First, higher GWh spillage rates occur for solar PV compared to wind generation under both transmission scenarios. Second, higher GWh spillage rates arise under the N-1 transmission scenario compared to the N transmission scenario. For example, 1029 GWh under the N-1 transmission scenario compared to 354 GWh under the N transmission scenario.

Table 17: Average VRE spillage rates for 2030 ISP central scenario

Panel (A): N Transmission Scenario

Node/VRE	FNQ	Ross	NQ	CWQ	GLAD	WB	TAR	SWQ	ARM	TAM
Wind	0.56%	3.58%	NA	0.37%	NA	NA	0.11%	0.42%	0.22%	NA
Solar	1.25%	0.45%	0.44%	2.89%	5.29%	7.30%	3.75%	1.80%	0.41%	0.83%

Panel (B): N-1 Transmission Scenario

Node/VRE	FNQ	Ross	NQ	CWQ	GLAD	WB	TAR	SWQ	ARM	TAM
Wind	1.09%	4.26%	NA	0.61%	NA	NA	0.17%	3.51%	0.22%	NA
Solar	2.13%	0.76%	0.75%	5.08%	1.81%	18.65%	3.72%	9.71%	0.42%	0.82%

The power flow results associated with the 2030 ISP central scenario are reported in Panels (A) and (B) of Table 18 for the N and N-1 transmission scenarios. A number of results are notable. First, there is a predominance of reverse direction power flows in North Queensland, especially from CWQ to NQ (79.2%) and from NQ to Ross (62.9%). Normal direction power flows, however, dominate from FNQ to Ross (68.5%) under the N transmission scenario [cited in Panel (A)]. This outcome reflects the relatively large scale of wind generation at the FNQ node of approximately 700 MW – see Table 7. In this case, this sizeable capacity would exhaust FNQ demand under windy conditions and surplus wind power would be available to service demand and thus flow south to the Ross node.

These trends continue to occur at similar magnitudes under the N-1 transmission scenario as well [see Panel (B)]. Recall, in this context, that reverse direction power flows refer to power flowing from a south to north direction (i.e. towards North Queensland). The other line experiencing significant reverse direction power flows is Line 14 linking the Gold Coast and Lismore nodes. In this case, power flows from Lismore towards the Gold Coast. This power flow is to be expected as power is flowing towards the node with larger demand which is the Gold Coast node in this case.

Second, under the N transmission scenario, there is little evidence of congestion apart from Line 14 (Directlink) which has a low thermal rating of 180 MW. However, apart from Line 14, congestion increases under the N-1 transmission scenario on Lines 4 [CWQ to Gladstone (8%)], Line 7 [WB to MN (24.2%)] and Line 10 [SWQ to MS (23.5%)]. These are the same sets of transmission branches that experienced congestion under the N-1 scenario of the 2030 pipeline scenarios. In the case of Line 7, however, the congestion results listed above are much lower in magnitude than occurred under the 2030 Pipeline scenarios, reflecting the absence of wind generation at the WB node under the 2030 ISP central scenario.

Table 18: Average transmission branch congestion and direction of flow results for 2030 ISP central scenario

	Line 1 FNQ-ROSS	Line 2 ROSS-NQ	Line 3 NQ-CWQ	Line 4 CWQ-GLAD	Line 5 CWQ-TAR	Line 6 GLAD-WB	Line 7 WB-NM	Line 8 TAR-SWQ	Line 9 TAR-SWQ
Node Paths	1-2	2-3	3-4	4-5	4-7	5-6	6-9	7-8	7-9
Flow direction: Normal (%)	68.51%	37.08%	20.84%	99.32%	97.04%	100.00%	99.93%	98.22%	100.00%
Flow direction: Reverse (%)	31.49%	62.92%	79.16%	0.68%	2.96%	0.00%	0.07%	1.78%	0.00%
Congestion (%)	0.00%	0.00%	0.00%	0.08%	0.00%	0.00%	0.98%	0.00%	0.00%

	Line 10 SWQ-SM	Line 11 SWQ-QNI-ARM	Line 12 NM-SM	Line13 SM-GC	Line 14 GC-DL-LIS
Node Paths	8-10	8-13	9-10	10-11	11-12
Flow direction: Normal (%)	100.00%	100.00%	97.01%	100.00%	60.75%
Flow direction: Reverse (%)	0.00%	0.00%	2.99%	0.00%	39.25%
Congestion (%)	0.03%	0.00%	0.00%	0.00%	24.13%

Panel (B): N-1 Transmission Scenario

	Line 1 FNQ-ROSS	Line 2 ROSS-NQ	Line 3 NQ-CWQ	Line 4 CWQ-GLAD	Line 5 CWQ-TAR	Line 6 GLAD-WB	Line 7 WB-NM	Line 8 TAR-SWQ	Line 9 TAR-SWQ
Node Paths	1-2	2-3	3-4	4-5	4-7	5-6	6-9	7-8	7-9
Flow direction: Normal (%)	65.70%	33.76%	16.53%	99.54%	97.99%	99.99%	99.97%	99.72%	100.00%
Flow direction: Reverse (%)	34.30%	66.24%	83.47%	0.46%	2.01%	0.01%	0.03%	0.28%	0.00%
Congestion (%)	0.61%	0.00%	0.01%	7.96%	0.00%	0.00%	24.16%	0.00%	0.00%

	Line 10 SWQ-SM	Line 11 SWQ-QNI-ARM	Line 12 NM-SM	Line13 SM-GC	Line 14 GC-DL-LIS
Node Paths	8-10	8-13	9-10	10-11	11-12
Flow direction: Normal (%)	100.00%	100.00%	98.52%	100.00%	56.87%
Flow direction: Reverse (%)	0.00%	0.00%	1.48%	0.00%	43.13%
Congestion (%)	23.47%	0.00%	0.00%	0.00%	20.90%

4.5 Analysis of ISP 2030 step change scenario

The 2030 ISP step change scenario was a scenario developed by AEMO to represent a situation whereby more effort was undertaken to meet the longer-term decarbonisation objectives consistent with Paris obligations. This scenario encompassed a number of differences compared to the 2030 central scenario considered in the previous section. First, more aggressive uptake of behind the meter technologies was assumed including the uptake of rooftop solar PV. In the modelling, this was accommodated by using the 2040 ISP central scenario's 2040 demand profile which had a similar level of rooftop solar PV uptake to that associated with the 2030 Step Change Scenario. Second, a more aggressive accelerated retirement of existing generation plant was adopted. In Queensland, the plant assumed to be retired included: (1) Callide B; (2) Swanbank E; (3) Gladstone; and (4) Tarong. This represented an aggregate capacity withdrawal of more than 4 GW's of generation capacity in Queensland alone.

In this section, separate sub-sections will address production share outcomes, spillage effects and branch flow outcomes.

4.5.1 Analysis of production shares by technology/fuel type

The production share results for the 2030 ISP step change scenario are presented in Table 19 with the results for the N transmission scenario again reported in Column 2 while the N-1 transmission scenario results are listed in Column 3.

A number of conclusions follow from inspection of this table. First, the renewable energy share for QLD under both transmission scenarios notionally falls well below 50% in the range of 36.9% to 37.6%. This compilation rests on production shares between 26.3% and 27.5% for wind, 10.0% to 10.6% for solar PV and 0.07% to 0.14% for conventional hydro. Pump-hydro dispatch contribution falls between 5.0% and 5.5%. These production shares are larger than the shares reported in Table 16 associated with the ISP 2030 central scenario as well as for all pipeline scenarios reported in Table 10. In the current case, the above production shares translate into an annual GWh energy range for pump-hydro dispatch of 4410 GWh to 4556 GWh in Table 19. This compares with the equivalent range of 2350 GWh to 3843 GWh in Table 10 and 3157 GWh to 3533 GWh in Table 16.

Of particular note is the increased production share associated with wind generation relative to that of solar PV. This reflects the underlying VRE composition determined by AEMO for this scenario which was particularly wind heavy.

Second, the VRE share is also quite close in magnitude under both transmission scenarios, in the range of 36.9% to 37.5%.

Third, the fossil fuel share is now below 50%, in the range of 41.2% to 46.5%, depending on transmission scenario. The lower value under the N-1 scenario primarily reflects lower production shares across coal, NGCC and OCGT power production.

In contrast to the 2030 central scenario, the energy associated with the energy-gap component has increased significantly, especially under the N-1 transmission scenario. In the case of the N transmission scenario, balancing activities utilised 10.8% of all energy produced, up from 5.5% in Table 16 for the ISP 2030 central scenario. Further, under the N-1 transmission scenario, this production share increased to 16.3%, up from 7.3% recorded in Table 16. In the current case, these production shares translate into annual GWh production totals of 9542 GWh and 13388 GWh for the N and N-1 transmission scenarios, respectively. These values represent significant increases on the equivalent values of 4905 GWh and 6389 GWh reported in Table 16 for the 2030 central scenario as well as the values listed for all pipeline scenarios in Table 10.

Table 19: Production shares for 2030 ISP step change scenario

Technology Type	N Transmission Scenario	N-1 Transmission Scenario
Coal	36.26%	34.16%
Gas & Diesel	10.23%	7.05%
Hydro	0.14%	0.07%
PHES Dispatch	5.02%	5.54%
Solar	10.01%	10.61%
Wind	27.49%	26.27%
Energy-Gap	10.85%	16.30%
Thermal	46.49%	41.21%
VRE	37.50%	36.88%
Renewable	37.64%	36.95%
Energy-Gap	10.85%	16.30%
Total Energy (GWh)	87914	82161
Spillage	571	3238
Solar (GWh)	124	204
Wind (GWh)	447	3034
Energy-Gap (GWh)	9542	13388
PHES Dispatch (GWh)	4410	4556

4.5.2 VRE spillage rates

VRE spillage results for the 2030 step change scenario are reported in Panels (A) and (B) of Table 20 for the N and N-1 transmission scenarios. Examination of Panel (A) indicates very little spillage with the highest rate being 5.5% for wind power at the Ross node. However, the magnitude of spillage rates increased noticeably under the N-1 transmission scenario as reported in Panel (B). In this case, the highest spillage rate is wind power at the FNQ node of 25.8% followed by 14.3% and 13.5% respectively for wind power at the neighbouring Ross node and at the SWQ node. In contrast to the results obtained in relation to the 2030 central scenario, in the step change scenario, spillage rates are generally higher across all the nodes for wind generation when compared to solar PV[21]. This, in turn, reflects the wind heavy composition of VRE generation assumed for this particular ISP scenario.

Inspection of Table 19 also indicates much higher spillage rates in the case of the N-1 transmission scenario. First, higher GWh spillage rates occur for wind compared to solar PV generation under both transmission scenarios. This result clearly represents a compositional shift in VRE resources relative to the results reported in Table 16. Second, higher GWh spillage rates continue to arise under the N-1 transmission scenario compared to the N transmission scenario. For example, 3238 GWh under the N-1 transmission scenario and 571 GWh under the N transmission scenario. This compares with 1029 GWh under the N-1 transmission and 354 GWh under the N transmission scenario associated with the 2030 ISP central scenario identified in Table 16.

4.5.3 Direction of power flow and branch congestion outcomes

The power flow results associated with the 2030 step change scenario are reported in Table 21 for the N and N-1 transmission scenarios which are reported in Panels (A) and (B), respectively. A

[21] The exceptions to this occur at the Tarong and Armidale nodes.

number of results can be identified. First, there is a predominance of normal direction power flows on all lines except for Line 14 linking Gold Coast and Lismore. This outcome deviates from the results found for many northern lines in the previous section relating to the ISP 2030 central scenario. This principally reflects the greater incidence of wind and solar PV generation capacity located at the FNQ, NQ and CWQ nodes which will be sufficient to more than satisfy demand prevailing in FNQ, Ross NQ and CWQ nodes when VRE resource yield is good. This means that surplus power from VRE is available to satisfy demand located further south of these nodes, effected through normal direction power flows from the northern nodes towards the southern located nodes.

Second, there is an 'increased' incidence of reverse power flow on Line 8 linking the Tarong and SWQ nodes. This implies that power from generation located in the SWQ node flows north to the Tarong node. Recall that in the case of the 2030 step change scenario, the Tarong power station has been retired with only Tarong North remaining in operation. This contrasts with sizeable wind and solar PV generation and thermal plant being located in the SWQ node under this scenario[22]. Power flowing to the Tarong node from the SWQ node can then flow into the demand heavy MN and MS nodes. Thus, the SWQ-Tarong-MN-MS pathway constitutes a second important transmission pathway that generation located in the SWQ node can supply the main South East Queensland demand centres located in the MN and MS nodes. The other main pathway is the more direct pathway on Line 10 linking SWQ to MS node.

Congestion patterns under the N transmission scenario are generally quite low with the highest rates being recorded for Line 14 (31.3%) followed by Line 4 connecting the CWQ and Gladstone nodes (17%).

Under the N-1 transmission scenario, some qualitative changes emerge. First, reverse direction power flows become relatively more prominent especially on Lines 2 and 3 connecting the Ross and NQ nodes and NQ and CWQ nodes, respectively. Recall that reverse direction flows signify power flowing from south to north, that is, towards the northern located node. Power flows on Line 1 continue to be predominantly in a normal direction, from north to south. This is not unexpected given the relatively large wind capacity located at the FNQ node under this scenario and with any surplus generation only being able to flow south from the FNQ node. There is also an increased incidence of reverse power flows on other transmission branches but they still have a predominant normal direction of power flow, that is from a north to south direction. This points to the fact that under the more restrictive N-1 transmission scenario with its reduced power transfer capability, more power has to be directed from more southern located nodes such as SWQ, Tarong and WB to more northern located nodes. Given that these lines still have predominantly normal direction power flows (e.g. north to south), it does not happen in general terms, but there is a definite uptick in such reverse power flows relative to that arising under the N transmission scenario. This trend is especially evident for Lines 5, 6, 7 and 8 interconnecting the CWQ and Tarong nodes, Gladstone and WB nodes, WB and MN nodes and Tarong and SWQ nodes.

There was also a significant increase in congestion on certain transmission branches under the more restrictive N-1 transmission scenario. This included Line 4 interconnecting the CWQ and Gladstone nodes (56.4%), Line 7 interconnecting the WB and MN nodes (13.9%), Line 10 connecting SWQ and MS nodes (52.1%) and Line 14 interconnecting Gold Coast and Lismore nodes (55%). In this context, it is of note that Lines 7 and 10 experienced no real congestion under the N transmission scenario[23].

The congestion observed on Line 10 is particularly worrisome as this constitutes one of the main transmission pathways that is available to supply power from the sizeable generation fleet located in the SWQ node (both renewable and thermal) to the large demand centres located in the MS node as well as further on to the Gold Coast node. With the closure of the Tarong power station, system balancing will become more dependent on power supplied from the large SWQ generation fleet

[22] It should be noted that there is also a significant wind generation component (e.g. 1549 MW) located at the Tarong node but a very small solar PV component (20 MW).

[23] Also discounting the extremely small congestion results of 0.15% associated with Line 10 in Panel (A) of Table 18.

balancing demand in South East Queensland. However, this function could be adversely affected if power is restricted from balancing demand by the incidence of branch congestion.

Second, the significant congestion on Line 4 is also problematic given the greater dependence potentially placed on the sizeable generation fleet in CWQ node to supply power to balance the large baseload demand occurring in Gladstone associated with aluminium and alumina smelting and processing, especially after the retirement of Gladstone power station.

Table 20: Average VRE spillage rates for 2030 ISP step change scenario

Panel (A): N Transmission Scenario

Node/VRE	FNQ	Ross	NQ	CWQ	GLAD	WB	TAR	SWQ	ARM	TAM
Wind	4.67%	5.50%	1.39%	1.42%	N.A.	N.A.	0.37%	0.66%	1.21%	N.A.
Solar	2.34%	0.81%	0.87%	0.88%	2.06%	4.25%	3.40%	0.50%	3.57%	1.35%

Panel (B): N-1 Transmission Scenario

Node/VRE	FNQ	Ross	NQ	CWQ	GLAD	WB	TAR	SWQ	ARM	TAM
Wind	25.76%	14.33%	8.11%	8.48%	N.A.	N.A.	0.30%	13.54%	1.03%	N.A.
Solar	10.41%	3.17%	3.26%	3.28%	0.37%	1.17%	3.88%	2.68%	2.95%	1.18%

Table 21: Average transmission branch congestion and direction of flow results for 2030 ISP step change scenario

Panel (A): N Transmission Scenario

	Line 1 FNQ-ROSS	Line 2 ROSS-NQ	Line 3 NQ-CWQ	Line 4 CWQ-GLAD	Line 5 CWQ-TAR	Line 6 GLAD-WB	Line 7 WB-NM	Line 8 TAR-SWQ	Line 9 TAR-SWQ
Node Paths	1-2	2-3	3-4	4-5	4-7	5-6	6-9	7-8	7-9
Flow direction: Normal (%)	82.42%	68.70%	69.56%	100.00%	95.25%	98.06%	95.25%	75.84%	100.00%
Flow direction: Reverse (%)	17.58%	31.30%	30.44%	0.00%	4.75%	1.94%	4.75%	24.16%	0.00%
Congestion (%)	1.02%	0.00%	0.00%	17.00%	0.00%	0.00%	0.00%	0.00%	0.00%

	Line 10 SWQ-SM	Line 11 SWQ-QNI-ARM	Line 12 NM-SM	Line13 SM-GC	Line 14 GC-DL-LIS
Node Paths	8-10	8-13	9-10	10-11	11-12
Flow direction: Normal (%)	100.00%	100.00%	95.45%	99.88%	31.85%
Flow direction: Reverse (%)	0.00%	0.00%	4.55%	0.12%	68.15%
Congestion (%)	0.15%	0.00%	0.00%	0.00%	31.32%

Panel (B): N-1 Transmission Scenario

	Line 1 FNQ-ROSS	Line 2 ROSS-NQ	Line 3 NQ-CWQ	Line 4 CWQ-GLAD	Line 5 CWQ-TAR	Line 6 GLAD-WB	Line 7 WB-NM	Line 8 TAR-SWQ	Line 9 TAR-SWQ
Node Paths	1-2	2-3	3-4	4-5	4-7	5-6	6-9	7-8	7-9
Flow direction: Normal (%)	76.97%	46.64%	42.07%	100.00%	81.25%	83.46%	75.98%	86.70%	100.00%
Flow direction: Reverse (%)	23.03%	53.36%	57.93%	0.00%	18.75%	16.54%	24.02%	13.30%	0.00%
Congestion (%)	3.82%	0.00%	0.00%	56.39%	0.00%	0.00%	13.93%	0.00%	0.00%

	Line 10 SWQ-SM	Line 11 SWQ-QNI-ARM	Line 12 NM-SM	Line13 SM-GC	Line 14 GC-DL-LIS
Node Paths	8-10	8-13	9-10	10-11	11-12
Flow direction: Normal (%)	100.00%	100.00%	96.96%	99.87%	13.54%
Flow direction: Reverse (%)	0.00%	0.00%	3.04%	0.13%	86.46%
Congestion (%)	52.13%	0.00%	0.00%	0.00%	55.01%

4.6 Analysis of ISP 2040 central scenario

The 2040 ISP central scenario was developed by AEMO and built on the 2030 central scenario to represent a situation where over the additional decade encompassing the 2030-2040 time-frame, further steps were taken to approach the longer-term decarbonisation objectives consistent with Paris obligations. A key feature of this scenario was the closure of many coal-fired power stations that reached their end of useful life status during 2030 to 2040 decade. In relation to Queensland, coal retirements arising during this decade included Gladstone, Tarong and Tarong North power stations. Other smaller plant closures in Queensland included Kareeya hydro, Mt Stuart, Barcaldine and Roma power stations. These closures are in addition to the 2030 closures associated with Callide B and Swanbank E assumed under the 2030 ISP central scenario. Restricting consideration to coal plant and Swanbank E only, the total combined capacity of these plant closures in Queensland represented 4608 MW of capacity. In NSW, over this decade all units of Eraring and Bayswater power stations were assumed to be retired amounting to 5520 MW, in addition, to the earlier plant closures of Liddell and Vales Point associated with the 2030 ISP central scenario, amounting to a combined capacity of 8840 MW of retired coal capacity by 2040 in New South Wales.

In this section, separate sub-sections will address production share outcomes, spillage effects and branch flow outcomes under this ISP scenario.

4.6.1 Analysis of production shares by technology/fuel type

The production share results for the 2040 ISP central scenario are reported in Table 22 with the results for the N transmission scenario in Column 2 while the N-1 transmission scenario results are in Column 3.

Examination of this table offers a number of conclusions. First, the renewable energy share for Queensland under the N transmission scenario remained below 50% at 41.5%. In the case of the N-1 transmission scenario, the renewable production also remains below 50% at 38.2%. These results rest upon production shares between 20.5% and 21.2% for wind and between 17.7% and 20.2% for solar PV and between 0.06% to 0.13% for conventional hydro. Pump-hydro dispatch contribution is between 5.2% and 5.8%, marginally up on the equivalent values cited in Table 19 associated with the 2030 step change scenario. In the current case, the above production shares translate into an annual GWh energy range for pump-hydro dispatch of 4675 GWh to 4860 GWh in Table 22.

Second, VRE shares listed in Table 22 fall in the range of 38.1% to 41.4% with the lower production share arising under the N-1 transmission scenario. This contrasts with the equivalent results in Table 19 which are between 36.9% and 37.5%.

Third, the fossil fuel share is now well below 50%, in the range of 38.0% to 42.3%, depending on transmission scenario. Of note again, the lower share is recorded under the N-1 transmission scenario.

The energy associated with the energy-gap component has increased slightly above the results for the 2030 step change scenario. In the case of the N transmission scenario, balancing activities utilised 11.0% of all energy produced, up from 10.9% in Table 19 for the ISP 2030 step change scenario. Further, under the N-1 transmission scenario, this production share increased to 17.9%, up from 16.3% recorded in Table 19. In the current case, these production shares translate into annual GWh production totals of 9826 GWh and 14925 GWh for the N and N-1 transmission scenarios, respectively. These values again represent slight increases on the equivalent values of 9542 GWh and 13388 GWh reported in Table 19 for the 2030 step change scenario.

Note that the larger energy-gap component under the N-1 transmission scenario helps balance the falls in both VRE and fossil fuel production shares reported in Table 22 relative to results associated with the N transmission scenario. Finally, the increase in energy-gap component associated with the 2040 central scenario would also reflect the larger extent of coal plant closures assumed under this scenario compared to the 2030 ISP step change scenario.

Table 22: Production shares for 2040 ISP central scenario

Technology Type	N Transmission Scenario	N-1 Transmission Scenario
Coal	29.67%	28.29%
Gas & Diesel	12.60%	9.76%
Hydro	0.13%	0.06%
PHES Dispatch	5.22%	5.83%
Solar	20.18%	17.67%
Wind	21.23%	20.48%
Energy-Gap	10.96%	17.92%
Thermal	42.28%	38.05%
VRE	41.42%	38.14%
Renewable	41.54%	38.20%
Energy-Gap	10.96%	17.92%
Total Energy (GWh)	89628	83307
Spillage	2641	7985
Solar (GWh)	1865	5237
Wind (GWh)	775	2748
Energy-Gap (GWh)	9826	14925
PHES Dispatch (GWh)	4675	4860

4.6.2 VRE spillage rates

VRE spillage results for the 2040 central scenario are reported in Panels (A) and (B) of Table 23 for the N and N-1 transmission scenarios. Examination of Panel (A) indicates low spillage rates with the highest rate (for a Queensland node) being 14.4% for solar power at the SWQ node although higher spillage rates are recorded across the NSW border for solar PV at both the Armidale and Tamworth nodes of 27.7% and 19.9%, respectively. The highest spillage rate recorded for wind is 9.2% at the FNQ node.

The magnitude of spillage rates increased noticeably under the N-1 transmission scenario across most of the nodes as reported in Panel (B). In this case, the highest spillage rate is solar PV is in the SWQ node at 40.5%, followed by wind power at the FNQ node with a spillage rate of 31.6%. Under the N-1 transmission scenario, the top two spillage rates are significant given that AEMO is targeting these two nodes explicitly with these sources of VRE generation.

Examination of Table 22 also indicates much higher spillage rates in the case of the N-1 transmission scenario. First, higher GWh spillage rates occur for solar compared to wind generation under both transmission scenarios. This outcome qualitatively mirrors the results associated with the 2030 central scenario (Table 16) but contrasts with the results associated with the 2030 step change scenario (Table 19) which had greater spillage of wind power. Second, higher GWh spillage rates continue to arise under the N-1 transmission scenario compared to the N transmission scenario. In the current case,7985 GWh under the N-1 transmission scenario and 2641 GWh under the N transmission scenario. This compares with 3238 GWh under the N-1 transmission and 571 GWh under the N transmission scenario associated with the 2030 ISP step change scenario identified in Table 19. Thus, aggregate GWh spillage is notably higher under the 2040 central scenario when compared with the 2030 step change scenario.

4.6.3 Direction of power flow and branch congestion outcomes

The power flow results associated with the 2040 central scenario are reported in Panels (A) and (B) of Table 24 for the N and N-1 transmission scenarios. A number of results are forthcoming from inspection of this table. First, under the N transmission scenario [Panel (A)], there is a predominance of normal direction power flows on all lines except for Lines 8 and 14 linking Tarong and SWQ and Gold Coast and Lismore nodes, respectively. This result mirrors the results associated with the 2030 step change scenario in that the greater incidence of wind and solar PV generation capacity located at the FNQ, NQ and CWQ nodes will be sufficient to more than satisfy demand prevailing in FNQ, Ross, NQ and CWQ nodes when VRE resource yield is good. This means that surplus power from VRE is available to satisfy the large demand centres located further south of these nodes.

Second, there is a predominance of reverse power flow on Line 8 linking the Tarong and SWQ nodes. This implies that power from generation located in the SWQ node generally flows north to the Tarong node. Recall that for the 2040 central scenario, both the Tarong and Tarong North power stations have been retired. This contrasts with sizeable wind and particularly solar PV generation and thermal plant located in the SWQ node under this scenario[24]. Power flowing to the Tarong node from the SWQ node can then flow into the demand heavy MN and MS nodes.

Under both the N and N-1 transmission scenarios,100% of the power flow on Line 11 (e.g. QNI) occurs in a normal direction, from SWQ to Armidale. Therefore, the power flow from SWQ to Tarong is being supplied purely from SWQ generation resources and not from power inflows from NSW on the QNI interconnector.

Congestion patterns under the N transmission scenario are generally quite low with the highest rates being recorded for Line 14 (24.8%) followed by Line 4 connecting the CWQ and Gladstone nodes (24.7%). This latter result is higher than under the previous 2030 ISP step change scenario of 17% (see Panel (A) of Table 21).

Under the N-1 transmission scenario, some distinctive changes occur. First, reverse direction power flows become more prominent especially on Lines 2 and 3 connecting the Ross and NQ nodes and NQ and CWQ nodes while also continuing to hold also on Line 8 (Tarong to SWQ). This was also observed under the 2030 ISP step change scenario. Similarly, power flows on Line 1 continue to be predominantly in a normal direction, linked to the relatively large wind capacity located at the FNQ node. There is also an increased incidence of reverse power flow on other transmission branches but they still have a predominant normal direction of power flow. This result again also mirrors the same result that was obtained under the N-1 transmission scenario of the 2030 ISP step change scenario in Panel (B) of Table 21.

There was also a significant increase in congestion on certain transmission branches under the more restrictive N-1 transmission scenario. This included Line 4 interconnecting the CWQ and Gladstone nodes (67.4%), Line 7 interconnecting the WB and MN nodes (23.2%), Line 10 connecting SWQ and MS nodes (58.0%) and Line 14 interconnecting Gold Coast and Lismore nodes (45.3). Once again, these results mirror the results associated with the 2030 step change scenario, where Lines 7 and 10 experienced no real congestion under the N transmission scenario but significant congestion under the N-1 transmission scenario. Furthermore, the rates of congestion on the transmission lines identified above have increased over the equivalent rates of congestion reported in Panel (B) of Table 21, with the exception of Line 14.

From the perspective of system balancing, the apparent high rates of congestion on Lines 4 and 10 are very significant outcomes as these lines represent key transmission pathways for supplying power to meet the high nodal demands at the Gladstone and MS nodes. Furthermore, significant congestion on Line 10 has serious ramifications for the efficacy of the SWQ node as a potential renewable energy zone being targeted by AEMO. Specifically, under the N-1 transmission scenario, the congestion on Line 10 will seriously constrain the ability of this node to effectively supply power from

[24] It should be noted that there is also a significant wind generation component (e.g. 728.5 MW) located at the Tarong node but a very small solar PV component (20 MW).

its expansive thermal and VRE generation fleet directly to the MS-MN-Gold Cost demand region via Line 10. Second, it is likely that greater dependence will need to be placed on reverse direction power flows on Line 8 to re-direct constrained off power to MN and MS from SWQ through the Tarong node. The modelling results strongly supported this proposition, under both the N and N-1 transmission scenarios.

Table 23: Average VRE Spillage Rates for 2040 ISP Central Scenario

Panel (A): N Transmission Scenario

Node/VRE	FNQ	Ross	NQ	CWQ	GLAD	WB	TAR	SWQ	ARM	TAM
Wind	9.20%	7.86%	2.06%	1.97%	N.A.	N.A.	0.30%	0.42%	2.39%	3.32%
Solar	0.68%	1.31%	1.44%	5.70%	1.63%	2.78%	3.61%	14.36%	27.74%	19.94%

Panel (B): N-1 Transmission Scenario

Node/VRE	FNQ	Ross	NQ	CWQ	GLAD	WB	TAR	SWQ	ARM	TAM
Wind	31.60%	15.23%	8.38%	8.40%	N.A.	N.A.	0.13%	3.52%	1.88%	2.55%
Solar	12.36%	4.73%	4.75%	17.14%	0.22%	0.85%	4.48%	40.54%	22.82%	15.44%

Table 24: Average Transmission Branch Congestion and Direction of Flow Results for 2040 ISP Central Scenario

Panel (A): N Transmission Scenario

	Line 1 FNQ-ROSS	Line 2 ROSS-NQ	Line 3 NQ-CWQ	Line 4 CWQ-GLAD	Line 5 CWQ-TAR	Line 6 GLAD-WB	Line 7 WB-NM	Line 8 TAR-SWQ	Line 9 TAR-SWQ
Node Paths	1-2	2-3	3-4	4-5	4-7	5-6	6-9	7-8	7-9
Flow direction: Normal (%)	81.32%	68.94%	68.94%	100.00%	99.09%	99.26%	98.21%	33.28%	100.00%
Flow direction: Reverse (%)	18.68%	31.06%	31.06%	0.00%	0.91%	0.74%	1.79%	66.72%	0.00%
Congestion (%)	2.30%	0.00%	0.00%	24.67%	0.00%	0.00%	0.05%	0.00%	0.00%

	Line 10 SWQ-SM	Line 11 SWQ-QNI-ARM	Line 12 NM-SM	Line13 SM-GC	Line 14 GC-DL-LIS
Node Paths	8-10	8-13	9-10	10-11	11-12
Flow direction: Normal (%)	100.00%	100.00%	83.74%	99.88%	36.49%
Flow direction: Reverse (%)	0.00%	0.00%	16.26%	0.12%	63.51%
Congestion (%)	0.78%	0.00%	0.00%	0.00%	24.77%

Panel (B): N-1 Transmission Scenario

	Line 1 FNQ-ROSS	Line 2 ROSS-NQ	Line 3 NQ-CWQ	Line 4 CWQ-GLAD	Line 5 CWQ-TAR	Line 6 GLAD-WB	Line 7 WB-NM	Line 8 TAR-SWQ	Line 9 TAR-SWQ
Node Paths	1-2	2-3	3-4	4-5	4-7	5-6	6-9	7-8	7-9
Flow direction: Normal (%)	77.08%	47.82%	45.70%	100.00%	95.24%	86.16%	80.09%	39.73%	100.00%
Flow direction: Reverse (%)	22.92%	52.18%	54.30%	0.00%	4.76%	13.84%	19.91%	60.27%	0.00%
Congestion (%)	3.65%	0.00%	0.00%	67.37%	0.00%	0.00%	23.25%	0.00%	0.00%

	Line 10 SWQ-SM	Line 11 SWQ-QNI-ARM	Line 12 NM-SM	Line13 SM-GC	Line 14 GC-DL-LIS
Node Paths	8-10	8-13	9-10	10-11	11-12
Flow direction: Normal (%)	100.00%	100.00%	94.48%	99.88%	21.12%
Flow direction: Reverse (%)	0.00%	0.00%	5.52%	0.12%	78.88%
Congestion (%)	58.01%	0.00%	0.00%	0.00%	45.27%

5 Modelling Transmission Losses

5.0 Introduction

Recall from the discussion in Section 3.4 that two transmission loss concepts are modelled in this project. The first concept refers to transmission losses on transmission branches associated with power flows on those branches determined by the DC OPF solution underpinning the modelling. Within this context, these transmission losses are calculated for each transmission branch using the methodology outlined in (AEMO, 2012, Section 5) as outlined in detail in Section 3.4 of this report. Losses are then allocated to nodes connecting each respective transmission branch by two alternative methods. The first involves allocating transmission losses to the receiving end node as an additional fictitious nodal demand. The second method involves allocating transmission losses as additional fictitious nodal demands to each of the connected nodes at each end of the transmission branch on a 50:50 basis. *It should be noted that the results reported in the previous chapter were based upon the first allocation method – to the receiving end node according to the direction of power flow.*

The second loss concept that is investigated in the project are marginal losses. Marginal losses are partial derivatives relating to the incremental change in transmission losses to an incremental net injection of power at a specific node. This is calculated given an existing solution obtained from the DC OPF solution and typically involves adding one extra MW of demand at a node and then numerically calculating the change in transmission losses that result from this incremental nodal injection (AEMO, 2012, Section 5). The methodology used to calculate marginal losses was also outlined in detail in Section 3.4 of this report.

This chapter will include detailed assessment of modelling results associated with both transmission loss concepts. Section 5.1 will examine the main results associated with transmission losses calculated from the DC OPF solution and applied within the modelling as fictitious nodal demands. Recall that this is done to ensure that the nodal demand targets are met in full by ensuring that generation supplies an additional amount of power to cover transmission losses incurred with power flows on transmission branches.

In Section 5.2, an investigation of marginal losses and marginal loss factors will be undertaken. This analysis will examine how marginal loss outcomes vary with: (1) transmission loss allocation method; (2) 2022 and 2030 baseline pipeline scenarios; (3) between N and N-1 transmission scenarios for the 2030 pipeline baseline scenario; and (4) between the 2030 pipeline scenario and scenarios B and C under the N transmission scenario.

5.1 Modelling transmission losses as fictitious nodal demands

The magnitude of the power flow on transmission branches will depend crucially on the nature of nodal demand-supply balance. If demand exceeds generation at a node, then power will need to flow into that node to balance demand with supply. In this case, the node would be at the receiving end of the transmission branch with power flowing into the node. On the other hand, if nodal generation exceeds demand, then generation will be available to supply power to balance demand at other nodes. In this case, the node will be on the sending end of the transmission branch and power will flow away from it towards other nodes requiring additional power to balance demand.

In the modelling conducted for this project, transmission losses are also likely to depend on the transmission scenario adopted in the modelling. Recall that two transmission scenarios were employed:

- N transmission scenario; and
- N-1 transmission scenario.

The first scenario involves applying the MW thermal limits determined from the sum of all individual transmission line thermal ratings in the group of transmission lines connecting two nodes. The second N-1

transmission scenario involves subtracting the largest individual line from the group of transmission lines connecting nodes.

Why these two scenarios might be important for transmission loss calculations is because under the N transmission scenario, the transmission branches will have higher maximum MW transfer capacities. In this circumstance, the magnitude of power flows could be greater than under the N-1 transmission scenario which, in turn, would produce higher transmission losses if higher magnitude power flows were to eventuate.

The above analysis clearly links transmission losses with the magnitude of power flows on transmission branches. Transmission branches, in turn, interconnect nodes and permit power flows (i.e. transfers) between these interconnected nodes to balance nodal demand and supply (e.g. generation) throughout the network. Therefore, in the first instance, ANEM calculates transmission losses associated with power flows on transmission branches with the branch transmission losses being determined by: (1) each transmission branch's line resistance; and (2) each transmission branch's squared magnitude of its calculated power flow. In the latter context, the direction of power flow as represented by the sign of the calculated power flow does not affect the transmission loss calculation because of the squaring operation and transmission losses will necessarily be positive by construction.

The second modelling task is to allocate these branch transmission losses to nodes. This allocation process will depend on the objective underpinning the application of calculated transmission losses. In the broader modelling, transmission losses were allocated to nodes to ensure that nodal demands became hard targets. This required that an additional fictitious nodal demand component corresponding to transmission losses be added to nodal demands to ensure that generation produced enough power to cover both the transmission losses involved in transmitting power over transmission lines as well as the underlying nodal demand arising at the receiving end node towards which the power is flowing on the transmission branch.

In order to fulfil this requirement, two allocation methods were investigated. The first method was to allocate the transmission losses completely to the receiving end node. Recall that the receiving end node is the node at the end of the transmission line towards which the power is flowing on that transmission line. In contrast, the sending end node is the node from which the power is flowing away from on the transmission branch. In this current case, the transmission losses are added to the nodal demand at the receiving end as an additional fictitious nodal demand to ensure that enough power is produced and supplied from the sending end node to meet the demand at the receiving end node.

The second allocation method involves employing a 50:50 allocation of the calculated transmission loss as fictitious nodal demands at the sending and receiving end nodes. This allocation method has been proposed in the academic on loss tracing methods literature [e.g. (Srinivasa Varma and Sankar, 2012) and (Chengaiah and Jyoshna, 2013)] and will also provide a useful benchmark for the purpose of comparison with the first allocation method outlined above.

The rest of this section will document the nature of transmission losses obtained under different modelling scenarios involving the 2030 pipeline scenario as well as under different loss allocation methods mentioned above and between the N and N-1 transmission scenarios.

5.1.1 Transmission loss outcomes

In this section, an investigation of the GWh energy value of transmission losses will be examined based upon:

- Comparison of results under direction of flow and 50:50 allocation methods for the 2030 pipeline scenario under both the N and N-1 transmission scenarios.
- Comparison of 2030 pipeline B and C scenarios under different loss allocation methods and transmission scenarios.

5.1.1.1 Transmission loss results for 2030 pipeline baseline

Transmission losses arising under the 2030 pipeline baseline scenario for the different loss allocation methods and transmission scenarios are presented in Figure 7. The most notable result in the figure is the much higher transmission loss result associated with the N transmission scenario and direction of power flow (dof) loss allocation method for the MN node. Under the N transmission scenario, the MN node receives higher magnitude power flows from the WB node from the significant solar PV and wind generation located at that node than occurs under the N-1 transmission scenario. Recall that the WB node has 1200 MW of wind generation and 808 MW of solar PV capacity under all of the 2030 pipeline scenarios. However, under the N-1 transmission scenario, considerable congestion and spillage of both solar PV and wind power was observed at the WB node.

The MN node also receives large power flows from the Tarong node from both the Tarong and Tarong North coal-fired generators as well as the VRE generation located at that node (513 MW of wind and 620 MW of solar PV). Furthermore, the requirement of high power flows into MN would be also buttressed by the significant charging loads occurring at the MN node associated with pump actions of Wivenhoe and Mt Bryon pump hydro generation. For example, this additional demand can exceed 1.5 GW's especially during the day.

These large power flow results will translate into high transmission losses in the case of the N transmission scenario, irrespective of whatever loss allocation method is employed (e.g. dof or 5050). However, the larger values obtained for the MN node under the dof allocation method reflects the fact that the MN node is the receiving end node for both WB to MN and Tarong to MN transmission branches which both record 100% normal direction power flows. That is, power flows from the Tarong and WB nodes to the MN node 100% of the time. Moreover, power does not flow into the MN node from the MS node on Line 12. Therefore, under the dof allocation method, the considerable transmission losses associated with the large power flows from WB and Tarong to MN node is completely allocated to the MN node. In contrast, under the '5050' allocation method, half of these same losses are allocated to the WB and Tarong nodes thereby producing the much smaller transmission losses values indicated in Figure 7 for the MN under the '5050' transmission loss allocation method and N transmission scenario.

Apart from the MN node, it is also apparent that WB and Tarong nodes have the next largest transmission loss outcomes reflecting their central locations in the major transmission pathways suppling power to the large demand centres in South East Queensland via the CWQ to Tarong and Gladstone to WB transmission branches. Both of these lines recorded a very high percentage of normal direction power flows so these nodes are receiving end nodes for those particular power flows under the N transmission scenario. However, the fact that transmission losses are slightly higher at the WB and Tarong nodes for the '5050' allocation method emphasises how large the power flow into MN from these two nodes are relative to power flowing into the WB and Tarong nodes from Gladstone and CWQ, respectively.

Another key result in Figure 7 points to transmission losses under the N-1 transmission scenario being smaller than the equivalent results under the N transmission scenario for the same loss allocation method. This reflects the lower maximum MW capacity values arising under the N-1 transmission scenario relative to the N transmission scenario. Results are a bit more variable when comparing across different allocation methods. For example, losses at CWQ, Gladstone, WB and Tarong nodes are generally higher under the '5050' loss allocation method than under the 'dof' method because these nodes are essentially sending end nodes under a regime of predominant normal direction (e.g. north to south) power flows. This clearly contrasts with the situation confronting the MN node. Moreover, the magnitude of the losses are smaller at North Queensland nodes across both loss allocation and transmission scenarios compared to Southern Queensland nodes. This would reflect the higher demands underpinning power flows in southern Queensland nodes.

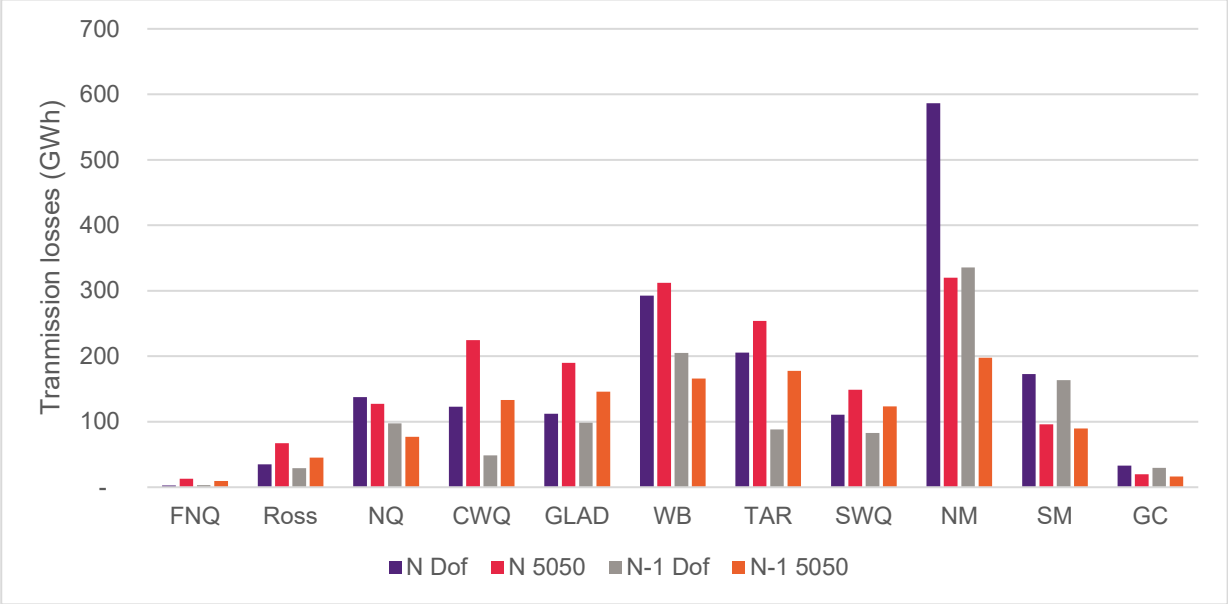

Figure 1: Comparison of transmission losses for the 2030 pipeline baseline scenario by loss allocation method and transmission scenario

Against this potential benefit of lower transmission losses under the N-1 transmission scenario, recall that in the case of the 2030 pipeline scenarios, that the energy-gap required for system balancing typically increased significantly under the N-1 transmission scenario. Moreover, renewable energy production shares were lower than under the N-1 transmission scenario and for all pipeline scenarios considered.

5.1.1.2 Transmission loss results for 2030 pipeline B scenario

Transmission losses arising under the 2030 pipeline B scenario for the different loss allocation methods and transmission scenarios are presented in Figure 8. Recall that this scenario implements an accelerated program of coal plant closures relative to then 2030 pipeline baseline scenario considered in the previous sub-section. Specifically, this scenario retires two units of Stanwell, four units of Gladstone, two units of Tarong and all four units of Eraring.

Once again, the most notable result in Figure 8 is the much higher transmission loss results associated with the N transmission scenario and direction of power flow (dof) loss allocation method for the MN node. However, compared with Figure 7, the magnitude of the transmission losses has fallen from around 600 GWh in Figure 7 to around 400 GWh in Figure 8 for the MN node assuming the N transmission scenario and dof loss allocation method. This overall reduction reflects, in part, the reduced output coming from Tarong power station following the retirement of two of its units. There have also been reductions in aggregate transmission losses at the Tarong and WB nodes, down from around 220 GWh to just over 150 GWh for Tarong and down from around 300 GWh to 160 GWh for WB under the 2030 pipeline B scenario.

There has also been a decline in losses at the Gladstone node and increase in losses across Northern Queensland nodes encompassing especially CWQ, NQ and Ross nodes. Of particular note is the relative shift in the magnitude of losses associated with the dof and '5050' allocation methods with a relative shift from reverse direction power flows to normal direction power flows on transmission branches connecting these particular nodes. This shift means that the incidence of times that Ross, NQ and CWQ become receiving end nodes has increased with the shift to a greater amount of north to south power flows under the pipeline B scenario compared to the baseline scenario. This occurrence, in turn, means that more transmission losses will be allocated to these northern nodes under the dof allocation method as indicated in Figure 8.

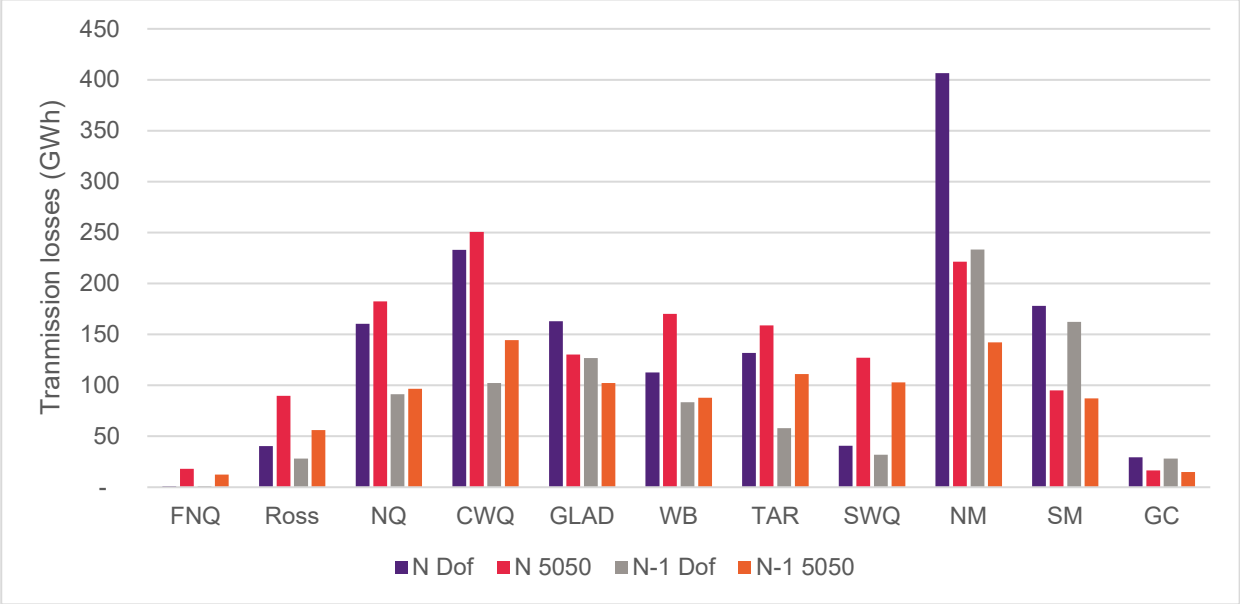

Figure 2: Comparison of transmission losses for the 2030 pipeline B scenario by loss allocation method and transmission scenario

5.1.1.3 Transmission loss results for 2030 pipeline C scenario

Transmission losses arising under the 2030 pipeline C scenario for the different loss allocation methods and transmission scenarios are documented in Figure 9. Recall that this scenario also implements an accelerated program of coal plant closures relative to then 2030 pipeline baseline scenario considered previously. This program involves retiring four units of Gladstone and Tarong power stations as well as all four units of Eraring. In this scenario, all four units of Stanwell power station remain operational.

Once again, the most notable result in Figure 9 is the much higher transmission loss results associated with the N transmission scenario and direction of power flow (dof) loss allocation method for the MN node. The loss patterns broadly match those identified in Figure 8 with the magnitude of transmission losses under the N transmission scenario and dof loss allocation method being around 400 GWh.

The amount of transmission losses allocated to Tarong, WB and Gladstone appear to be higher than equivalent results pointed to in Figure 8. Specifically, under the N transmission scenario, the highest transmission loss values for these three nodes in Figure 9 are around 220 GWh [Tarong, dof], 210 GWh [WB, 5050] and 210 GWh [Gladstone, dof]. This compares with equivalent results in Figure 8 of 155 GWh [Tarong, 5050],160 GWh [WB, 5050] and 160 GWh [Gladstone, dof]. These results also point to some switching between loss allocation methods that produce the higher transmission loss outcomes.

There has also been a notable increase in transmission losses at the CWQ node under the pipeline C scenario of 300 GWh under the '5050' allocation method compared to values of around 250 GWh in Figure 8 for the N transmission scenario. This result in Figure 9 would point to significant power transfers from CWQ to Gladstone and Tarong from all generation sources located at the CWQ node, including from all operational units of Stanwell. For example, results in Table 5 for the N transmission scenario pointed to an increase in normal direction power flow on Line 5 linking CWQ to Tarong of 99.2% under the 2030 pipeline C scenario, up from 91.9% under 2030 pipeline scenario B.

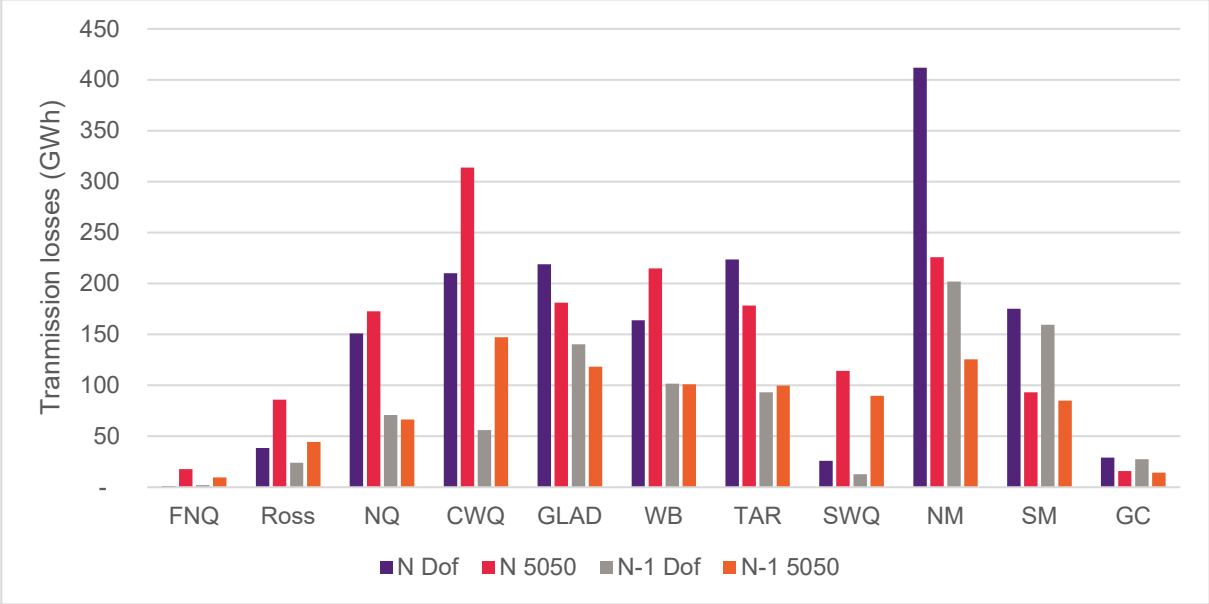

Figure 3: Comparison of transmission losses for the 2030 pipeline C scenario by loss allocation method and transmission scenario

5.2 Modelling marginal loss factors

Recall that marginal losses are partial derivatives relating to the incremental change in transmission losses to an incremental net injection of power at a specific node. This is calculated heuristically given an existing solution obtained from the DC OPF solution and typically involves adding one extra MW of demand (load) at a node and then numerically calculating the change in transmission losses that result from this incremental nodal injection. In this project, a conventional implementation of numerical methods for calculating partial derivatives was employed.

The application of marginal loss factors in a nodal model framework differs in certain respects to the typical application in more aggregated zonal model frameworks. While hub or zonal market concepts can be included in a nodal framework as an aggregation of a number of different nodes, nodal pricing applied to generation and marginal loss calculations are based strictly on the underlying nodal structure. As such, zonal structures do not play any real role in relation to marginal loss calculations. Marginal losses for generation will also not be based relative to any zonal or regional reference market structure. Instead, marginal losses and power flows will be more closely aligned with the nature of net nodal balance across the nodes in the network reflecting the particular location of generation and load within the network. As such, the regional reference nodes associated with the zonal market structure underpinning other wholesale market models of the NEM would just become normal nodes within the nodal model structure. Further, the inter-state interconnectors would also become typical transmission branches interconnecting nodes, except in this case, in different states. Importantly, power flows on all transmission lines in the nodal model, irrespective of whether they are intra-state or inter-state transmission branches would have to be solved as decision variables jointly with generator dispatch in the broader DC OPF problem. This would be necessary if marginal losses are going to be calculated on a real-time basis as both transmission losses and marginal losses would have to be calculated from the squared magnitude of optimised power flows determined from the DC OPF solution itself.

The methodology employed for calculating the marginal losses rests heavily on determining how the nodal demand increment changes power flows on interconnected transmission branches. In implementing the

calculation, it is applied on a node by node basis, holding demand and generation at all other nodes fixed. This is then performed sequentially over each node in the model to get a complete set of marginal losses.

Recall that once the marginal loss has been determined, Marginal Loss Factors (MLF) can be calculated simply as one plus the marginal loss. If the marginal loss is negative, then the MLF will be less than one. In this context, a negative marginal loss indicates that an incremental increase in nodal demand will reduce transmission losses. The rationale for this is that more generation will have to be offered to meet nodal demand and less will be available to transmit to other nodes and producing transmission losses as a by-product of this power transfer. Under these circumstances, adding demand would be expected to reduce losses while adding generation would be expected to increase losses as more generation relative to demand would be available to be transmit to other nodes which would produce increased transmission losses, *ceteris paribus*.

The allocation methodology applied in relation to the marginal loss calculations is to allocate the marginal losses to the sending node. This approach was adopted because power flow on a transmission branches commences at the sending node end of the transmission branch with power flowing over the transmission branch to the receiving end node and, in doing so, incurring the transmission loss. Under these circumstances, the sending node is more likely to have significant surplus nodal generation. In contrast, receiving nodes will not have the marginal losses allocated to them as they are at the end of the power transfer process on the transmission branch and losses have been already incurred in getting the power to that node from the sending node.

5.2.1 Results from modelling of marginal losses

In this section, an investigation of the marginal losses will be undertaken for the following scenarios:

- Comparison of marginal losses for the 2022 pipeline scenario under the two fictious nodal demand allocation methods: (1) direction of power flow (e.g. to receiving node); and (2) 50:50 allocation to receiving and sending nodes;
- Comparison of marginal losses for 2022 and 2030 pipeline scenarios under the N-1 transmission scenario; and
- Comparison of 2030 baseline scenario with 2030 pipeline B and C scenarios for the N transmission scenarios.

5.2.1.1 MLFs for the 2022 scenario: Comparison of dof and 5050 loss allocation methods assuming the N-1 transmission scenario

The MLF's arising under the 2022 pipeline scenario for both loss allocation methods are presented in Figure 10. Recall that the 2022 pipeline scenario includes all VRE projects that are operational, under construction or have financial close and some prospect for completion by 2022. Examination of Figure 10 depicts the closeness of the MLF's across the nodes indicating, in this case, that that they are not affected by whatever loss allocation methods is chosen (e.g. dof and 5050 methods).

The values of the MLF's in Figure 10 are crucially linked to the direction of power flow on transmission lines. The MLF's for FNQ, Ross and NQ are close to unity because in the 2022 simulations, a high proportion of power flows on the transmission lines connecting FNQ and Ross and Ross and NQ were reverse direction power flows. This mean that these three nodes were often receiving end nodes as power flow under reverse direction flow travels from the south to the north. In contrast, the other transmission branches experienced a very high proportion of normal direction power flows meaning that the MN, MS and Gold Coast nodes were receiving end nodes.

However, marginal losses are allocated to the sending end nodes of transmission branches from where the power flow commences on the transmission line and from where the transmission loss was incurred.

Therefore, if a node is a receiving end node, the marginal loss allocated to that node is zero and the MLF unity. That is why the MLF's of FNQ, Ross, NQ, MN, SM and Gold Coast are very close to if not unity.

The CWQ node is important because it is a key sending node from which originating power flows commence in both a northern direction (i.e. reverse direction power flow to the NQ node) and in a southern direction via normal direction power flows from the CWQ node to the Gladstone and Tarong nodes. In the latter case, the normal direction power flows continue from Gladstone to WB to MN and from Tarong to MN and SWQ. Because these power flows are in a north to south direction, the sending nodes are always the northern located node interconnected by specific transmission branches. As such, the CWQ, Gladstone, WB and the Tarong nodes will all be sending end nodes and subject to having marginal losses (and MLF's) assigned to them as indicated in Figure 10. The MLF's associated with these nodes have values of 0.923 for CWQ, 0.919 for Gladstone, 0.928 for WB and 0.935 for the Tarong node. Because all MLF's are less than one means that all marginal losses were negative. MLF's are also allocated to the SWQ and MN nodes reflecting power flow on Line 10 from SWQ to MS and on Line 12 from MN to MS. These two MLF are higher at 0.965 and 0.982, respectively.

Thus, the 2022 MLF results are tied closely to the direction of power flow on transmission branches determined by the DC OPF solution and categorisation of nodes into receiving and sending nodes.

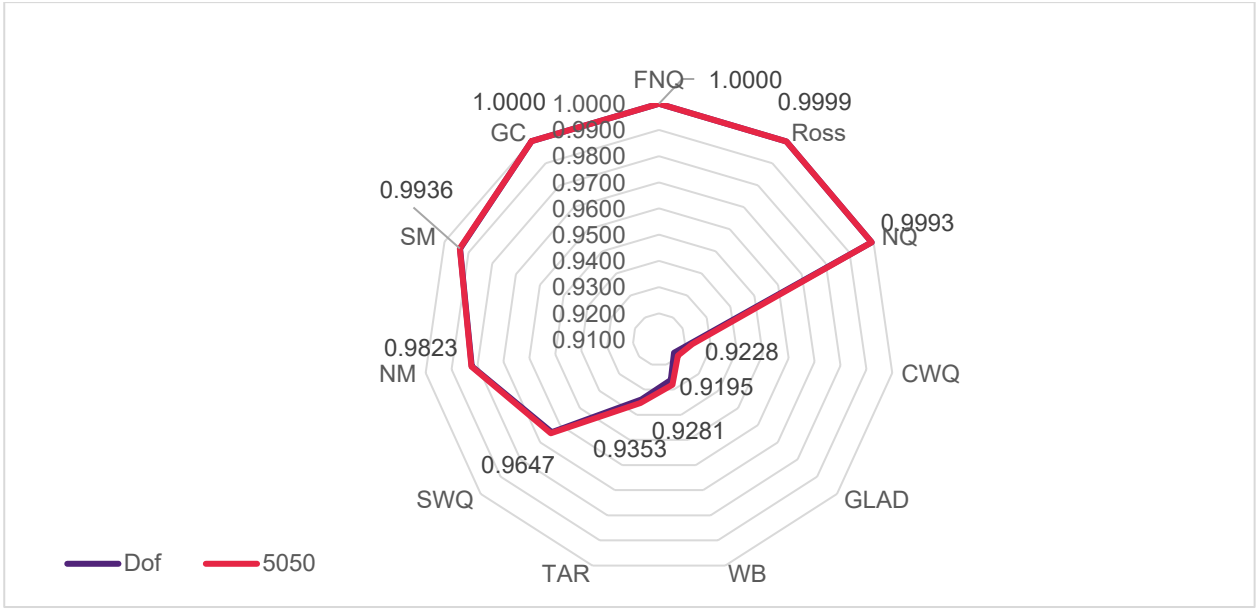

Figure 4: Comparison of MLFs for the 2022 Pipeline Scenario: Comparison of loss allocation methods

5.2.1.2 Comparison of MLFs for 2022 and 2030 pipeline baseline scenarios: Assuming N-1 transmission scenario and dof allocation method

The quantification of the differences between the MLF's associated with the 2022 and 2030 pipeline baseline scenarios assuming the N-1 transmission scenario and dof loss allocation method are documented in Figure 11. The 2022 results were discussed in the previous section. Discussion will centre on the 2030 results.

The role-out of VRE resources underpinning the 2030 results were very substantial relative to the equivalent capacities underpinning the 2022 scenario results. This included substantial wind and solar resources at the FNQ, Ross, and NQ nodes. As a consequence, there was a substantial turn around in the extent of reverse direction power flows with normal direction power flows now the dominant form of power flow on lines connecting these northern nodes. This would reflect the fact that the VRE capacity at these nodes circa 2030

is now sufficient to more than meet local nodal demand and have surplus power available to supply power elsewhere within the network. This would be affected via normal direction power flows in a north to south direction towards the larger demand centres in central and southern Queensland.

Under this regime of dominant normal direction power flows, the FNQ, Ross and NQ nodes will become sending end nodes and have marginal losses allocated to them. The resulting MLF's for these three northern nodes were 0.969 for FNQ, 0.962 for Ross and 0.962 for NQ nodes. For the other nodes, the 2022 and 2030 MLF values are quite close to each other with the 2030 MLFs being slightly smaller in magnitude. Thus, the big changes between 2022 and 2030 pipeline scenarios relates to the three northern nodes reflecting the greater MW capacity and dispatch of VRE resources in these nodes to not only meet local nodal demand as also supply power to more southern located nodes.

To see how the range of MLF values for the three northern nodes has changed in 2030 relative to 2022, Figure 12 lists the effective range of MLF values under both pipelines scenarios. This figure clearly shows that the range of MLF values for all three nodes has increased significantly in 2030 relative to the extremely narrow range about unity in 2022. The other interesting feature of Figure 12 is how the 2030 ranges demonstrates the variability in marginal loss outcomes (feeding into the MLF outcomes) that can emerge in a real time dispatch setting. The actual 'dispatch' outcomes show considerable variation in MLF's about the median values cited in Figure 11.

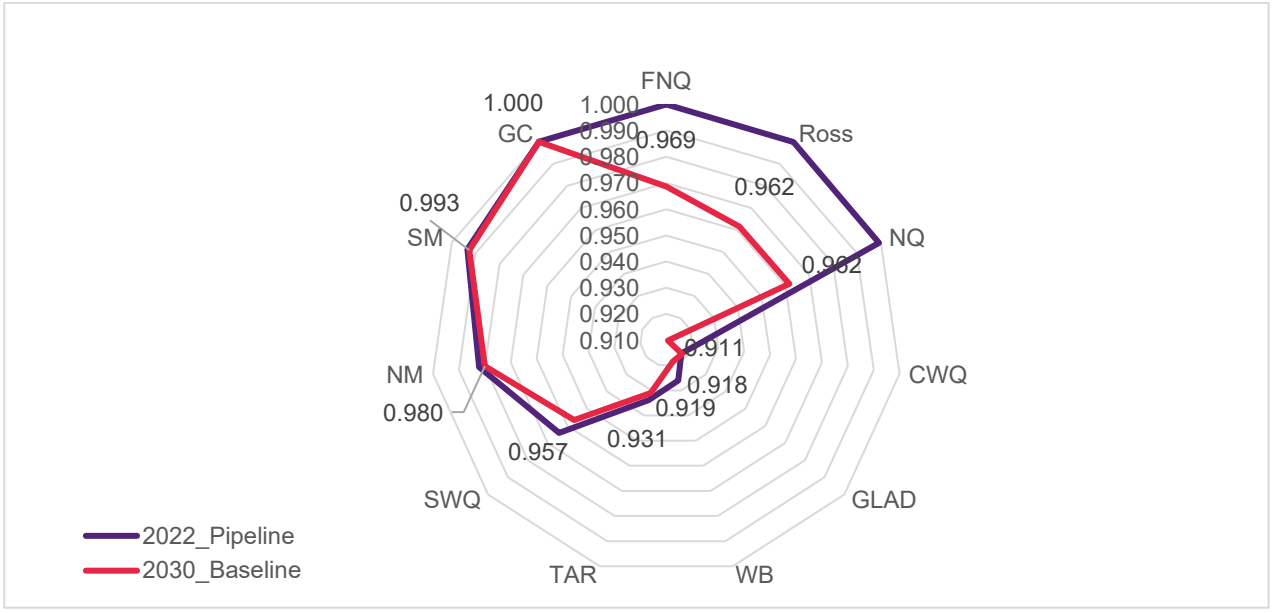

Figure 5: Comparison of MLFs for 2022 and 2030 pipeline baseline scenarios: dof loss allocation and N-1 transmission scenario

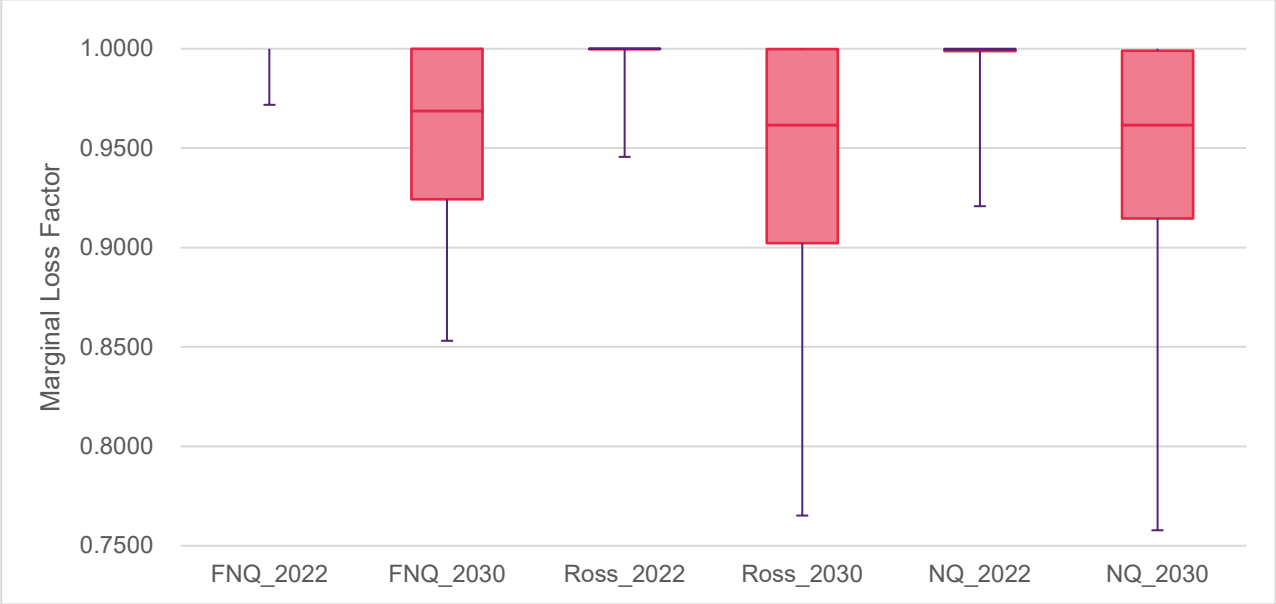

Figure 6: Comparison of MLFs for 2022 and 2030 pipeline baseline scenarios: Northern nodes

5.2.1.3 Comparison of MLFs for 2030 pipeline baseline scenarios: N and N-1 transmission scenario and dof allocation method

The quantification of the differences between the MLF's associated with the 2030 pipeline baseline scenarios for N and N-1 transmission scenario and assuming the dof loss allocation method are documented in Figure 13. The N-1 results were discussed in the previous section so this section will focus on results under the N transmission scenario.

Examination of Figure 13 indicates two key differences between nodal MLF's. The first and largest is at the WB node where the median MLF under the N transmission scenario is notably smaller than under the N-1 transmission scenario, e.g. 0.868 compared to 0.919. The second is a smaller difference at the CWQ node with the median MLF for the N transmission scenario being 0.893 compared to the N-1 value of 0.911. The lower values under the N transmission scenario reflect the greater transfer capacity under that particular scenario.

From Panel (A) of Table 12, there is no congestion on any lines connecting CWQ-Gladstone-WB except for the small rate of 1.8% on Line 4 connecting CWQ to Gladstone. As such, there is no network restriction on power flows under the N transmission scenario. In contrast, in Panel (A) of Table 13, there is significant congestion on two transmission lines capable of influencing power flow and dispatch of VRE under the N-1 transmission scenario. That is, congestion rates of 32.5% on Line 4 connecting CWQ and Gladstone and 52.6% on Line 7 connecting WB and MN. Thus, under the N-1 transmission scenario, there are real network limits capable of restricting the ability of power to reach the Gladstone node and for WB to export surplus VRE power to the MN node. These network constraints also served to increase the spillage of solar resources at the CWQ and Gladstone and especially solar PV and wind at the WB node under the N-1 transmission scenario.

Therefore, under the N-1 transmission scenario, because of significant congestion, less power can reach the Gladstone node from CWQ or supply the MN node from WB compared to dispatch outcomes arising under the more expansive N transmission scenario. Therefore, the greater dispatch levels and power flow capacity

from CWQ to Gladstone and WB to MN under the N transmission scenario would be expected to reduce the MLF of these two nodes relative to the N-1 transmission scenario results as depicted in Figure 13.

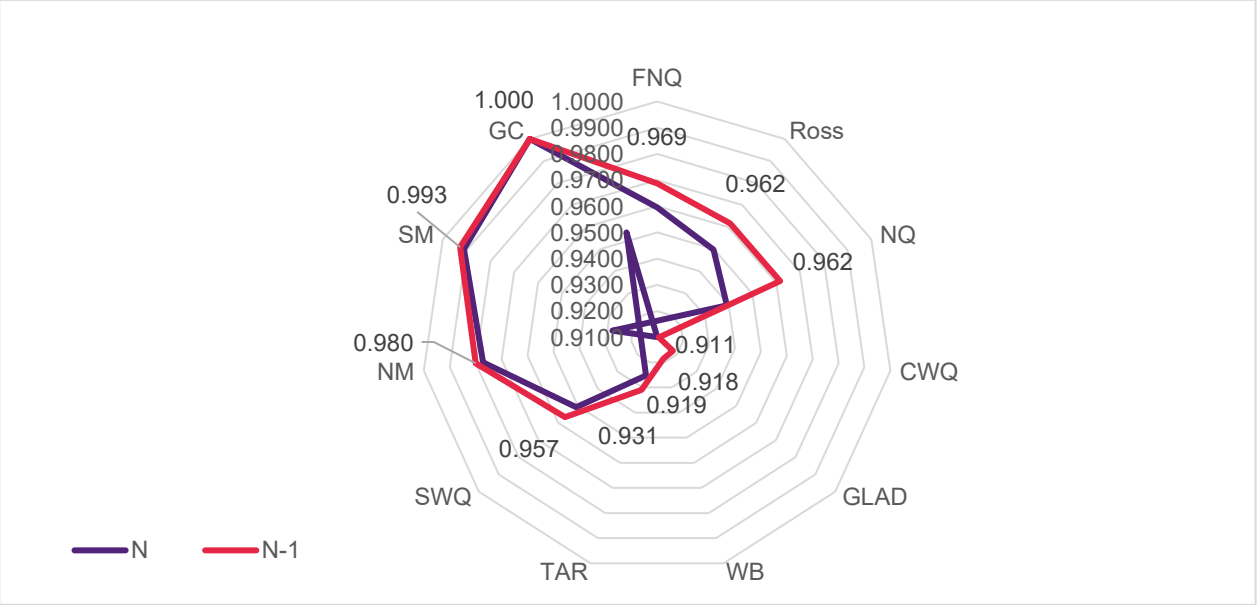

Figure 7: Comparison of MLFs for 2030 pipeline baseline scenario for N and N-1 transmission scenario: dof loss allocation method

These trends can be observed in Figure 14. Under the N transmission scenario, the range associated with with MLF's of WB and CWQ nodes are wider and lower than for those nodes under the N-1 transmission scenario. For example, for the WB node, the range for MLF values is between 0.85 and 0.9 compared with the very narrow range under the N-1 scenario around 0.91. Similarly, under the N transmission scenario, the range of the MLF outcomes for the CWQ node is between 0.87 and 0.92. This contrasts with the equivalent range under the N-1 transmission scenario between 0.9 and 0.935 which is narrower and higher. Similar arguments can also be clearly applied to the NQ node which is also depicted in Figure 13.

It should be noted that the greater range associated with the MLF values under the N transmission scenario follows from the greater natural variability (e.g. intermittency) in VRE power production that is available for dispatch and not restricted by network constraints that arise under the N-1 transmission scenario*. The increased variability in full VRE dispatch will also drive variability in MLF values producing the greater range indicated in Figure 14 associated with the N transmission scenario.*

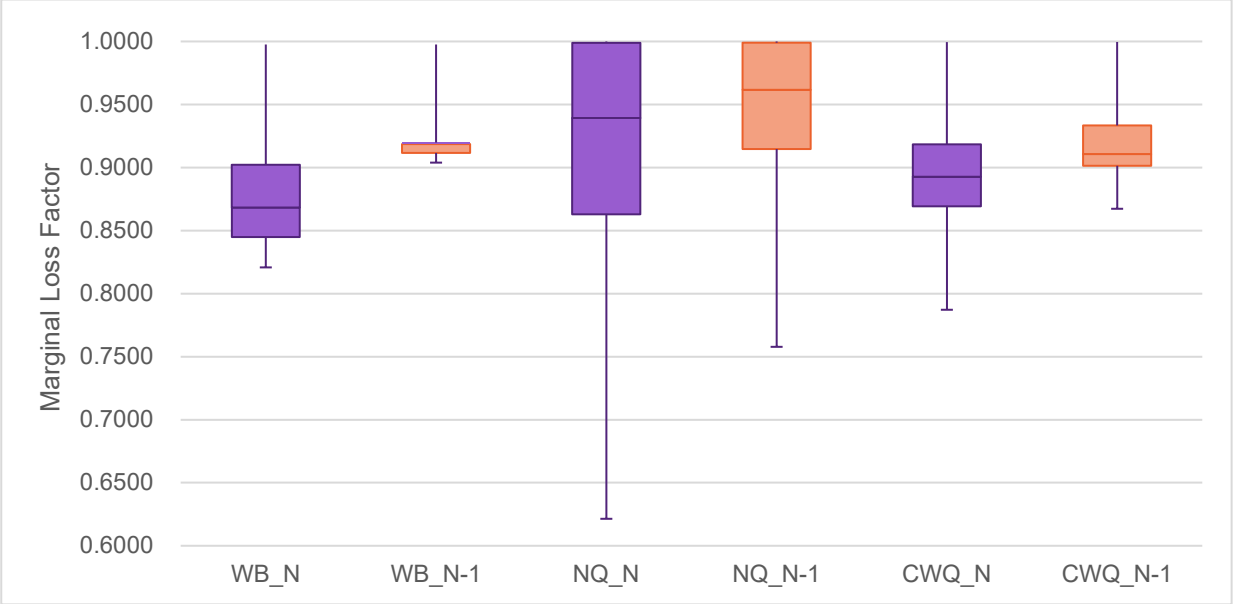

Figure 8: Comparison of MLFs for 2030 pipeline baseline scenario for N and N-1 transmission scenario: Selected nodes

5.2.1.4 Comparison of MLFs for 2030 pipeline baseline and B scenarios: N transmission scenario and dof allocation method

A comparison between the MLF's for the 2030 pipeline baseline and B scenarios for N transmission scenario and dof loss allocation method are displayed in Figure 15. The results for the 2030 pipeline baseline scenario under the N transmission scenario and dof loss allocation method was discussed in the previous sub-section so this sub-section will focus on results associated with the 2030 pipeline scenario B.

Recall that the 2030 pipeline scenario B entails an accelerated closure of coal plant. In addition to the closure of Callide B under the 2030 pipeline baseline scenario, scenario B also assumes, in addition, the retirement of two units of Stanwell, four units of Gladstone, two units of Tarong as well as all units of Eraring in New South Wales. In the context of Queensland, these closures represent significant reductions in generation capacity in the CWQ, Gladstone and Tarong nodes.

Inspection of Figure 15 indicates two key results. First, MLF's at the northern nodes (e.g. FNQ, Ross and NQ) have declined relative to their 2030 baseline results. Specifically, the median MLF value for FNQ declined from 0.959 to 0.937, for Ross from 0.95 to 0.923 and more markedly from 0.939 to 0.879 for the NQ node.

Second, the MLF's associated with CWQ, Gladstone, WB and Tarong have all increased relative to their 2030 baseline values. For example, the median MLF value for CWQ has increased from 0.823 to 0.902, from 0.91 to 0.946 for Gladstone, from 0.868 to 0.907 for WB, 0.925 to 0.944 for Tarong and from 0.977 to 0.981 for the MN node.

The first set of results mentioned above are consistent with more output flowing south from those three northern nodes (especially NQ) in response to the reduction in capacity in central Queensland associated with the additional closures of the Stanwell and Gladstone units. Support for this proposition can be found in Panel (C) of Table 12 which indicates a sizeable increase in the proportion of normal direction power flows on transmission branches connecting the three northern nodes compared to the baseline results reported in Panel (A) of Table 12. For example, the percentage of normal direction flows on Lines 1 to 3 in Panel (C) have increased to 85.5%, 78.9% and 82.6%, up from 71.7%, 67.0% and 68.2% in Panel (A) of Table 12.

The second result is consistent with the expected impact of capacity closures in nodes on MLF's. That is, the sizable capacity closures in CWQ and Gladstone nodes will restrict the amount of power that is available to be used to both meet local nodal demand or to supply power to other parts of the network. This reduction in capacity would be expected to increase the MLF's at those nodes directly. Moreover, this capacity reduction has also prompted an increase in reverse power flows from more southern located nodes including WB, MN and even MS (if marginally) – see Panel (C) of Table125. This means that to the extent that these nodes become receiving end nodes associated with an increased incidence of south to north power flows, then a MLF of unity would be allocated thereby driving up the median value of their MLF's compared to the 2030 baseline scenario values.

Examination of the results for the N-1 transmission scenario indicated that the patterns identified above continued to hold. The main difference between the N and N-1 transmission scenario results related to a slight increase in the magnitude of the median MLF values for both the 2030 baseline and B scenario under the N-1 transmission scenario relative to median MLF results under the N transmission scenario. This reflected the role that network capacity limitations as well as branch congestion arising under the N-1 transmission scenario played in restricting the magnitude of power flows especially between CWQ and Gladstone and WB and MN nodes. These various affects also combined to compress the magnitude of the difference between MLF estimates under both scenario across all nodes whilst still preserving the patterns observed above.

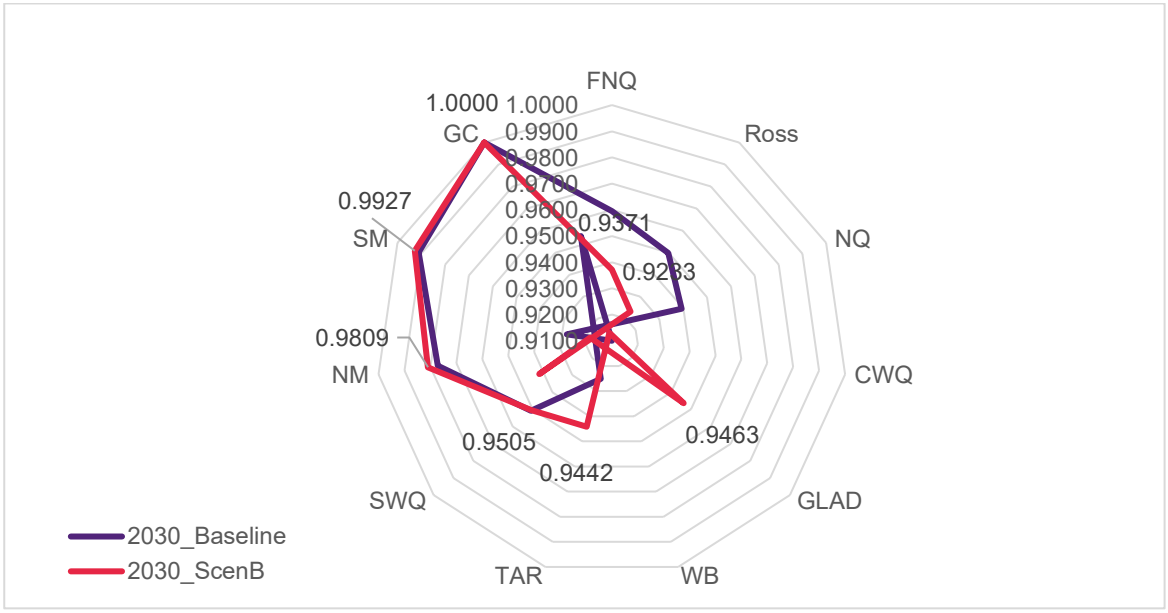

Figure 9: Comparison of MLFs for 2030 pipeline baseline and B scenarios: N transmission scenario and dof loss allocation method

5.2.1.5 Comparison of MLFs for 2030 pipeline baseline and C scenarios: N transmission scenario and dof allocation method

A comparison between the MLF's for the 2030 pipeline baseline and C scenarios for N transmission scenario and dof loss allocation method are displayed in Figure 16. The results for the 2030 pipeline baseline scenario under the N transmission scenario and dof loss allocation method have been discussed previously so this sub-section will focus on results associated with the 2030 pipeline scenario C.

Recall that the 2030 pipeline scenario C entails an accelerated closure of coal plant. In addition to the closure of Callide B under the 2030 pipeline baseline scenario, scenario C assumes, in addition, the retirement of four units of Gladstone, four units of Tarong as well as all units of Eraring power station. In comparison to scenario B discussed in the previous sub-section, scenario C assumes that Stanwell remains operational whilst all units of Tarong power station are retired. As such, the generation capacity in the CWQ node remains intact relative to the baseline scenario whilst significant reductions in generation capacity occur in the Gladstone and Tarong nodes.

Inspection of Figure 16 indicates that the broad trends identified in relation to scenario B continue to hold under Scenario C. Specifically, median MLF values at the northern nodes (e.g. FNQ, Ross and NQ) declined relative to their 2030 baseline results with larger falls being recorded at the NQ node in particular. However, in addition to the nodes listed above, the CWQ node now also enters this list with a fall in MLF from 0.893 under the baseline scenario to 0.8720 under scenario C. This differs from scenario B where the MLF at the CWQ node in fact increased reflecting the reduction in generation capacity at the CWQ node with the closure of the two Stanwell units under scenario B. In contrast, under scenario C, there is no capacity reduction at the CWQ node because Stanwell remains operational and increased power flow from the northern nodes including CWQ flow south to help balance the network at nodes that have experienced significant capacity reductions under scenario C, notably at the Gladstone and Tarong nodes.

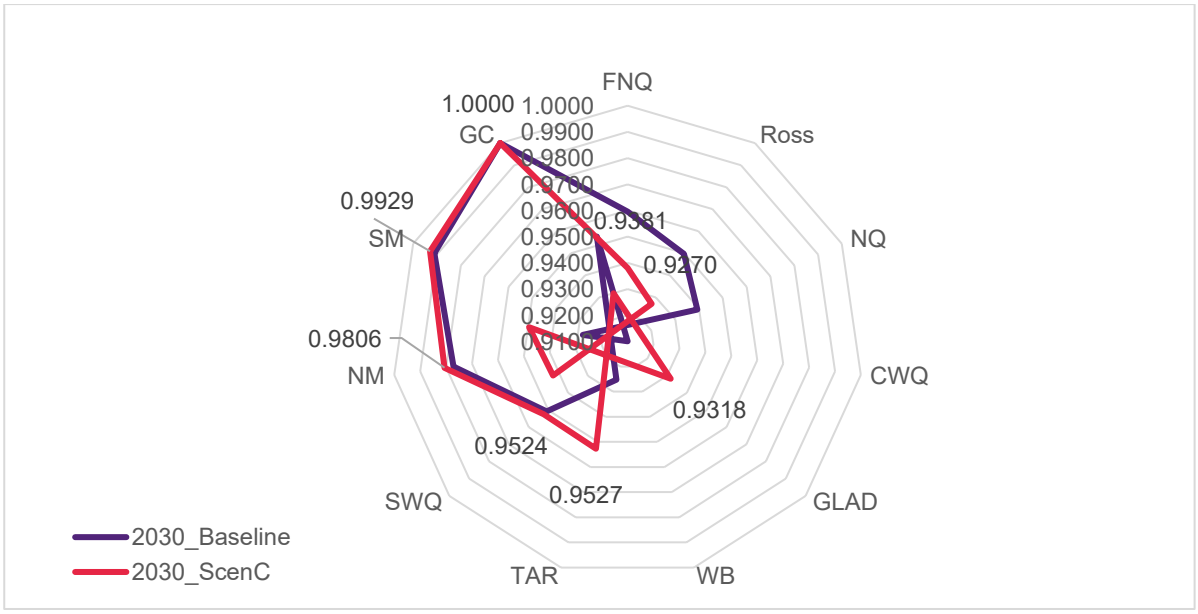

Figure 10: Comparison of MLFs for 2030 pipeline baseline and C scenarios: N transmission scenario and dof loss allocation method

At these more southern nodes, the median MLF value under scenario C have increased relative to their baseline values, mirroring the results associated with scenario B. Recall that this increase was linked to: (1) significant reductions in generation capacity; and (2) increases in the incidence of reverse power flows to help balance the demand at these nodes. It should be noted that the extent of reverse power flows is not as great as under scenario B however with, instead, more power flowing from the SWQ node to Tarong to help balance the network. With Stanwell fully operational, larger power flows from both CWQ to Gladstone can help supply crucial power needed to balance the sizeable demand located at the Gladstone node, thereby requiring less reverse power flows from nodes located to the south of Gladstone.

These trends can also be observed in Figure 17. In the case of the results associated with the Tarong and WB nodes, the range and median MLF results increase under scenario C compared to the baseline values (in blue). These results contrast with those of the NQ node where the median MLF value under scenario C

declined. The greater range associated with scenario C reflects the higher VRE production shares arising under scenario C compared to the baseline scenario as indicated in Panel (A) of Table 10. Under these circumstances, the increased range reflects the higher variability in output coming from the VRE resources.

Furthermore, in a similar manner to scenario B, the same patterns observed above can also be extended to comparison of the 2030 pipeline scenario and scenario C under the N-1 transmission scenario. The main difference continues to be a slight increase in the magnitude of the MLF value across both scenarios associated with the limitations that the N-1 transmission scenario exerts on capacity especially linked to congestion on lines linking CWQ and Gladstone and WB to MN. These various affects combine to compress the magnitude of the difference between MLF estimates under both scenario at many of the nodes whilst preserving the patterns identified above.

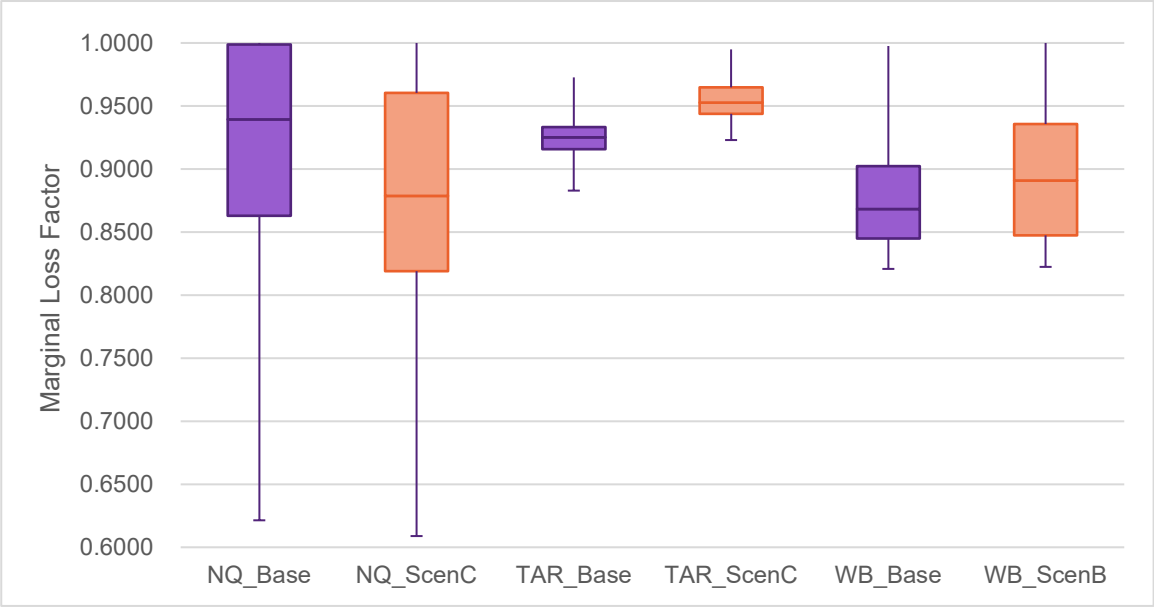

Figure 11: Comparison of MLFs for 2030 pipeline baseline and C scenarios: Selected nodes

6 Discussion

6.0 Introduction

In this report, detailed analysis of the 2030 pipelines scenario was undertaken with a view to examining how an accelerated program of coal generation plant closures might contribute to attaining a 50% renewable energy target by 2030. In this modelling, attention was focused entirely on the centralised power system – that is, on the role that large-scale centralised generation, whether thermal or renewable, might contribute to balancing centralised demand as well as meeting the 2030 renewable energy target. The results of this modelling were presented and discussed in Chapter 4

This modelling was extended to include analysis of three AEMO ISP scenarios. These scenarios were:

- 2030 central scenario;
- 2030 step change scenario; and
- 2040 central scenario.

In the 2030 step change Scenario modelling, the 2040 central scenario demand profiles were utilised because these profiles represented a better match to the 2030 Step Change Scenario change demand profiles especially in relation to assumed uptake of behind the meter technologies including rooftop solar and also in terms of underlying generation retirements. The results of this modelling were also presented in Chapter 4.

In both sets of modelling, the objective was to examine the four specific output metrics related to:

- Renewable energy production shares;
- VRE spillage rates;
- Direction of power flows and congestion on transmission branches; and
- Nature of any additional energy requirements (e.g. energy-gap) needed to balance the system.

This modelling was performed under two different transmission scenarios termed the N and N-1 transmission scenarios. The first scenario involves applying the MW thermal limits determined from the sum of all individual transmission line thermal ratings in the group of transmission lines connecting two nodes. The second N-1 transmission scenario involves subtracting the largest individual line from the group of transmission lines connecting nodes. Under these definitions, the N transmission scenario will have higher MW power transfer capacities than arising under the N-1 transmission scenario. As such, congestion is more likely to feature under the latter scenario.

A number of transmission augmentations were also applied across the 2030 pipeline and ISP related modelling. These augmentations were:

- EnergyConnect - double circuit 330 kV branch;
- HumeLink - two double circuit 500 kV branches;
- KerangLink - 500 kV double circuit branch with 330 kV branches also to the Red Cliffs and Glenrowan nodes;
- QNI Stage 2 - double circuit 500 kV branch linking QNI to Newcastle and Bayswater nodes through the Armidale, Tamworth and Liddell nodes; and
- Stage 1 ‘Battery-Of-The-Nation’ (BON): 750 MW HVDC branch from Burnie (Tasmania) to Hazelwood (Victoria).

Furthermore, under the ISP 2030 step change and 2040 central scenarios, the Stage 2 ‘Battery-Of-The-Nation’ (BON) augmentation was also applied in the modelling.

Distinct sets of plant closure assumptions were applied to the 2030 pipeline scenario and for each ISP scenario. In relation to the 2030 pipeline modelling, three different programmes of accelerated plant closures were applied in addition to the baseline scenario. Under the 2030 pipeline baseline scenario, the following Queensland plant closures were applied:

- Callide B; and
- Swanbank E.

Three accelerated plant closure programs were subsequently applied within the 2030 pipeline scenario modelling program, termed:

- Scenario A with additional closures:
  - Stanwell, unit 1
  - Gladstone, units 1,2,5 and 6
  - Tarong, unit 1
  - Eraring, unit 2
- Scenario B with additional closures:
  - Stanwell, units 1 and 2
  - Gladstone, units 1,2,5 and 6
  - Tarong, units 1 and 2
  - Eraring, units 2 to 4
- Scenario C with additional closures:
  - Gladstone, units 1,2,5 and 6
  - Tarong, units 1 to 4
  - Eraring, units 2 to 4.

Different generation plant closure programs were also applied in modelling the ISP scenarios with the 2030 central scenario having the same plant closure assumptions as the 2030 pipeline baseline scenario.

In the case of the 2030 step change scenario, the following additional plant closure assumptions were applied:

- Gladstone and Tarong, all units;
- Loy Yang A.

In the case of the 2040 ISP central scenario, the following additional plant retirements were also assumed:

- Gladstone and Tarong, all units;
- Tarong North;
- Bayswater and Eraring, all units; and
- Loy Yang A and B, all units.

Analysis of results in Chapter 4 indicated that the underlying transmission network structure assumed in the modelling played a key defining role in determining modelling outcomes. These different structures were encapsulated in the two transmission scenario assumptions outlined above, namely the N and N-1 transmission scenarios.

The second key issue warranting further discussion in this chapter relates to the findings made about system balancing requirements (e.g. energy-gap) in an environment containing significant coal plant closures and penetration of VRE resources.

Finally, further discussion about other issues affecting the attainment of a 50% renewable energy target will also be provided in Section 6.3.

These three broad issues will be addressed in the following three sections of this chapter.

6.1. Transmission Network Adequacy

Analysis of results in Chapter 4 indicated that the underlying transmission network structure assumed in the modelling played a key defining role in determining modelling outcomes. These different transmission structures were encapsulated in the N and N-1 transmission scenarios. These structures were crucial to determining power flows and the extent of transmission branch congestion and affected production share outcomes, VRE spillage rates and network balancing (e.g. energy-gap) requirements.

Across all the scenarios considered, significant congestion rates emerged under the N-1 transmission scenario on transmission branches interconnecting CWQ to Gladstone (Line 4), WB to MN (Line 7) and SWQ to MS nodes (Line 10). On the other hand, congestion on these transmission branches were significantly lower or non-existent under the N transmission scenario.

The congestion impacts under the N-1 transmission scenario reflect much lower MW transfer capacities operating under this transmission scenario compared to the more expansive N transmission scenario.

A number of key findings emerged under the N transmission scenario:

- Renewable and VRE production shares were higher than under the N-1 scenario;
- VRE spillage rates were notably lower;
- Apart from Line 14 (Gold Coast to Lismore), congestion rates were much lower compared to equivalent congestion rates under N-1 transmission scenario;
- GWh energy-gap required for balancing activities was significantly lower than under the N-1 transmission scenario across all modelled scenarios;
- Transmission losses were higher and marginal losses factors lower because of the potential for higher magnitude power flows under the N transmission scenario due to higher maximum MW transfer capacities associated with this scenario.

From the modelling results, some worrisome congestion patterns occurred under the N-1 transmission scenario across all modelled scenarios. This specifically related to observed branch congestion on: (1) CWQ to Gladstone; (2) WB to MN; (3) SWQ to MS; and (4) Gold Coast to Lismore (e.g. Directlink interconnector) transmission branches.

The first three are of strategic importance. First, congestion on the CWQ to Gladstone transmission branch (Line 4) can further restrict the magnitude of power flowing to Gladstone (below the 980MW 1126MW summer winter capacity limits under an N-1 scenario), adversely impacting attempts to balance the large industrial demand (average of 1104MW) at Gladstone. This will become especially critical as units of Gladstone power station are retired.

The second strategic congestion point is on the SWQ to MS transmission branch. This branch represents one of two key pathways to supply power to the large MS node which is Queensland's largest nodal demand centre (average of 1544MW). Congestion on this branch would restrict the ability to supply power from the SWQ node (below the 1096 1231 MW summer winter capacity limits under an N-1 scenario) to balance this demand. This consideration is especially relevant when recognition is given to the sizeable thermal (3687MW) and VRE (3219 MW pipeline, 2989MW ISP central) resources located in the SWQ node under all modelled scenarios. This node is also a nominated Queensland Renewable Energy Zone (REZ) by AEMO.

However, significant congestion on one of the main intra-state transmission branches that interconnects to the major South East Queensland demand centres would potentially mitigate the value of SWQ as a RES.

A potential solution to the above issue would be to, at least initially, focus attention more around the Tarong node which has a strong network backbone, interconnects into the same South East Queensland demand centres and will have more transfer capacity as coal generation plant at this node, is scheduled to close over the period 2035 to 2037 before the thermal units (Milmerran, Kogan Creek) at the SWQ node which are scheduled to close after 2040.

The final strategic congestion point is Line 7 connecting the WB and MN nodes. Why this congestion might be problematic is that a large 1200 MW wind farm has been proposed for the WB node with State Government backing together with sizeable solar PV pipeline of 800 MW. The 2030 pipeline scenarios modelled found that significant congestion and spillage of both solar and wind power arose. Significant spillage rates also remained even after significant coal plant closures were modelled associated with the 2030 pipeline B and C Scenarios. This congestion not only constrained the output of VRE resources located in the WB node, but restricted power flow into MN which had significant demand and pump-hydro resources. Thus, the possibility of significant transmission congestion affecting power flow from VRE generation sources located in the WB node to MN (and further on to MS and the Gold Coast nodes) will need to be considered further if the State Government wishes to designate the Wide Bay region as a REZ for consideration within the broader ISP process.

Another key consequence of transmission congestion under the N-1 transmission scenario is to impose more onerous balancing (energy-gap) requirements which will be discussed in the next section.

6.2. Balancing Requirements

The energy-gap component identified in Chapter 4 referred to balancing requirement associated with the additional dispatch of new generation that was needed over and above existing generation resources to ensure system balance was secured. By design, this dispatch is priced very highly and is intended to act in a role as dispatch of last resort when existing generation resources could not meet this requirement for some reason. Moreover, the modelling of this component is technologically agnostic. Instead, the focus is on dispatch requirements albeit with this new generation being dispatched according to the highest supply offers accommodated in the modelling.

This particular pricing methodology would, under the cost minimisation principles underpinning the wholesale market modelling, seek to promote the use of existing sources of generation to balance the system whenever possible and technically feasible. As such, it would also seek to minimize the use of new generation sources for this purpose.

Two key findings emerged in relation to balancing requirements:

- Balancing requirement increased sharply with the extent of coal plant retirements; and
- Required balancing energy (e.g. energy-gap) was always significantly lower under the N transmission scenario.

The results relating to balancing requirements are pervasive enough to indicate that some type of strategy will be needed to be put in place to focus attention of Planning Authorities on these requirements when investigating decarbonisation options. The modelling results, rather than providing answers, should more appropriately be interpreted as flagging issues requiring attention.

The modelling, as a whole, established a definite trade-off between transmission augmentation and the need for balancing services, especially in terms of the underlying balancing energy requirements. That is, augmentation of the MW transfer capacity of the transmission network would generally reduce the energy-gap requirements of the system significantly while the energy-gap would generally become larger and more

onerous when the MW transfer capacity on the transmission network was reduced or constrained because of congestion.

Whatever the underlying system design, a question remains about ***how the (potentially) infrequently used but significant 'back-up' infrastructure associated with the energy-gap component would be incentivised and what are appropriate ownership models for this infrastructure***. While the author provides no definitive answer to the above question, the following considerations appear to be material to consideration of this issue:

- Would a capacity market incentivise investment;
- Would an extension of the Emergency and Reserve Trader (RERT) facility be an appropriate market mechanism perhaps operating under the auspices of a formal balancing market; and
- Can investments be accommodated within a day ahead and real time balancing framework in operation in overseas jurisdictions and being investigated by the ESB.

In relation to the third point, a complicating feature relates to the applicability and ease to which VRE resources could potentially enter into day ahead contractual arrangements commonly entered into by participants in day ahead markets. Typically, the forecast error of output from VRE generation is likely to decline the closer the real-time operational setting is approached. Furthermore, balancing requirements operationally will not be fully determined until the output of VRE resources are also firmed which is only likely to eventuate in a real-time setting.

In terms of *ownership model*, the following considerations appear to also be material to consideration of this issue:

- Is it appropriate for State Governments to take over responsibility of constructing of balancing capacity given that its infrequent usage might preclude private sector investment in this type of capacity;
- If Government seeks to co-opt private sector investment in this type of investment, can this be incentivised under a reverse auction process; and
- Would Government investment in seasonal storage technologies provide an alternative mechanism that provides enough capacity to provide deeper balancing services.

In relation to the last point, to-date most storage options in the public domain in Queensland including pump hydro proposals appear to be capable of providing shallow storage services operating on a daily timescale. However, to the author's knowledge, Queensland does not appear to have an equivalent of Snowy 2.0 or Tasmania's Battery-of-the-National project, both of which are capable of providing deep storage on a seasonal scale.

6.3. Other Considerations

As investment in VRE increases, balancing requirements similar to those discussed in the previous section would also be expected to increase. As such, deep cuts in emissions from power generation will also require the development of clean energy technologies that can operate on the back of the role out of high penetration of VRE. While many of these technology options are already available, the only technology that has been deployed at the scales suggested by the modelling is pump hydro. The deployment at a similar scale of other clean technology options remains to be proven. However, these clean energy options will be needed and need to work to lock in emission gains to and beyond 2030.

Beyond 2030, to achieve larger emission cuts will require the further retirement of coal and gas assets in Queensland. At 2040, according to the schedule published by AEMO as part of the ISP process, Stanwell, Callide C, Kogan Creek and Millmerran coal fired power stations will still be in operation with a combined capacity of 3956 MW. A sizeable gas fleet is also operational including 1128 MW of NGCC plant. Thus,

further emission reductions will require much of that plant to also be retired with the resulting implications for VRE resourcing and provision of balancing services. As such, the energy-gap associated with balancing requirements is likely to increase beyond that identified in this report.

A significant proportion of the operating fleet circa 2040 mentioned immediately above is located in the SWQ node. In the presence of congestion on the SWQ to MS transmission branch (i.e. Line 10), the co-location of very large VRE generation in the SWQ with the existing thermal fleet could reduce the value of SWQ node as a REZ until significant coal closures begin to occur in the SWQ node. A better medium-term prospect for locating sizeable VRE generation might be the Tarong node with coal plant closures in this node currently scheduled to occur over the 2035-38 time period. This node has a strong network backbone with strong transmission pathways to MN and SWQ nodes.

Appendix A: Glossary of Terms

Abbreviation	Meaning
AC	Alternating Current
AEMO	Australian Energy Market Operator
AMES	American Agent-Based Modelling of Electricity Systems Model
ANEM	Australian National Electricity Market Model
Armidale	Armidale (an ANEM NSW node)
CWQ	Central West Queensland (an ANEM QLD node)
DC	Direct Current
DC OPF	Direct Current Optimal Power Flow
DirectLink	HVDC Queensland-New South Wales Interconnector
EnergyConnect	New South Wales-South Australia Interconnector
FNQ	Far North Queensland (an ANEM QLD node)
FOM	Fixed Operation and Maintenance
GC	Gold Coast (an ANEM QLD node)
GLAD	Gladstone (an ANEM QLD node)
GT	Gas Thermal
GW	Gigawatt
GWh	Gigawatt-hour
HVDC	High Voltage Direct Current
ISO	Independent System Operator
ISP	Integrated System Plan
LMP	Locational Marginal Price
LSE	Load Serving Entity
MN	Moreton North (an ANEM QLD node)
MS	Moreton South (an ANEM QLD node)
MW	Megawatt
MWh	Megawatt-hour
NEM	National Electricity Market
NGCC	Natural Gas Combined Cycle
NQ	North Queensland (an ANEM QLD node)
NSW	New South Wales
OCGT	Open Cycle Gas Turbine
POE	Probability of Exceedance
QLD	Queensland
QNI	Queensland-New South Wales Interconnector
Ross	Ross (an ANEM QLD node)
SA	South Australia
SCQP	Strictly Convex Quadratic Programming
SWQ	South West Queensland (an ANEM QLD node)
TARONG	Tarong (an ANEM QLD node) and power station in the Tarong node
TAS	Tasmania
VIC	Victoria
VOM	Variable Operation and Maintenance
VRE	Variable Renewable Energy
WB	Wide Bay (an ANEM QLD node)

Appendix B. List of Wind and Solar farms included in the VRE scenarios

List of Queensland solar farms (and MW capacity) included in pipeline scenarios

Node/scenario	2022	2025	2030
FNQ	Kidston S1 (49)	Kidston S2 (271)	
Ross	Haughton S1 (100) Clare S1 (100) Ross River (118) Sunmetals (124) Hughenden S1 (35)	Haughton S2 (100) Majors Creek (200) Clare S2 (36)	Big Kennedy (575)[25] Haughton S3-S5 (300) Rollingstone (88)
NQ	Hamilton (57.5) Whitsunday (57.5) Daydream (150) Hayman (50) Collinsville Ratch (41.6)	North Collinsville (100) Boulderombe (280) Broadsound (290)	
CWQ	Barcaldine S1 (20) Longreach S1 (15) Rugby Run S1 (65) Clermont (75) Emerald (68) Lilyvale (100)	Barcaldine S2 (21.7) Longreach S2 (25) Rugby Run S2 (105) Tieri (76.8)	Moura (91.7) Rolleston (100) Ullogie (180)
Gladstone		Aldoga (265) Bororen (250) Raglan (280)	
WB	Childers (75) Susan River (98)	Lower Wonga (350) Aramara (112)	Teebar (52.5) Munna Creek (120)
Tarong	Bakers Board (19.9)	Chincilla (100)	Harlin S1 (500)
SWQ	Darling Downs (110) Oakey (80) Yarranlea (121) Warwick (68) Columboola (162) Brigalow (30) Gangarri (120)	Bulli Creek S1 (300) Wandowan South S1 (250)	Bulli Creek S2 (300) Wandowan South S2 (250) Western Downs (500)

[25] CopperString 2.0 transmission project connecting Mt Isa to Ross is assumed to be complete so that the wind and solar components of the 'Big Kennedy' project can deliver their output to the NEM.

List of Queensland wind farms (and MW capacity) included in pipeline scenarios

Node/scenario	2022	2025	2030
FNQ	Windy Hill S1 (12) Mt Emerald (180.5)	Lakeland (108) Kaban (130.5) Forsayth (65.8) Kidston S3 (149.3)	
Ross	Kennedy 1 (43.2)		Big Kennedy (601.2)
NQ		Clark Creek (799.2)	
CWQ		Banana Range (180)	
Wide Bay			Forest WF (1200)
Tarong	Coopers Gap (449.2)	Manneum (64)	
SWQ		Macintyre (540) Dulucca (240.8)	

List of New South Wales solar farms (and MW capacity) included in pipeline scenarios

Node/scenario	2022	2025	2030
Armidale	Moree (56) White Rock (20) Metz (100)	Sapphire (170)	Newstead (600) Uralla (600)
Tamworth	Walget (29)	Narrabri S1 (60) Gunnedah S1 (275)	Narrabri S2 (90) Gunnedah S2 (47.5) Wee Waa (55) Walcha (650)
Mt Piper			Brewongle (120)
Wellington	Nyngan (102) Parkes (55) Dubbo (29) Manildra (46.7) Beryl (87) Wellington (BHP Lighthouse) (176) Nevertire (105) Jemalong (50) Goonumbla (68.7)	Suntop 1 (170) Gilgandra (40) Maryvale (125)	Suntop 2 (165) Mumbil (140) Wellington North (300)
Marulan		Brayton (144)	Parkesbourne (500)
Yass		Gunnings (160)	
Canberra	Royalla (20) Mugga Lane (13)	Springdale (100)	
Wagga	Griffith (30) Coleambally (150) Finley (142) Darlington Point (230) Bomen (122) West Wyalong (90)	Hay (100) Hillston (85) Gregadoo (40)	Warrabee (900) Currawarra (160)
Buronga	Sunraysia (200) Limondale (250)		
Broken Hill	Broken Hill (53)		

List of New South Wales wind farms (and MW capacity) included in pipeline scenarios

Node/scenario	2022	2025	2030
Armidale	White Rock 1 (175) Sapphire (270)	White Rock 2 (170.9) Glen Innes (90)	
Tamworth			Winterbourne (700)
Mt Piper	Blayney (9.9) Crudine Ridge (133.2)		
Wellington	Bodangora (113.2)	Flyers Creek (136.8)	Liverpool Range (961.2) Uungula (410.2)
Marulan	Crookwell 1 (4.8) Crookwell 2 (96) Gullen Range (165.5) Taralga (106.8) Biala (100.1)	Crookwell 3 (120.1)	
Yass	Bango (255.6)	Coppabella (315) Rye Park (317.4)	
Canberra	Capital 1 (140.7) Cullerin Range (30) Gunning (46.5) Boco Rock 1 (113) Woodlawn (48.3) Collector (198)	Capital 2 (100.1) Boco Rock 2 (144.1)	
Broken Hill	Silverton (198.9)		

List of Victorian solar farms (and MW capacity) included in pipeline scenarios

Node/scenario	2022	2025	2030
Kerang	Gunnawarra S1 (50.6) Swan Hill (15.2) Cohuna (30)	Kerang (32) Prairie (240)	Gunnawarra S2 (60.7)
Glenrowan	Winton (85) Numurkah (100) Glenrowan West (119.2)	Wangaratta (16) Shepparton (100)	
Horsham		Murra Warra (188) Horsham (104)	
Red Cliffs	Wemen (87.8) Karadoc (89.6) Bannerton (88) Yatpool (84.8) Carwarp (100) Kiamal 1 (239)	Kiamal 2 (111)	Nowingi (200)

List of Victorian wind farms (and MW capacity) included in pipeline scenarios

Node/scenario	2022	2025	2030
Melbourne		Inverleigh (55.2)	
Morwell	Bald Hills (106.6) Toora (21) Wonthaggi (12)		
South West VIC	Codrington (18.2) Macarthur (420) Oakland Hill (66.9) Portland (102) Portland 4 (47.2) Yambuk (30) Mt Gellibrand (132) Salt Creek (54) Mortons Lane (19.5) Stockyard Hill (530.4) Mortlake South (157.5) Berrybank (180) Dundonnel (336)	Woolsthorpe (69) Hawkesdale (104) Ryan's Corner (224)	Willatook (412.8) Goldens plains (820.8) Woakwine Range (372)[26]
Ballarat	Challicum Hills (51.9) Mt Mercer (131.2) Waubra (192) Ararat (242.3) Hepburn (4) Chepstowe (6.2) Lal Lal (216) Moorabool (321) Yalock South (28.7) Crowlands (80)		
Kerang	Coonooer Bridge (19.8)	Berrimal (72)	
Glenrowan	Cherry Tree (57.6)		
Horsham	Murra Warra 1 (225.7) Kiata (103.5) Bulgana (193.8)	Murra Warra 2 (203.5) Rifle Butts (39)	

[26] Whilst the Woakwine Range Wind farm is located in Lake Bonney region of South Australia, it is assumed that transmission connection is via underground cable connecting at or near the Heywood interconnector with particular focus on higher demand in South West Victoria.

List of South Australian solar farms (and MW capacity) included in pipeline scenarios

Node/scenario	2022	2025	2030
South East SA	Tailem Bend S1 (100)	Tailem bend S2 (87)	Pallamana (176)
Riverlands	Solar Rivers S1 (200)	Solar Rivers S2 (200)	Robertstown (500) Morgan (330)
Mid North SA		Crystal Brook (110)	Chaff Mill (100) Bungama (280) Goyder (500)
Upper North SA	Bungala 1 (120) Bungala 2 (120) Port Augusta 1 (110)	Port Augusta 2 (500)	Bridle Track (300) Kingfisher (120)
Eyre peninsular	Cultana (220)	Whyalla-Adani S1 (113.7)	Whyalla-Adani S2 (26.3)

List of South Australian wind farms (and MW capacity) included in pipeline scenarios

Node/scenario	2022	2025	2030
South East SA	Canunda (45.4) Lake Bonney S1 (78.3) Lake Bonney S2 (158) Lake Bonney S3 (38.7)		
Adelaide	Starfish Hill (33.7)	Ceres 1 (319)	Ceres 2 (315.6)
Mid North SA	Hallett 1 (94.5) Hallett 2 (71.4) North Brown Hill (132.3) Bluff (52.5) Wattle Point (90.8) Snowtown 1 (98.7) Snowtown 2 (270) Waterloo (129) Clements Gap (56.7) Hornsdale 1 (102.4) Hornsdale 2 (102.4) Hornsdale 3 (112) Willogoleche (119.4)	Palmer (374.9) Crystal Brook (124.8)	Twin Creek (183.6)
Upper North SA	Lincoln Gap (212.4) Port Augusta (210)		
Eyre Peninsular	Cathedral Rocks (66) Mt Millar (70)		

List of Tasmanian wind farms (and MW capacity) included in pipeline scenarios

Node/scenario	2022	2025	2030
George Town		Low head (30)	
Sheffield		Hellyer (152)	Guildford (304)
Burnie	Woolnorth (139.8)	Jimmy Plains (200) Robbins Island 1 (340) Western Plains (46.8)	Robbins Island 2 (660)
Farrell	Granville Harbour (111.6)		
Hadspen	Musselroe (168)		
Tarraleah	Cattle Hill (150)		

References

AEMO. 2012. Treatment of Loss Factors in the National Electricity Market, July 2012. Available: https://www.aemo.com.au/-/media/Files/Electricity/NEM/Security_and_Reliability/Loss_Factors_and_Regional_Boundaries/2016/Treatment_of_Loss_Factors_in_the_NEM.pdf. [Accessed 2020].

AEMO. 2018a. Integrated System Plan, July 2018. For the National Electricity Market, July 2018. Available: https://www.aemo.com.au/-/media/Files/Electricity/NEM/Planning_and_Forecasting/ISP/2018/Integrated-System-Plan-2018_final.pdf. [Accessed 2020].

AEMO. 2018b. 2018 Integrated System Plan database. Available: https://aemo.com.au/energy-systems/major-publications/integrated-system-plan-isp/2018-integrated-system-plan-isp/2018-isp-database [Assessed 2020].

AEMO. 2019a. Electricity Demand Forecasting Methodology Information Paper" August 2019. Available: https://www.aemo.com.au/-/media/Files/Electricity/NEM/Planning_and_Forecasting/NEM_ESOO/2019/Electricity-Demand-Forecasting-Methodology-Information-Paper.pdf. [Accessed 2020].

AEMO. 2019b. Draft 2020 ISP chart data [Online]. Melbourne: Australian Energy Market Operator. Available: https://aemo.com.au/-/media/files/electricity/nem/planning_and_forecasting/isp/2019/draft-2020-isp-chart-data.zip?la=en [Accessed 2020].

AEMO.2020. 2020 Integrated System Plan database. Available: https://aemo.com.au/energy-systems/major-publications/integrated-system-plan-isp/2020-integrated-system-plan-isp/2019-isp-database. [Accessed 2020].

Bradbury, L (2015), Wind Power Program, viewed 22 Apr 2015, http://www.wind-power-program.com/index.htm.

Bureau of Meteorology: BOM (2015) 'Australian Hourly Solar Irradiance Gridded Data.', http://www.bom.gov.au/climate/how/newproducts/IDCJAD0111.shtml.

Chengaiah, C, and P. Jyoshna (2013), "Allocation of Transmission Losses in Deregulated Power System", Global Journal of Researches in Engineering, Electrical and Electronics Engineering, 13(12), 1-7.

ElectraNet (2019) "SA Energy Transformation RIT-T - Network Technical Assumptions Report", February 2019, https://www.electranet.com.au/wp-content/uploads/projects/2016/11/Network-Technical-Assumptions-Report.pdf

Gilman, P. (2015) 'SAM Photovoltaic Model Technical Reference.' National Renewable Energy laboratory (NREL), May,http://www.nrel.gov/docs/fy15osti/64102.pdf.

INL: Wind Power, Idaho National Laboratory (2015), Wind Power, Idaho National Laboratory, viewed 22 Apr 2015, https://inlportal.inl.gov/portal/server.pt/community/wind_power/424/software.

Jacobsen, HS (2015), Wind Analysis Program (WAsP), viewed 22 Apr 2015, http://www.wasp.dk/.

Mosek (2014), High performance software for large-scale LP, QP, SOCP, SDP and MIP, viewed 16 Mar 2014, http://www.mosek.com/.

Powerlink (2019) "Transmission Annual Planning Report 2019", https://www.powerlink.com.au/sites/default/files/2019-09/Transmission%20Annual%20Planning%20Report%202019%20-%20Full%20report.pdf.

Repast (2014), The Repast Suite is a family of free agent-based modelling libraries, viewed 16 Mar 2014, http://sourceforge.net/projects/repast/files/.

Srinivasa Varma, P, and V. Sankar (2012) “Comparison of Transmission Loss Allocation Methods in Deregulated Power Systems”, International Journal of Advanced Electrical and Electronics Engineering, 1(1), 70-79.

Sun, J & Tesfatsion, L (2007a), DC Optimal Power Flow Formulation and Solution Using QuadProgJ, ISU Economics Working Paper No. 06014, Department of Economics, Iowa State University, IA 50011-1070, http://www.econ.iastate.edu/tesfatsi/DC-OPF.JSLT.pdf.

Sun, J & Tesfatsion (2007b), Dynamic testing of Wholesale power Market Designs: An Open-Source Agent Based Framework, ISU Economics Working Paper No. 06025, July 2007, Department of Economics, Iowa State University, IA 50011-1070, http://www.econ.iastate.edu/tesfatsi/DynTestAMES.JSLT.pdf.

Wild, P, Bell, WP & Foster, J (2012), An Assessment of the Impact of the Introduction of Carbon Price Signals on Prices, Production Trends, Carbon Emissions and Power Flows in the NEM for the period 2007-2009, EEMG Working Paper No 4/2012, Energy Economics and Management Group, School of Economics, University of Queensland, April 2012, http://www.uq.edu.au/eemg/docs/workingpapers/17.pdf.

WRF 2015, The Weather Research and Forecasting Model, viewed 22 Apr 2015, http://www.wrf-

Contact details

[Name]
T +61 7 [0000 0000]
M +61 [0000 000 000]
E [email]@uq.edu.au
W uq.edu.au

CRICOS Provider Number 00025B